CZECH TECHNICAL UNIVERSITY IN PRAGUE

FAULTY OF MECHANICAL ENGINEERING

DEPARTMENT OF PROCESS ENGINEERING

PRODUCTION OF CERAMIC AGGREGATES IN ROTARY KILN

MASTER THESIS

2021

ALESSANDRO SECHI

Supervisor: DOC. ING. JAN SKOCILAS PH.D.

MASTER'S THESIS ASSIGNMENT

I. Personal and study details

Student's name: **Sechi Alessandro** Personal ID number: **491105**

Faculty / Institute: **Faculty of Mechanical Engineering**

Department / Institute: **Department of Process Engineering**

Study program: **Mechanical Engineering**

Branch of study: **Process Engineering**

II. Master's thesis details

Master's thesis title in English:

Production of ceramic aggregates in rotary furnace

Master's thesis title in Czech:

Výroba keramických částic v rotační peci

Guidelines:

Ceramic gravel aggregates are made from clay and slate. The granules are formed from mined clay, and they are expanding in a rotary furnace during heating up to a temperature of 1150°C. The expanded granules are cooled down and are used for civil engineering purposes. Perform analysis of particle movements in the rotary kiln. Focus on the effect of the build-in construction in the furnace on residence time distribution.
1) Perform literature search of processes for the production of gravel aggregates in a rotary kiln.
2) Perform literature search of simulation of the particle movement in rotating geometry.
3) Perform simulation of particle movement in the rotary kiln without inserts and with three newly designed inserts affecting residual time distribution.
4) Compare results with and without inserts and describe the effect of the inserts.
5) Draw blueprints of proposed inserts.

Bibliography / sources:

Perry, R. H., & Green, D. W.: Perry´s Chemical Engineer´s Handbook. Mc Graw Hill, 1999.
Boateng, A. A.: Rotary Kiln, Butterworth-Heinemann 2008. ISBN: 9780128037805.
Liu, X. Y., & Specht, E.: Mean Residence Time and Hold-up of solids in Rotary Kilns. Chemical Engineering Science, 2006.

Name and workplace of master's thesis supervisor:

doc. Ing. Jan Skočilas, Ph.D., Department of Process Engineering, FME

Name and workplace of second master's thesis supervisor or consultant:

Date of master's thesis assignment: **21.04.2021** Deadline for master's thesis submission: **04.06.2021**

Assignment valid until: **19.09.2021**

doc. Ing. Jan Skočilas, Ph.D. Supervisor's signature	prof. Ing. Tomáš Jirout, Ph.D. Head of department's signature	prof. Ing. Michael Valášek, DrSc. Dean's signature

III. Assignment receipt

The student acknowledges that the master's thesis is an individual work. The student must produce his thesis without the assistance of others, with the exception of provided consultations. Within the master's thesis, the author must state the names of consultants and include a list of references.

. _____
Date of assignment receipt

_____
Student's signature

I confirm that the diploma work was disposed by myself and independently, under leading of my thesis supervisor. I stated all sources of the documents and literature.

In Prague …… ……

Alessandro Sechi

Annotation sheet

Name: Alessandro

Surname: Sechi

Title Czech: Výroba keramických částic v rotační peci

Title English: Production of Ceramic aggregates in rotary kiln

Scope of work: number of pages: 93

number of figures: 84

number of tables: 18

number of appendices: 2

Academic year: 2020/2021

Language: English

Department: Mechanical Engineering

Specialization: Process Engineering

Supervisor: Doc. Ing. Jan Skocilas Ph.D.

Reviewer: Doc. Ing. Karel Petera, Ph.D.

Submitter: Alessandro Sechi

Annotation – Czech: Keramického kameniva je vyráběno z jílů a břidlic. Z vytěženého jílu se vytvoří granule, které expandují v rotační peci při teplotě 1150°C. Expandovaný granulát je následně schlazen a používá se pro stavební účely. Proveďte hmotovou a energetickou bilanci stávající rotační pece s cíle popsat celý proces ohřevu, expanze a vypálení granulátu. Zaměřte se na výpočet přestupu tepla v peci a vliv vestaveb pro lepší distribuci tepla ve vsádce. Nalezněte kritická místa ohřevu a expanze materiálu v peci a navrhněte zlepšení stávajícího stavu.

Annotation - English: A ceramic gravel aggregates are made from clay and slate. The granules are formed from mined clay, and they are expanding in rotary furnace during heating up to temperature 1150°C. The expanded granules are cooled down and they are used for civil engineering purposes. Perform analysis of mass and energy balance of rotary furnace with aim to describe whole process of heating, expansion and burn-out of the granules. Focus on the calculation of the heat transfer in the batch and effect of the build-in construction in the furnace on the heat transfer efficiency and better distribution. Find out critical points of material treatment and propose the arrangements which will led to improvement of the actual state.

Keywords: Rotary kiln, CFD, clay, rotary cylinder, particles, mean residence time, analysis, simulations, design, Fluent, DPM, DDPM.

INDEX

1. INTRODUCTION 2

2. THE ROTARY KILN 3

2.1 DIFFERENT TYPES OF KILN 4
2.2 DESIGN ELEMENTS 7
2.3 STRUCTURAL ELEMENTS 8

3. HEAT TRANSFER 10

3.1 FLUID DYNAMICS 13
3.2 TRANSVERSE SOLID BED MOTION 14
3.3 CONTACT HEAT TRANSFER 14
3.4 HEAT TRANSFER BETWEEN THE COVERED WALL AND BULK BED 15
3.5 THE CONVECTIVE HEAT TRANSFER COEFFICIENT IN A ROTARY KILN 16
3.6 THE RADIATIVE HEAT TRANSFER COEFFICIENT IN A ROTARY KILN 16
3.7 HEAT LOSS OF THE OUTER WALL 17

4. MATERIALS 18

4.1 CLAY 18
4.1.1 CLAY FORMATION 19
4.1.2 TYPE OF CLAY 20
4.2 CERAMIC 20

5. EXPANDED CLAY IN THE ROTARY KILN 23

5.1 WHY CLAY AS A LIGHT AGGREGATE 23
5.2 THE PRODUCTION PROCESS OF EXPANDED CLAY 24

6. DESCRIPTION OF THE ANALYZED TASK 25

6.1 EXPLANATION 25
6.2 PARTICLE INTERACTION 25
6.3 MEAN RESIDENCE TIME 30
6.3.1 BOATENG MEAN RESIDENCE TIME 31
6.3.2 SAI RESIDENCE TIME 33
6.3.3 PEARY RESIDENCE TIME 33
6.3.4 BERNARD RESIDENCE TIME 34
6.3.5 LUI RESIDENCE TIME 34
6.3.6 PERRY RESIDENCE TIME 34
6.4 HOW TO ANALYSE MEAN RESIDENCE TIME 35
6.5 CALCULATION OF THEORETICAL MEAN RESIDENCE TIME 38
6.6 REYNOLD NUMBER AND CONFIGURATION OF THE SOFTWARE ANSYS FLUENT 40
6.6.1 CONSTITUTIVE EQUATIONS 41
6.7 METHODS FOR THE SIMULATIONS 42

7. SIMULATIONS OF BASIC GEOMETRIES 44

7.1 CONFIGURATIONS OF MESH 44
7.2 SIMULATIONS OF A SMOOTH CYLINDER TO COMPARE THE METHODS OF SIMULATION 45
7.2.1 DDPM 45
7.2.2 DPM 51
7.2.3 COMPARISON OF THE MODELS FOR A SMOOTH CYLINDER 53

7.3 SIMULATIONS OF DAM, HOOKS, AND MIXERS 57
7.3.1 CYLINDER WITH DAM 57
7.3.2 CYLINDER WITH HOOKS 59
7.3.3 CYLINDER WITH MIXERS 62
7.4 THE FIRST STUDY OF DESIGN 64
8. PROPOSED DESIGNS 70
8.1 PROPOSED GEOMETRIES 70
8.1.1 HOOKED BLADE DESIGN 70
8.1.2 INCLINED MIXERS WITH DAM DESIGN 71
8.1.3 SHOVELS WITH DAM DESIGN 73
8.2 CONFIGURATIONS OF MESH 74
8.3 SIMULATIONS 76
8.4 RESULTS AND COMPARISON 77
8.4.1 RESULTS HOOKED BLADE DESIGN 77
8.4.2 RESULTS INCLINED MIXERS WITH DAM DESIGN 79
8.4.3 RESULTS SHOVELS WITH DAM DESIGN 80
8.5 THE SECOND STUDY OF DESIGN 82
8.5.1 INCLINED MIXERS WITH DAM 82
8.5.2 SHOVELS WITH DAM 84
9. DISCUSSION OF THE FINAL RESULTS 88
10. CONCLUSION 91

FIGURES

FIGURE 1 - TYPES OF ROTARY KILNS [8] 4
FIGURE 2 - ROTARY KILN DIRECT-FIRED TYPE [18] 5
FIGURE 3 - ROTARY KILN INDIRECT-FIRED TYPE [9] 5
FIGURE 4 - ROTARY SMOOTH BARREL 6
FIGURE 5 - ROTARY KILN WITH DAM 6
FIGURE 6 - ROTARY KILN WITH HOOKS 7
FIGURE 7 - ROTARY KILN WITH MIXERS 7
FIGURE 8 - STRUCTURAL ELEMENTS OF ROTARY KILN [9] 9
FIGURE 9 - ROTARY KILN HEAT TRANSFER MEDIA [9] 10
FIGURE 10 - MODELS OF HEAT TRANSFER IN A ROTARY KILN: (A) INTERNAL HEATED; (B) EXTERNALLY HEATED [3] 11
FIGURE 11 - TEMPERATURE AND WATER CONTENT PROFILE OF FEED [1] 12
FIGURE 12 - SCHEMATIC OF THE HEAT TRANSFER IN THE CROSS-SECTION OF INDIRECTLY HEATED ROTARY KILNS [4] 14
FIGURE 13 - QUALITATIVE HEAT TRANSFER FROM A HOT WALL SURFACE TO A SOLID BED [4] 15
FIGURE 14 - MECHANISM OF HEAT TRANSFER BETWEEN THE COVERED WALL AND BULK BED IN A ROTARY KILN [3] 16
FIGURE 15 - RADIATION NETWORK WITHIN THE FREEBOARD OF ROTARY KILN USING ONE-ZONE WALL MODEL [3] 17
FIGURE 16 - CLAY NORMAL COMPOSITION PARAMETERS [5] 19
FIGURE 17 - DRYING PROCESS, HEAT TREATMENT [6] 21
FIGURE 18 - PORE STRUCTURE FOR 1 MM PARTICLES [3] 22
FIGURE 19 - PRODUCTION PROCESS OF EXPANDED CLAY [4] 24
FIGURE 20 - PARTICLE - PARTICLE COLLISION [14] 26
FIGURE 21 - ASSUMPTION FOR THE SPHERE MODEL [14] 27
FIGURE 22 - PARTICLE COLLIDING WITH A WALL [14] 29
FIGURE 23 - EROSION RATE OF ALUMINUM AND HIGH CHROMIUM CAST IRON BY ALUMINA PARTICLES IMPINGING AT 50 M/S [14] 30
FIGURE 24 - MOVEMENT OF THE PARTICLE ON FREUD NUMBER [9] 32
FIGURE 25 - SKEWNESS AND ORTHOGONAL QUALITY SMOOTH CYLINDER 45
FIGURE 26 - FLUENT LAUNCHER DDPM 46
FIGURE 27 - GENERAL SET FLUENT DDPM 46
FIGURE 28 - MULTIPHASE MODEL DDPM 47
FIGURE 29 - ROSIN-RAMMLER DISTRIBUTION 47
FIGURE 30 - INJECTION PROPERTIES DDPM 48
FIGURE 31 - SETTING DISCRETE PHASE DDPM 49
FIGURE 32 - SETTING INLET VELOCITY DDPM 49
FIGURE 33 - MOVING WALL DDPM 50
FIGURE 34 - RUN CALCULATION PROPERTIES 51
FIGURE 35 - GENERAL SET FLUENT DPM 51
FIGURE 36 - SET INJECTION PROPERTIES DPM 52
FIGURE 37 - SET CELL ZONE CONDITIONS DPM 52
FIGURE 38 - DPM SETTING FOR DPM 53
FIGURE 39 - RUN CALCULATION PARAMETERS DPM 53
FIGURE 40 - RESULT SMOOTH CYLINDER DDPM 54
FIGURE 41 - RESULT SMOOTH CYLINDER DPM 54
FIGURE 42 - SKEWNESS AND ORTHOGONAL QUALITY CYLINDER WITH DAM 58
FIGURE 43 - DESIGN CYLINDER WITH DAM 58
FIGURE 44 - RESULT CYLINDER WITH DAM 59
FIGURE 45 - SKEWNESS AND ORTHOGONAL QUALITY CYLINDER WITH HOOKS 60
FIGURE 46 - DESIGN CYLINDER WITH HOOKS 60

FIGURE 47 - RESULT CYLINDER WITH HOOKS 61
FIGURE 48 - SKEWNESS AND ORTHOGONAL QUALITY CYLINDER WITH MIXERS 62
FIGURE 49 - DESIGN CYLINDER WITH MIXERS 62
FIGURE 50 - RESULT CYLINDER WITH MIXERS 63
FIGURE 51 - NORMAL DISTRIBUTION SMOOTH CYLINDER 65
FIGURE 52 - NORMAL DISTRIBUTION CYLINDER WITH DAM 65
FIGURE 53 - NORMAL DISTRIBUTION CYLINDER WITH HOOKS 65
FIGURE 54 - NORMAL DISTRIBUTION CYLINDER WITH MIXERS 66
FIGURE 55 - COMPARISON DIAMETER AND PARTICLE MEAN RESIDENCE TIME FOR SMOOTH CYLINDER 67
FIGURE 56 - COMPARISON DIAMETER AND PARTICLE MEAN RESIDENCE TIME FOR A CYLINDER WITH DAM 67
FIGURE 57 -COMPARISON DIAMETER AND PARTICLE MEAN RESIDENCE TIME FOR A CYLINDER WITH HOOKS 68
FIGURE 58 - COMPARISON DIAMETER AND PARTICLE MEAN RESIDENCE TIME FOR A CYLINDER WITH MIXERS 68
FIGURE 59 – HOOKED BLADE DESIGN 70
FIGURE 60 - DETAILS OF THE HOOKED BLADE DESIGN 71
FIGURE 61 – INCLINED MIXERS WITH DAM DESIGN 71
FIGURE 62 - DETAILS OF THE INCLINED MIXERS WITH DAM DESIGN 72
FIGURE 63 – SHOVELS WITH DAM DESIGN 73
FIGURE 64 - DETAILS OF THE SHOVELS WITH DAM DESIGN 74
FIGURE 65 - SKEWNESS AND ORTHOGONAL QUALITY FOR HOOKED BLADE DESIGN 75
FIGURE 66 - SKEWNESS AND ORTHOGONAL QUALITY FOR INCLINED MIXERS WITH DAM DESIGN 75
FIGURE 67 - SKEWNESS AND ORTHOGONAL QUALITY FOR SHOVEL WITH DAM DESIGN 76
FIGURE 68 - RESULT OF HOOKED BLADE DESIGN 78
FIGURE 69 - COMPARISON DIAMETER AND PARTICLE MEAN RESIDENCE TIME FOR THE HOOKED BLADE DESIGN 78
FIGURE 70 - RESULT INCLINED MIXERS WITH DAM DESIGN 79
FIGURE 71 - COMPARISON DIAMETER AND PARTICLE MEAN RESIDENCE TIME FOR THE INCLINED MIXERS WITH DAM DESIGN 80
FIGURE 72 - RESULT SHOVELS WITH DAM DESIGN 81
FIGURE 73 - COMPARISON DIAMETER AND PARTICLE MEAN RESIDENCE TIME FOR THE SHOVELS WITH DAM DESIGN ... 81
FIGURE 74 – INCLINED MIXERS WITH DAM DESIGN, FIRST CONFIGURATION 83
FIGURE 75 – INCLINED MIXERS WITH DAM DESIGN, SECOND CONFIGURATION 83
FIGURE 76 – INCLINED MIXERS WITH DAM DESIGN, THIRD CONFIGURATION 84
FIGURE 77 – SHOVELS WITH DAM DESIGN, FIRST CONFIGURATION 85
FIGURE 78 – SHOVELS WITH DAM DESIGN, SECOND CONFIGURATION 86
FIGURE 79 – SHOVELS WITH DAM DESIGN, THIRD CONFIGURATION 86
FIGURE 80 - COMPARISON DIAMETER AND PARTICLE MEAN RESIDENCE TIME FOR INCLINED MIXERS WITH DAM DESIGN WITH 20° OF INCLINATION 89
FIGURE 81 - COMPARISON DIAMETER AND PARTICLE MEAN RESIDENCE TIME FOR SHOVELS WITH DAM DESIGN WITH 90° OF INCLINATION 89
FIGURE 82 - FINAL RESULT INCLINED MIXERS WITH DAM DESIGN 20° 90
FIGURE 83 - FINAL RESULT SHOVELS WITH DAM DESIGN 90° 90
FIGURE 84 – DISCUSSION OF DIAMETER AND PARTICLE MEAN RESIDENCE TIME FOR ALL DESIGNS 92

TABLES

TABLE 1 - EARTH COMPOSITION [6] 18
TABLE 2 - RANGES OF FROUDE NUMBER [9] 32
TABLE 3 - SUMMARY MEAN RESIDENCE TIME 35
TABLE 4 - DATA OF THE ANALYZED CASE 39
TABLE 5 - RESULTS OF ANALYTICAL CALCULATIONS 39
TABLE 6 - COMPARISON BETWEEN ANALYTICAL SOLUTIONS AND SIMULATION FOR MEAN RESIDENCE TIME 55
TABLE 7 - CHECKING OF THE SIMULATION TIME 56
TABLE 8 - COMPARISON OF RESULTS FOR MEAN RESIDENCE TIME FOR BASIC GEOMETRIES 64
TABLE 9 - COMPARISON MEAN RESIDENCE TIME CYLINDER WITH DAM BETWEEN SAI RESIDENCE TIME AND SIMULATION 69
TABLE 10 - STATISTICAL RESULTS FOR MEAN RESIDENCE TIME OF HOOKED BLADE DESIGN 77
TABLE 11 - STATISTICAL RESULTS FOR MEAN RESIDENCE TIME OF INCLINED MIXERS WITH DAM 79
TABLE 12 - STATISTICAL RESULTS FOR MEAN RESIDENCE TIME OF SHOVEL WITH DAM 80
TABLE 13 - COMPARISON ANALYTICAL SOLUTIONS FOR MEAN RESIDENCE TIME OF PROPOSED DESIGNS 81
TABLE 14 - COMPARISON ANALYTICAL RESULTS FOR MEAN RESIDENCE TIME OF INCLINED MIXERS WITH DAM DESIGN .. 84
TABLE 15 - COMPARISON ANALYTICAL RESULTS OF MEAN RESIDENCE TIME OF SHOVELS WITH DAM DESIGN 86
TABLE 16 - COMPARISON ANALYTICAL RESULTS FOR MEAN RESIDENCE TIME OF GEOMETRIES AFTER THE SECOND STUDY OF DESIGN 88
TABLE 17 - RESULTS OF MEAN RESIDENCE TIME EXPRESSED IN PERCENTAGE FOR SELECTED DESIGNS 88
TABLE 18 - DISCUSSION OF ALL RESULTS 92

ABSTRACT

The contents of this work are aimed at creating an internal structure for a rotary kiln used to produce expanded clay to increase the average residence time and the mixing process of the particles inside it.

The particles analysed are clay particles with a diameter from 1 mm to 16 mm.

CFD simulations are carried out using the ANSYS 2020 R1 software with student licenses.

After a phase of framing the problem with theoretical explanations of the kiln and the properties of the clay, we move on to the design phase.

The first phase of analysis focuses on framing the best possible simulation methods that can be used.

After this, the work moves on to the simulation of the given geometries to analyse them and be able to understand how the particles behave by changing the internal structure of the kiln.

Subsequently, three different structures were proposed to satisfy the aim of this work of increasing the average residence time and mixing the particles inside the rotating kiln.

1. Introduction

I present the rotary kiln, its industrial application, and the main principles acting on it during this work.

The rotary kiln that we analyse is designed to produce ceramic gravel aggregates from the clay. The product is used for civil engineering purposes. There is a focus on the properties of the clay.

Some basic CFD simulations are performed that help us better understand the interaction between particles of clay and rotating smooth barrel. This is useful to design alternative geometries of the internal structure of the kiln and compare the result of these models with the results obtained from the previous simulations and the analytical solutions.

The software used to perform these simulations is Ansys 2020 R1 with an academic license.

I focus only on the part of the kiln where the solidified ceramic gravel particles are already formed during this work. This part is located at the end of the kiln, which is the outlet section of the particles. The investigated segment of the kiln is approximately 10 meters long.

Due to the complexity of the model, the rarity of the equipment, and the not simple access to the information on it, I assume some approximation and simplification. For example, the last part of the kiln, usually long 10 meters, is assumed equal to 3 meters due to the demand for computation power and its restriction for student academic software license.

Truly complex physical laws dictate the flow of particles in the rotating kiln. To summarize them all, to have an adequate number of variables to consider, various scientific research and experiments carried out in the engineering past have been used.

2. The rotary kiln

The rotary kiln is a cylindrical reactor that, through the inclination and rotation, causes a continuous movement of the load inside it. The rotary kiln is a heat treatment furnace that is used to process solid material; they are treated at extremely high temperatures to cause a chemical reaction and/or a physical change to take place in them and reduce the water content [2].

The most common application today is the production of cement clinker. However, other applications are used, and they are organic combustion, thermal desorption, calcination, heat setting, and thermal desorption.

The rotary kiln has been developed for use in the cement industry. Today, thanks to their flexibility, they are used in various types of industry. They are used to convert raw material into cement clinker and other key components for the cement industry. [2]

The typical application of the rotary kiln is to heat the solids to the point where a chemical reaction takes place. Its function is to maintain the material temperature at a high temperature for a specific period. To determine the optimal processing temperature of an element and retention times, chemical and thermal analyses of the material are performed. In practical use, the kiln load, in order not to compromise the heat transfer, must never exceed 13% of the volume [2].

The rotary kiln is composed of a rotating cylinder, called a drum, which is sized based on the data collected to ensure that it can meet the material's time and temperature requirements concerning demanded production. These kilns are always installed with an inclination in such a way as to allow the effect of gravity in the treated material and therefore allow its movement within the cylinder [2].

2.1 Different types of kiln

We can find different designs regarding the rotary kiln configuration, and they can be easily expressed in figure 1:

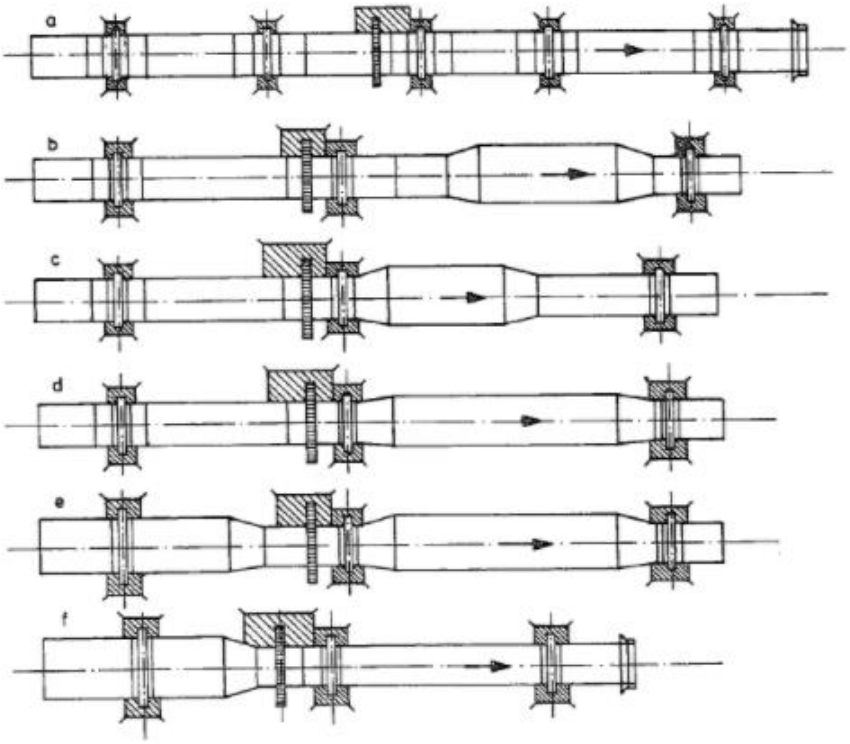

FIGURE 1 - types of rotary kilns [8]

From top to bottom, we find the following types of kiln, straight rotary kiln, rotary kiln with enlargement in the combustion area, rotary kiln with expansion in the calcination area, rotary kiln with expansion in the calcination and combustion area, rotary kiln with enlargement in the drying, calcination and combustion zone and rotary kiln with enlargement in the drying zone or the preheating zone [8].

The flow direction of the treated material is from left to right. The parts of the kilns are preheating zone, drying zone, calcination zone, and combustion zone.

The purpose of enlarging the diameter of a zone is to increase the resistance time of the material within a predefined zone; in parallel to this, a decrease in the speed of gases is also obtained, allowing a better heat transfer from the gas to the material present in the kiln. This modification, however, has not only positive aspects but also causes a passage of the material with irregular times, which compromises the correct functioning of the kiln. At the transition points between large and small diameters, a phenomenon called stowage occurs; it causes abrasion and dust [8].

The research carried out, and the theoretical deliberations affirm that the rotating kiln without size changes represents the most valuable construction.

There are two main categories of the rotary kiln regarding the combustion process, the one direct-fired and the other one with indirect-fired.

In a direct combustion kiln, as shown in figure 2, the combustion takes place directly in the drum, and the material is processed in direct contact with the fumes produced by combustion. Usually, the production of expanded clay is performed using this type of combustion process. This type of kilns can be counter-current or co-current; usually, the most used configuration is the counter-current one because it is more efficient. There is also no problem feeding the kiln by raw material – construction and material demand for high temperatures.

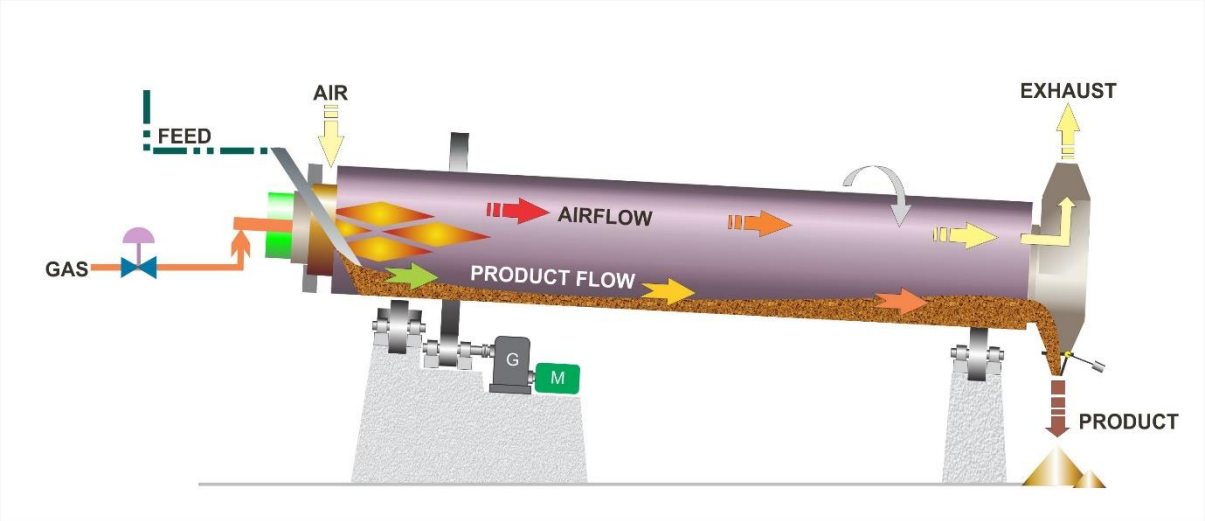

FIGURE 2 - rotary kiln direct-fired type [18]

Inside the indirect-fired kiln, as shown in figure 3, the combustion occurs in a chamber adjacent to the cylinder itself; for this reason, the material undergoes heating through contact with the shell of the furnace, which, as said above, is heated from the outside.

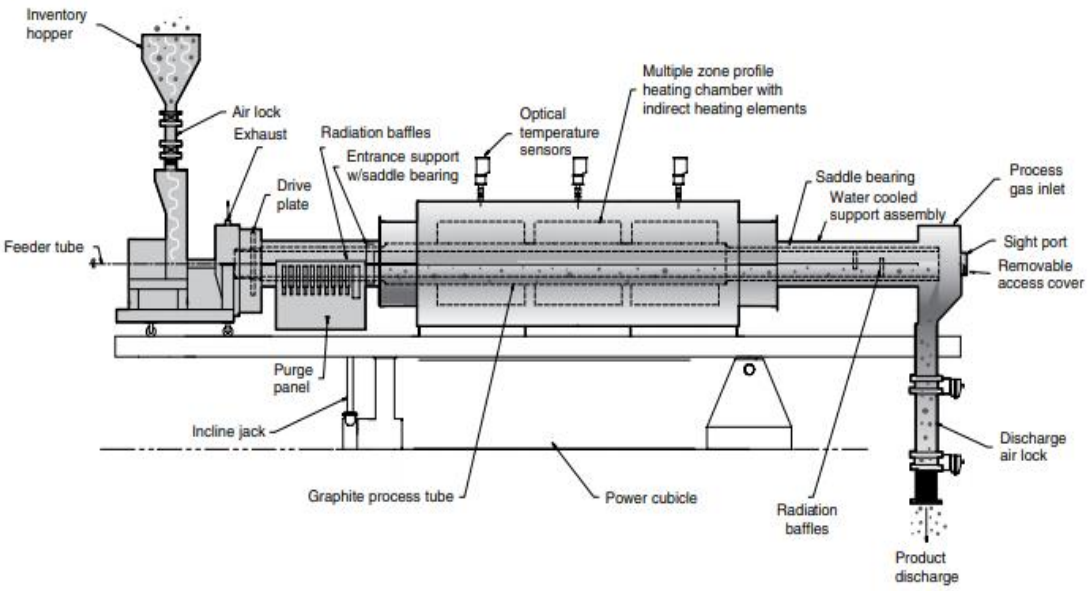

FIGURE 3 - rotary kiln indirect-fired type [9]

The heat required by the real physical and chemical processes that take place inside the kiln is provided by the material that is lifted and turned upside down as it moves.

Historically, the rotary kiln is related to the production of cement for civil engineering purposes; the increase of the production capacity of a large quantity of cement has depended on the evolution that the rotary kiln has undergone over the years. The first proposal for a rotary kiln defined as above is 1865, but it was considered with success only in 1895.

We can also have different types of classifications regarding the internal structure of the kiln, mainly we find four different types of configurations, and they are:

1) Rotary smooth barrel: it is the most common type and the less efficient; inside it, we do not find any insert but just a simple smooth barrel.

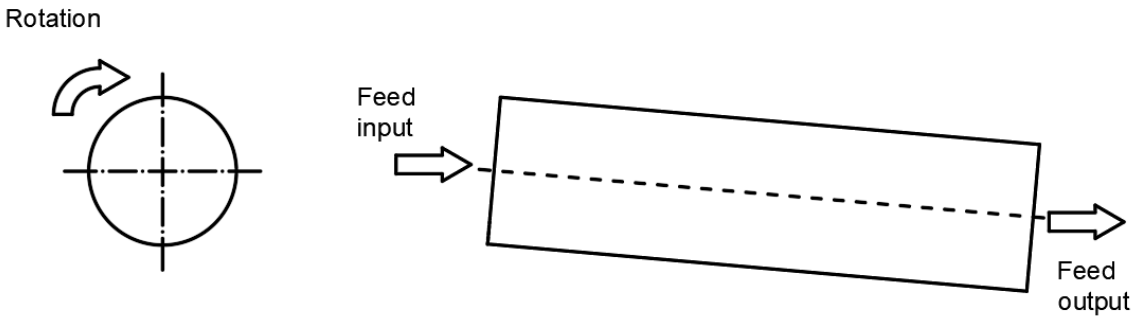

FIGURE 4 - rotary smooth barrel

2) Rotary kiln with Dam: an insert is installed inside that assumes the same functions as a water dam, namely those stopping the flow, making it accumulate and release after this phase. The primary purpose of this element is to increase the residence time of the material inside the furnace; by changing the height of the dam, we also change the level that the material must reach to advance to the next insert. The disadvantage of this geometry is that it cannot mix the flow and exposes the material to the effect of the hot gases.

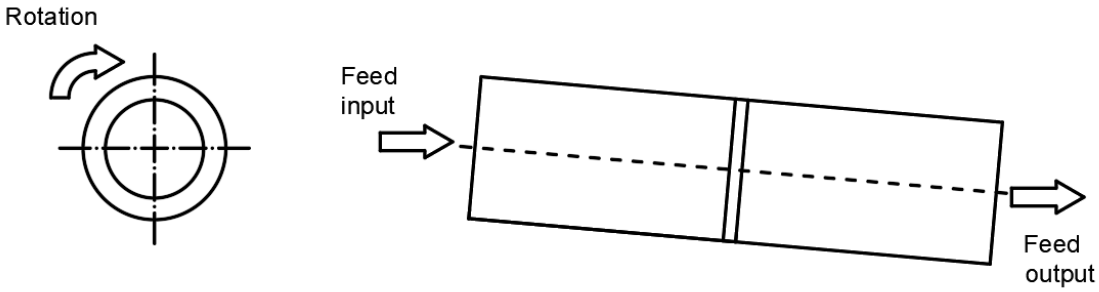

FIGURE 5 - rotary kiln with dam

3) Rotary kiln with hooks: inside the kiln, in this case, we find a structure that takes the form of many repeated hooks. They have the function of taking the material from the bottom and lifting it; in this case, the driving force is used. These hooks have the function of increasing the heat exchange by convection as they expose the time of the material.

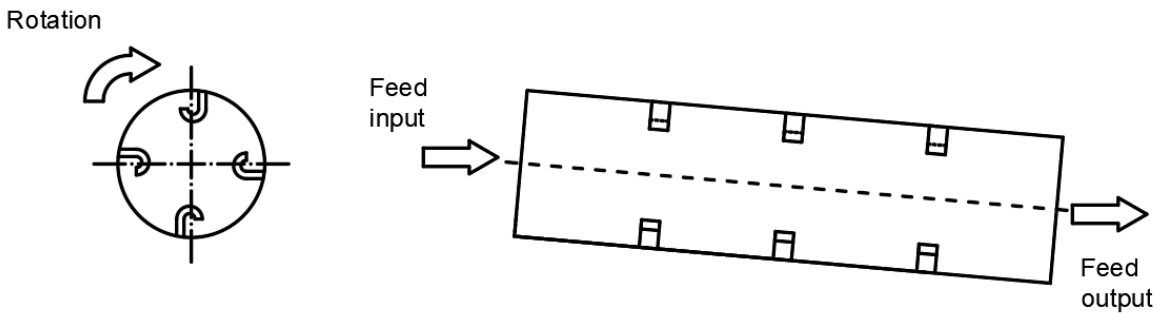

FIGURE 6 - rotary kiln with hooks

4) Rotary kiln with mixers: it is a geometry present inside the cylinder that allows creating a better mixing for the flow of material, thus allowing a more homogeneous exposure of the material to the hot air flow; thanks to this work, it increases efficiency.

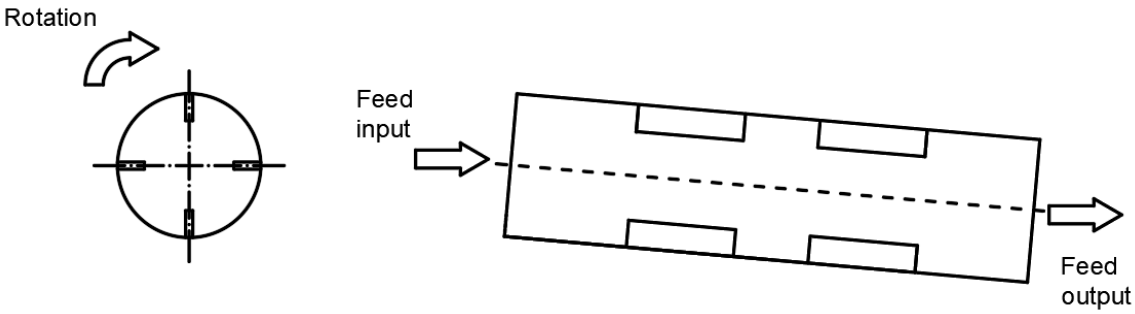

FIGURE 7 - rotary kiln with mixers

2.2 Design elements

A hollow coated cylinder forms the rotary kiln, it is mounted inclined on rollers and is rotated slowly by drivers. The material being processed undergoes a displacement from the feed end to the discharge of the cylinder. They must have a very resistant structure; they must rotate under their axis while maintaining a fixed input and output point. Usually the inclination of the kiln is between 2° and 6° concerning the horizontal axis, while the rotation of the kiln can vary between 2 rpm and 9 rpm [8].

There are no specific rules for establishing the inclination of the kiln. Initially, rotary kilns used higher slopes, compensating for this with lower rotational speeds. By increasing the rotation speed, we better mix the feed, combined with more intensive heat exchange. It's necessary to find optimal revolution for the kiln representing efficient mixing of the rotary drive's treated material and energy consumption [8].

In practical use, the kiln load, not compromising the heat transfer, must never exceed 13%.

It is essential to have good insulation of the kiln, it reaches a temperature up to 1500°C; for this reason, the construction materials are not subject only to weight and rotating stresses but also to the action of high temperatures. There are two main methods of doing a good coating; the first one, the castable way, uses dough material as the internal lining of the kiln; thanks to this method, we can superimpose different layers of different

materials. The second is called the brick model, and in this method, permanent bricks are fixed inside the kiln [9].

2.3 Structural elements

The kiln is made up of different types of components, which we describe better below and shown in figure 8.

- Oven shell: the shell of the oven has a cylindrical shape at the end but can also have tapered sections. It undergoes a twisting due to the stresses generated by the weight. Generally, due to the partial filling and tip support, the shell is deformed to an oval shape. Indirect heating kiln, having to withstand higher temperatures, are made with specific alloys that are more heat resistant [20].
- Drive group: Thanks to this, we have the rotation of the kiln. The system consists of a chain and pinion drive, direct drive assembly, and friction drive. The selection of one type of unit over another is dictated only by the required power [20].
- Guide rings: these have the task of providing a surface for the distribution of the furnace load. The riding moves relative to the shell when it is rotating. The correct sizing of the ring is essential [20].
- Push rollers: have the function of preventing the drum from moving horizontally by pushing against the guide rings. They allow smooth and concentric rotation during operation. They act as worn piece as they are easier to replace and less expensive than the guide ring. Two rotation rollers per guide ring, keyed on the pins, rotate in bearings with pressure flow or immersion lubrication [20].
- Oven discharge head: the first use is to allow products to leave the kiln, the second use is to permit a counter-current system.
- Inlet head of the furnace: the inlet head of the furnace has an exhaust gas system whose size varies whether there is a direct flame. In this apparatus, the exhaust gases leave the system and are purified before being released into the environment or sent to the waste boiler [20].
- Refracts of the oven: it has the purpose of insulating and therefore protecting from high temperatures and minimizing heat loss. The thickness, physical properties, and chemical composition of the refractory are decided based on the process to be performed. In some applications, monolithic refractories are used.
- Burner: it provides the energy required by the process. Typically, the burner is mounted on the exhaust head. They must be able to accommodate different types of fuels such as gaseous, liquid, or solid [20].
- Feeding of the raw material: it is the point where the raw material enters the kiln. This is usually accomplished by using a slide made from a more heat-resistant material. Attention should be paid to the design of this part as no build-up of material should occur.
- Sealing: helps prevent system process gas escaping and air escaping. It is important to be able to keep the temperature constant for the desired chemical reaction to occur. It is therefore important to choose the right type of gasket [20].

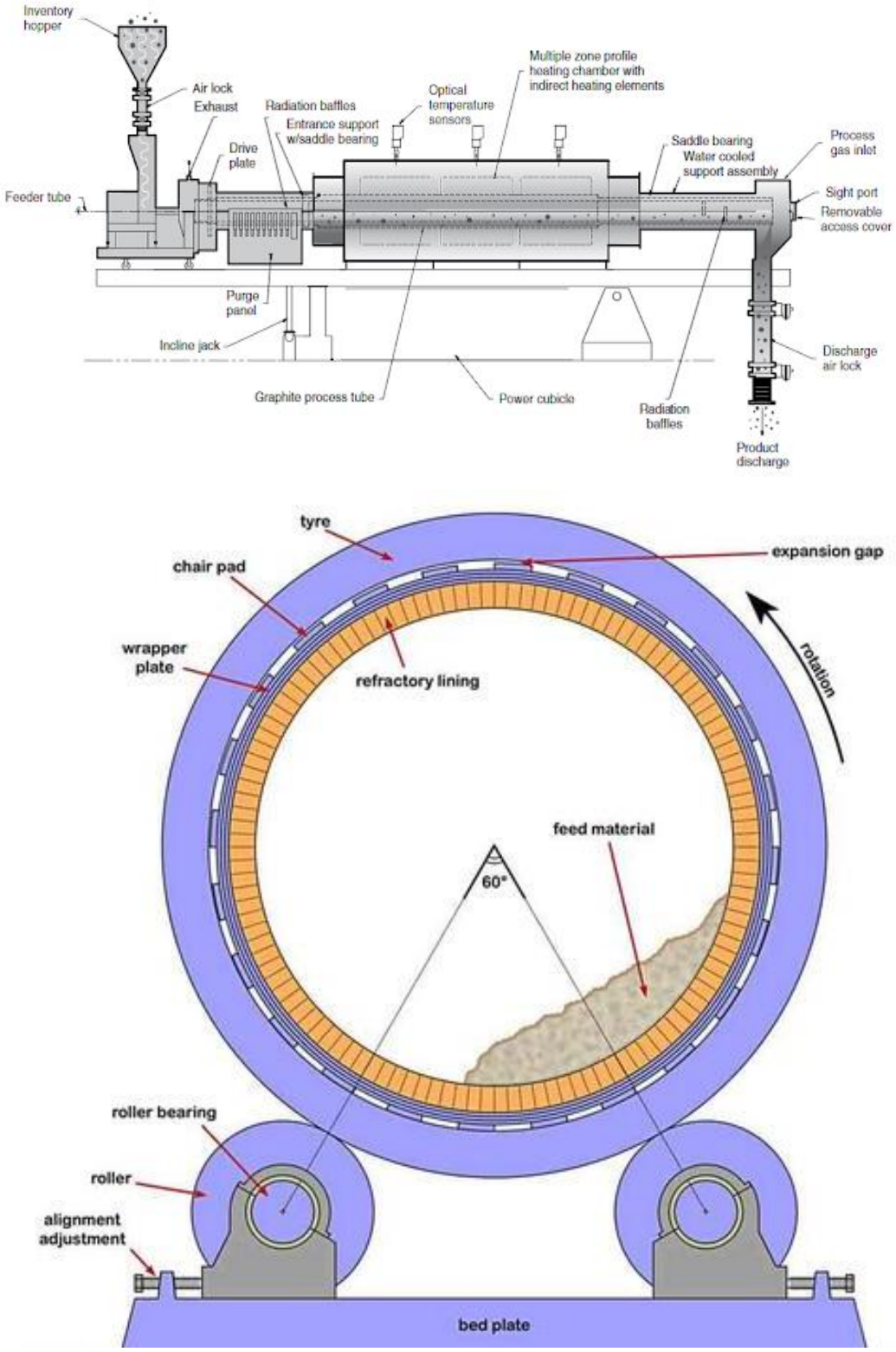

FIGURE 8 - structural elements of rotary kiln [9]

3. Heat transfer

As in most natural phenomena, even in the rotary kiln, we have the presence of all three phenomena of heat exchange. However, they do not have the same impact on the amount of heat transferred. To have a simpler model, we can simplify some of them, and this depends on the characteristics of the kiln and which properties are being studied in it. If, for example, the kiln has some hooks or mixers in its internal structure, we can assume that the temperature of the feed bed is constant due to the constant interruption of the feed flow [9].

The heat exchange in the gas-solid flow involves a complex coupling between mechanical flow and thermal behaviour. A variety of techniques have been developed in the literature to solve this problem [5].

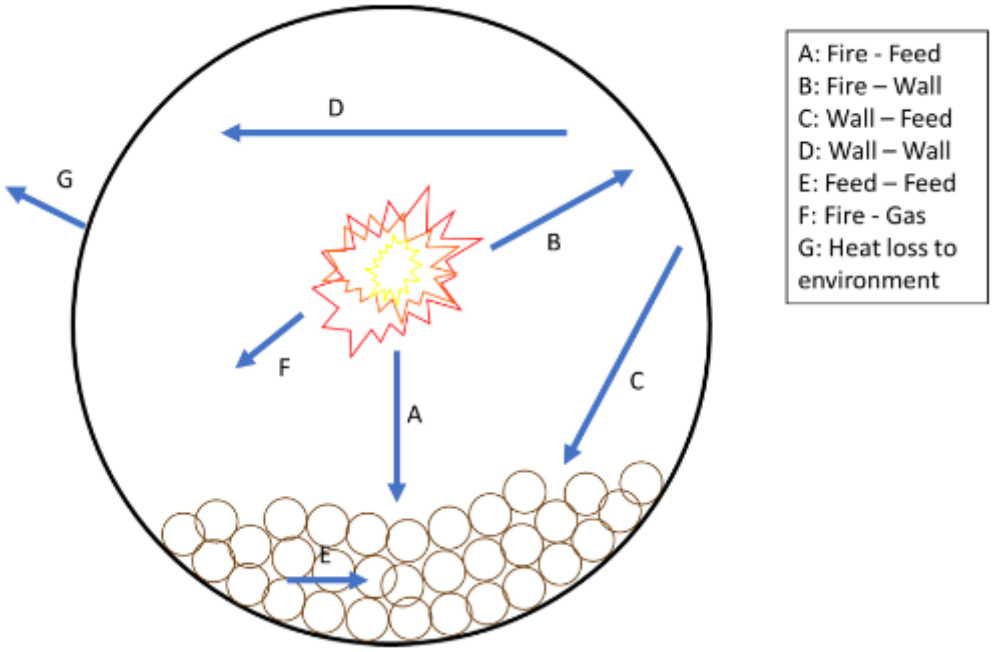

FIGURE 9 - rotary kiln heat transfer media [9]

Figure 9 is a representation of the interaction of the bodies within the kiln. Conduction, convection, and radiation may occur between them; as mentioned previously, however, there may be cases in which some of them are weak and therefore can be omitted. Usually, in rotary kilns, the most dominant type of heat transfer is that of convection. If close to the flame in a direct flame kiln, the radiation phenomenon becomes more important [9].

The slow rotation of an inclined kiln allows the correct mixing of the material during its transport from inlet to outlet. A flexible adjustment of the residence time can produce optimal conditions for perfect thermal destruction of the waste particles [3].

In the design of the model of a rotary kiln, four different important aspects can be considered from the point of view of process engineering: heat exchange, the flow of materials through the rotary kiln, gas-solid mass exchange, and kinetic reaction [3].

Comparing the rotary kiln with the other gas-solid reactors, the heat exchange inside the rotary kiln also includes:

- Coefficients of heat exchange between the gas and the rotating wall and between the gas and the surface of the rotating bed are affected by the drum rotation.
- The inlet part of the wall is in contact with high gas temperatures and certain intervals with the bulk bed; thus, the heat absorbed from the high temperatures of the gas is delivered indirectly to the bed [8].
- Radiation heat exchange cannot be ignored in an environment with relatively high temperatures, significantly when temperatures exceed 1000°C.

This type of heating takes place using coal, gas, or oils directly. The high-temperature gases are directly inserted inside the cylinder with two possible designs, one co-current and the other counter-current for the flow of particles.

The heat exchange inside a rotary kiln takes place through these five mechanisms:

$\boldsymbol{Q_{wc-cb}}$: heat exchange between the covered wall and the low covered bed [3].
$\boldsymbol{Q_{g-ew}}$: the heat exchange between the exposed wall and the free gases includes both the exchange by convection and the exchange by radiation [3].

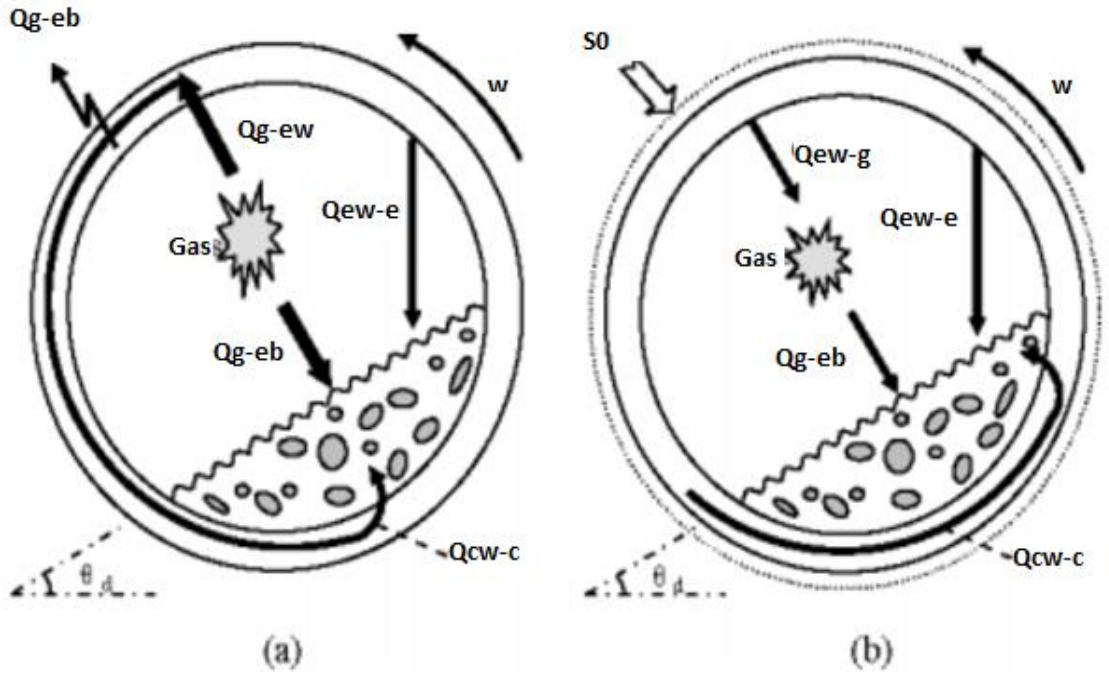

FIGURE 10 - models of heat transfer in a rotary kiln: (a) internal heated; (b) externally heated [3]

$\boldsymbol{Q_{g-eb}}$: the heat exchange between the exposed upper bed and the free gases [3].
$\boldsymbol{Q_{ew-eb}}$: the heat exchange between the exposed bed and the exposed wall [3].
$\boldsymbol{Q_{sh}}$: the lost heat of the wall for heating inside the rotary kiln, or $\boldsymbol{S_0}$, External heat sources for heat external to the rotary kiln.

The phenomena of heat exchange inside the rotary kiln are very complex and therefore require great attention. Thanks to the granular power supply, spaces filled with gas are

created inside the oven, allowing phenomena such as radiation and convection. Conduction is another important phenomenon of heat exchange. It occurs between the wall and the supplied bed due to the rotation of the wall. At a given moment, it is subject to radiation and convection of the fire and fumes produced. In practice, the same point receives and transmits heat at different times [3].

It is possible to divide the kiln into three main sections, and this division is based on the different supply temperatures. We can also divide the percentage of water present in the feed.

The presence and length of each of the sections depending on the working conditions of the furnace and treated material, and we can show here some examples:

- Initial temperature and humidity of the power supply
- Dimension of the kiln
- Location, source, and intensity of heat
- The internal construction of the kiln, dams, hooks, mixers, or smooth kiln.

As for water present and the supply temperature, we can divide the kiln into three different sections, which are:

1) Heating
2) Drying
3) Burning

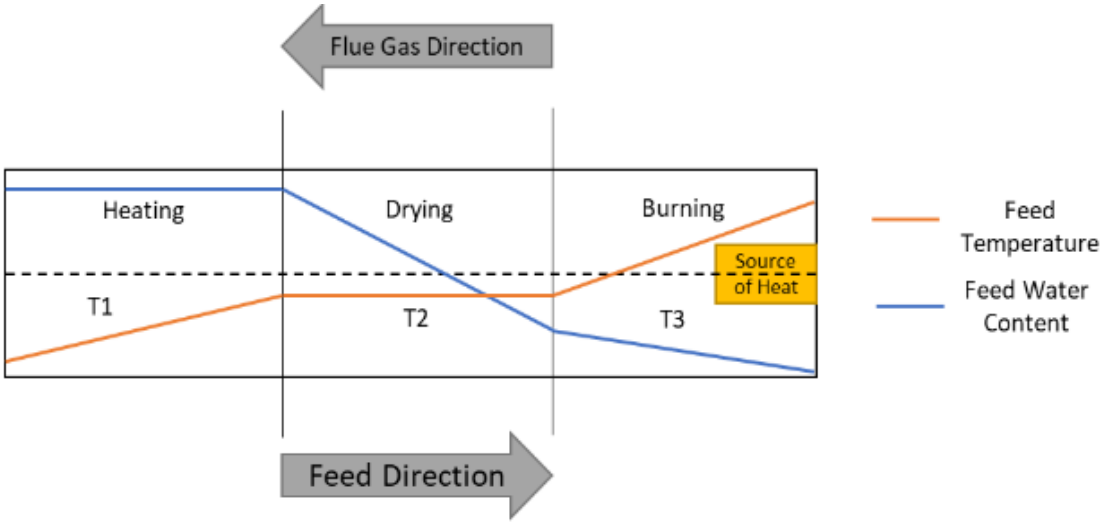

FIGURE 11 - temperature and water content profile of feed [1]

Heating: this section beings at the suction of the feed. If the kiln is in a counter-current configuration, we note that the colder fumes are in contact with the colder feed. Within the section, you want to increase the temperature of the supply until it reaches the evaporation point of the water present in the material. For this reason, the delta temperature of the power supply inside the piece of the kiln can be easily calculated; we know that the final temperature in this zone to be reached is that of 100°C, knowing the ambient temperature at which our load is introduced we can establish how much delta T we have. To not have a too large heating section, we tend to increase the inlet

temperature of the power supply to reach a lower delta T and therefore need less space [8].

Drying: in this phase, the evaporation of the water takes place for this reason. The temperature of the material surface remains constant, around 100°C. Usually, to optimize this section, hooks are used which lift the feed particles, bringing them to the highest point and, by doing this, increase the contact time with the hot gas and the relative velocity of the particles concerning the hot gases [8].

Combustion: chemical reactions usually take place in this section. In this section, the highest temperatures of the entire process are reached, from about 100°C, which we find in the drying phase, to 1000/1500°C depending on the application that we run and from the present process. We must be careful what type of internal construction we use because due to the high temperatures reached, a few materials can maintain their strength and resistance unaltered. To optimize this phase, it is important to insulate the system well to reduce heat loss. In this phase, 90% of the heat exchange occurs by radiation, 9% by convection, and only 1% by conduction. [8]

3.1 Fluid dynamics

Anderson and Jackson (1967) formulated the continuity equation representing the momentum from Navier-Stokes's point of view and the continuity equation using the concept of local mean variables.

The continuity equation is expressed as:

$$\frac{\boldsymbol{\delta(\varepsilon\rho_g)}}{\boldsymbol{\delta t}} + \boldsymbol{(\nabla * \varepsilon\rho_g u)} = \mathbf{0} \qquad \textit{Equation 1}$$

The equation for the momentum is expressed as:

$$\frac{\boldsymbol{\delta(\varepsilon\rho_g u)}}{\boldsymbol{\delta t}} + \left(\nabla * \varepsilon\rho_g \boldsymbol{uu}\right) = -\boldsymbol{\varepsilon}\nabla \mathbf{p} - \boldsymbol{\Sigma}(\varepsilon \mathbf{F_d}) - \nabla * \varepsilon\boldsymbol{\tau}_\mathbf{g} + \varepsilon\rho_\mathbf{g}\boldsymbol{g} \qquad \textit{Equation 2}$$

Where $\boldsymbol{\Sigma(\varepsilon F_d)}$ expresses the sum of the drag force for all particles per unit volume. The transport equations are solved using a semi-implicit scheme in which rectangular staggered grids are employed. To cover the kiln, a square area that bounds the circle is mapped. First, an equidistant grid divides the domain into cells of width three times the particle diameter is used. Then, some lines are added around the sides of the square to make the kiln boundary does not cross any side of the control volume, where the kiln boundary only crosses the corner of the corresponding control volumes. The pressure, void fraction, and temperature are defined at the centre of each control volume. The circular kiln boundary is approximated as lines that connect the corners of related control volumes [5].

3.2 Transverse solid bed motion

The fill state is defined by the ratio of the solid area in the cross-section and the total cross-section of the rotating cylinder. The filling angle can be expressed in terms of angular filling ϒ and the height of the solid bed h with:

$$F = \frac{A_{solidbed}}{A_{drum}} = \gamma - sin\gamma * \frac{cos\gamma}{\pi} \qquad \textit{Equation 3}$$

With: γ = arcos(1 - $\frac{h}{R}$)

The movement of the solid bed in the rotating cylinder is rotary. This movement is characterized by the division of the bed into an active layer and a passive layer in the lower part of the bed surface [4].

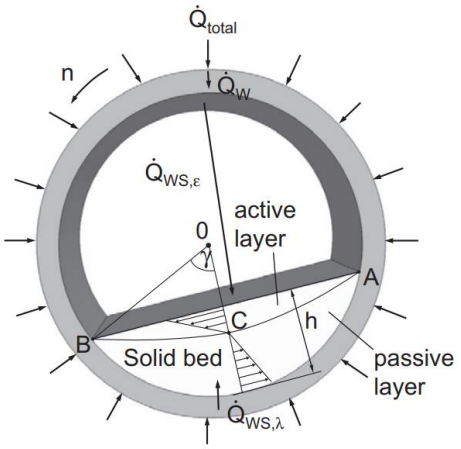

FIGURE 12 - schematic of the heat transfer in the cross-section of indirectly heated rotary kilns [4]

3.3 Contact heat transfer

The contact coefficient of the heat exchange is composed of a series of connections of the contact resistance between the wall and the particles $\alpha_{ws,contact}$ and the coefficient of penetration inside the solid bed $\alpha_{s,penetration}$.

$$\alpha_{ws\lambda} = \frac{1}{\frac{1}{\alpha_{ws,contact}} + \left(\frac{1}{\alpha_{s,penetration}}\right)} \qquad \textit{Equation 4}$$

A high-temperature gradient between the wall and the first layer of particles occurs close to the wall from the contact resistance. By replacing the thermo-physical properties of the particles with the actual properties of the bulk bed, the bed can be classified as nearly continuous. Assuming a constant wall temperature, we can obtain the penetration coefficient from the Fourier differential equation as:

$$\alpha_{s,penetration} = 2 * \sqrt{\frac{\rho_s * c_{ps} * \lambda_s}{\pi * t_{contact}}} \qquad \textit{Equation 5}$$

Where the contact time depends on the degree of filling and the speed of rotation, it was shown that, for small contact times, the heat transfer coefficient was sought at a finite value and the contact time by the contact coefficient of the heat exchange [4].

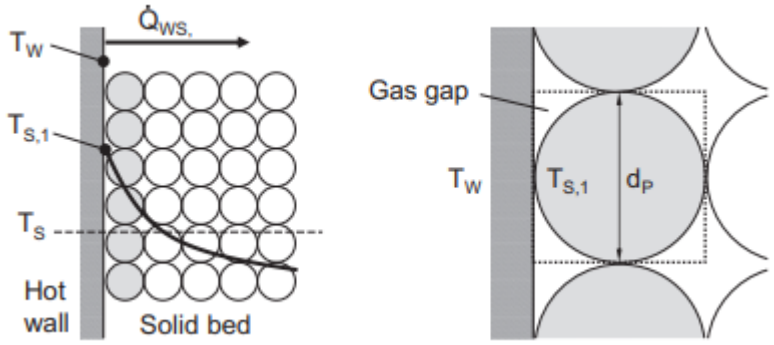

FIGURE 13 - qualitative heat transfer from a hot wall surface to a solid bed [4]

3.4 Heat transfer between the covered wall and bulk bed

The heat transfer coefficient between the covered wall and the bulk bed does not include only the heat exchange of the bed surface with the solid bulk but also the wall surface and the bed surface. To better evaluate the term $\boldsymbol{h_{wb}}$, Schlunder assumed that there is a thin layer of gas film at the contact point of the particles and the slipper wall. Using the theory of penetration into the rotary kiln reactor, he assumes that the wall temperature and the bulk temperature at the contact point are equal. Lehmberg postulated that there is a small space between the wall and the bed, and the temperature jumps in this space [3].

Three aspects mainly control the Heat exchange of the covered wall and the bulk bed, and they are:

1) $\frac{1}{h_{wb}}$: the contact resistance caused by $\boldsymbol{g_{ilm}}$ gases between the covered wall and the bed surface [3].
2) $\frac{2}{h_b^{ad}}$: the thermal resistance gave the unstable state of the conductive heat exchange from the surface of the bed to the bulk bed in which the temperature is reduced from $\boldsymbol{t_b}$(0) to $\boldsymbol{t_b}$(infinite) [3].
3) $\frac{1}{h_b^{ad}}$: the thermal resistance is given by the advection of the heat exchange with the solid bulk [3].

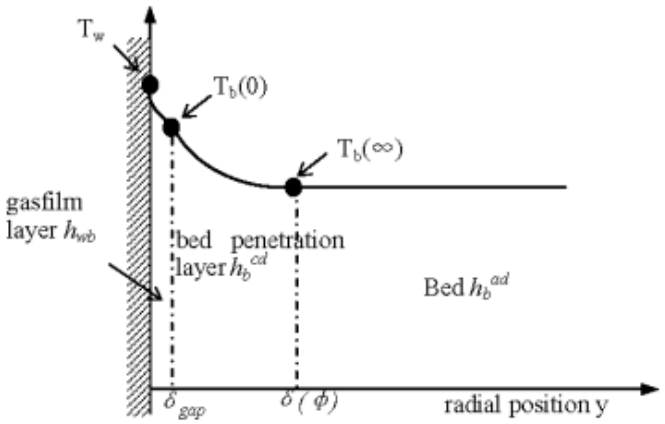

FIGURE 14 - mechanism of heat transfer between the covered wall and bulk bed in a rotary kiln [3]

3.5 The convective heat transfer coefficient in a rotary kiln

Convective heat transfer includes two main aspects: the heat exchange between the gas freeboards and the exposed wall and the heat exchange between the gas freeboards and the other surface of the bed.

The classical equations that we usually use for turbulent convection in a non-rotating kiln are not valid for the rotating kiln.

The regression analysis of experimental data takes the following dimensionless form [13]:

$$\boldsymbol{Nu_{gew} = \frac{h_{gew}^{c} D_e}{k_g} = 1.54 Re_g^{0.575} Re_w^{-0.292}} \qquad \textit{Equation 6}$$

$$\boldsymbol{Nu_{geb} = \frac{h_{geb} D_e}{k_g} = 0.46 Re_g^{0.535} Re_w^{0.104} \eta^{-0.341}} \qquad \textit{Equation 7}$$

Where the Reynolds number is expressed as $\boldsymbol{Re_g = V_g D_e / v}$.

The rotational Reynolds number as $\boldsymbol{Re_w = D_e^2 \frac{w}{v}}$, the filling percentage is η, the equivalent diameter *De*.

The equivalent diameter is a function of the solid's fill percentage. These equations are valid if 1600<$\boldsymbol{Re_g}$< 7800 and 10 < $\boldsymbol{Re_w}$ < 800.

3.6 The radiative heat transfer coefficient in a rotary kiln

These heat exchanges are influenced by the characteristic emissivity and temperature distribution of the freeboard gas inside the wall and bed surface. In general, the radiation heat transfer is not considered for temperatures below 400°C; however, it becomes comparable with the convective heat exchange for temperatures between 700°C and 900°C, it assumes a dominant aspect instead when the temperatures exceed 1000°C [3].

The radiation conditions can be simplified, and we assume the following approximations:

- The surface of the wall and the bed are taken as grey surfaces because the emission spectrum of the solid and the wall are not known.
- The inlet and outlet of the cylinder are considered adiabatic.
- The gas is taken as grey radiation, also because it contains $\boldsymbol{CO_2}$ and $\boldsymbol{H_2O}$ which emit and absorb radiations on different frequencies.
- The material is sufficiently mixed.
- The effect of the axial temperature gradient is solid, in the wall and the gas freeboard is negligible.
- There are no flames or fires inside the rotating kiln.

The electrical analogy of the resistor is shown in the figure below:

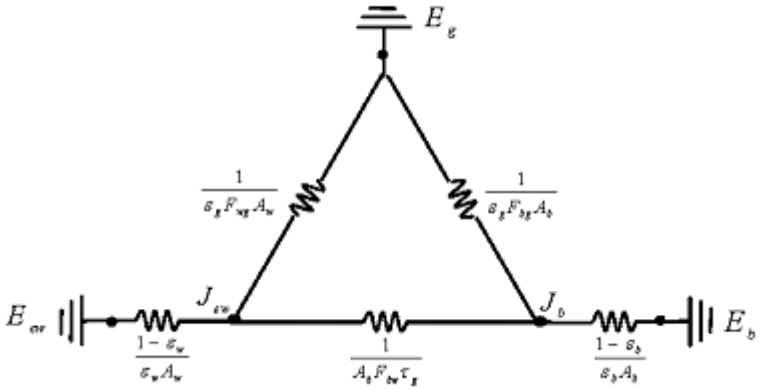

FIGURE 15 - radiation network within the freeboard of rotary kiln using one-zone wall model [3]

3.7 Heat loss of the outer wall

The heat lost in the inlet wall to the exhaust environment includes different heat transfer processes.

The conduction resistance between the entrance and the exit ($\frac{\mathbf{1}}{\boldsymbol{h_{xsh}^{cd}}}$), the convection resistance between the exit wall and the environment ($\frac{\mathbf{1}}{\boldsymbol{h_{sha}^{c}}}$) and the radioactive resistance ($\frac{\mathbf{1}}{\boldsymbol{h_{sha}^{r}}}$). So, the total resistance can be expressed as neglecting the curvature of the surface [4]:

$$\frac{\mathbf{1}}{\boldsymbol{h_{wa}}} = \frac{\mathbf{1}}{\boldsymbol{h_{wsh}^{cd}}} + \frac{\mathbf{1}}{\boldsymbol{h_{sha}^{r}}} + \frac{\mathbf{1}}{\boldsymbol{h_{sha}^{c}}} \qquad \textit{Equation 8}$$

4. Materials

Clay is the raw material that the rotary kiln that we describe in this work use.

Mineral in the form of rocks can be classified into three main groups: igneous or magmatic, sedimentary, and metamorphic.

- Magmatic rocks: they are formed following the solidification of magmas. They make up approximately 65% of the top of the earth's crust. These rocks have no organic material inside them [6].
- Sedimentary rocks: These rocks are formed because of erosion caused by water or wind, which causes a deposit of material. This process tends to generate a relative deposit because the particles tend to subdivide about their density, shape, and size [6].
- Metamorphic rocks: are formed within the earth's crust because of mineralogical and structural transformations such as exposure to water and pH. These elements change the composition of the rocks [6].

The composition of the earth can be summarized in the following table:

TABLE 1 - earth composition [6]

Element	Mass%	Volume%	Density
Oxygen	47	92	0,00143
Silicon	28	0,8	2,33
Aluminum	8	0,8	2,7
Iron	5	0,7	7,87
Calcium	4	1,5	1,55
Sodium	3	1,6	0,97
Potassium	3	2,1	0,86
Magnesium	2	0,6	1,74
Titanium	1	0,2	4,5

4.1 Clay

Clay is a term that defines extremely fine sediment, consisting mainly of hydrated aluminosilicates belonging to the class of filo silicates. The formation of clays as loose clastic sediments, such as soils, occurs through the washing away of rocks containing clayey minerals, with the concentration of fine sediment, following a long transport mainly in water, il lake, marine, lagoon environments. The minerals that made up the clay are all belonging to the category of clay minerals. The clay minerals have peculiar physicochemical characteristics, such as the micrometric size of the crystals that involve considerable capacity for water absorption, ion exchange, and cation fixation. These characteristics give the clayey sediment sensitive plasticity when mixed with water and

refractoriness if dehydrated, properties that have allowed the development of the brick and ceramic industry [5].

The composition, properties, and characteristics of the clay may vary due to its formation. It is formed through components that are deposited as a result of a natural erosion phenomenon; these components are subsequently transformed into clay through chemical processes generated by pressure and/or temperature [6].

For this reason, we can have a wide range of types of clay, and for this reason, it cannot be seen as a single component but as a group of components [6]

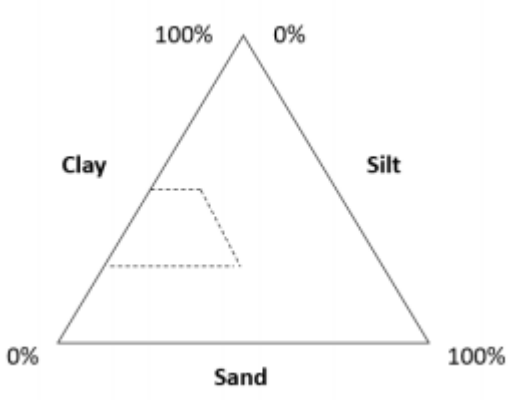

FIGURE 16 - clay normal composition parameters [5]

We can divide the clay into too big categories, and they are:

- Light clay: composed of 40 to 60 wt. % of the sand [5].
- Weight clay: composed of less than 40 wt. % of sand [5].

4.1.1 Clay formation

Clay, as mentioned above, is formed from the natural phenomenon of erosion of sedimentary and igneous rocks and the composition of all climatic factors, vegetation, types of rocks, and topography of the soil [6].

We can have two main types of erosion, mechanical and chemical.

- Mechanical erosion: it is a process that is obtained from the result of different stresses that are generated by:
    - Thermal erosion: we find a temperature difference within the areas of the deposited material; for this reason, a thermal expansion occurs. Due to this expansion and the lack of space to move, our rocks crack, water is added to the inside of these cracks, which, freezing, enlarges the size of these cracks even more [6].
    - Erosion due to wind and water: this type of erosion is created by the interaction between the solid phase and the fluid phase; this interaction generates friction. With the presence of sand, granules of other particles that may be present in the fluid, we have an increase in this friction [6].

    - Vegetation erosion: this type of erosion is generated by the weight of the vegetation in the area and by the roots in the soil [6].
    - Ice erosion: erosion generated by sheets of ice that move on a surface such as that of a valley.
- Chemical erosion: for this process to take place, the presence of water is essential. This type of erosion is a complex process in which concentration gradients play a fundamental role [6].
  Other aspects that greatly influence this type of erosion are the acidity and alkalinity of the solutions and crystalline structures.
  We can divide chemical erosion according to the type of solution present in it:
  1) Hydrolysis: occurs in the presence of water with pH = 7
  2) Acidolysis: occurs in the presence of water and acid, pH<7
  3) Alkalinolysis: water and acid, pH > 7
  4) Salinolydid: occurs in the presence of a saline solution with pH = 7

  In general, we can describe the chemical erosion process through this formula:

  Primary minerals + supplied solution = secondary minerals + drained solution

4.1.2 Type of clay

There are several ways to classify clay, based on the size of its particles, based on the colour it presents, its composition, based on its period and place of formation.

In the world, we have different types of clay, the main ones are [5]:

- Ball clay: this type has a high carbohydrate content; it is created in a deposit of water.
- Stoneware clay: this type is a cross between ball clay and refractory clay; as such it has mixed properties between the two types; it is a rare type of clay to find.
- Fire clay: this type has a wide spectrum of colours, has a high amount of metal oxides and quartz. It was formed by transport and wind erosion.
- Chinese clay: this type does not undergo erosion; it is found in the same formation point. It comes in white colour. Its main use is to produce porcelain objects
- Kaolin: this type is very plastic because it has a small particle size, the colour is yellowish.

4.2 Ceramic

We know synthetic ceramics as non-clayey ceramics. They are used when the natural components are not found in nature or if the material's properties do not occur in nature.

There are three main processes of ceramic heat treatment; in the drying phase, it is necessary to ensure that the relative temperature is high, there is a flow rate, and the operation is performed in an environment with low moisture content [6].

During this phase, the drying phenomenon takes place.

In the following diagram, we can see which are the phases that characterize the drying process:

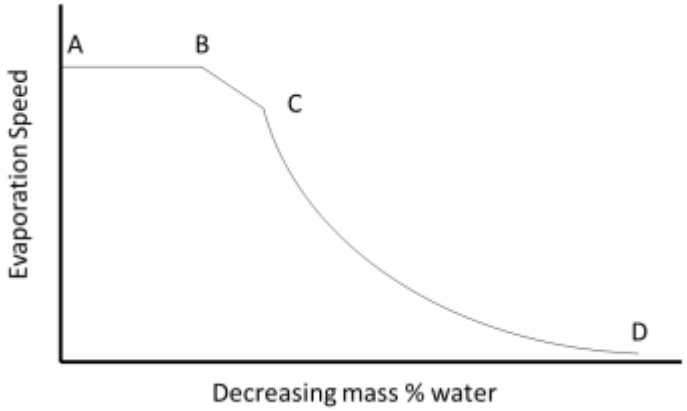

FIGURE 17 - drying process, heat treatment [6]

We note that from point A to point B, there is an evaporation phase from the exposed surface; subsequently, from point B to point C, the evaporation of the water is reduced, and some pores of the clay become dry. From point C to point D, the evaporation rate is adjusted by the diffusion of water inside the clay [6].

In the Firing phase, through pyrolysis, the decomposition of binder and flocculating elements takes place that is not desired within the system. For decomposition to take place, temperatures between 200 and 400°C are required, while for combustion and evaporation, we have temperatures between 400 and 600°C [6].

Care must be taken not to increase the treatment temperature too quickly to avoid cracks or explosions.

Once the Firing phase is over, we have an increase in temperature up to 1600°C, and in this phase, a phenomenon occurs in which the pores from which the water came out are dissolved and leave a denser body with greater cohesion is obtained. This phase is called sintering [6].

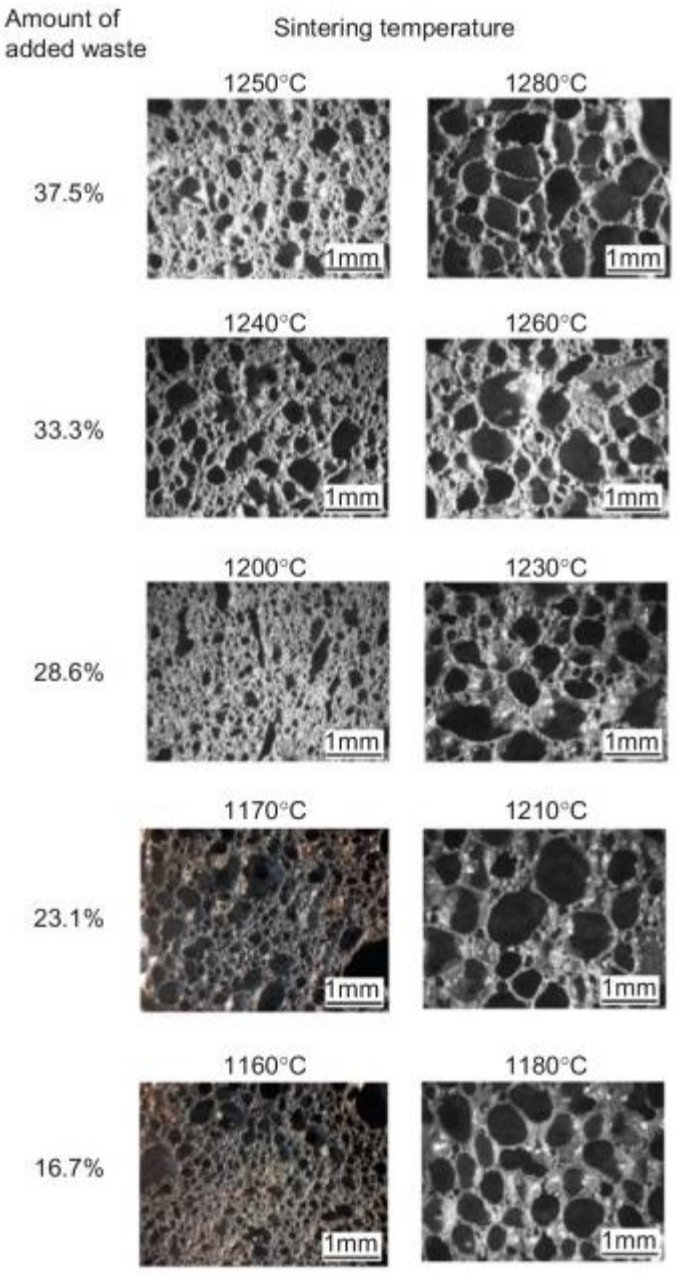

FIGURE 18 - pore structure for 1 mm particles [3]

5. Expanded clay in the rotary kiln

The rotary kiln is designed to produce expanded clay particles. They are used for civil engineering applications such as concrete aggregates, decorations, a pebble for decoration and insulation.

These aggregates are also called esclays or LECA (light expanded clay aggregates).

Expanded clay is a material used as a lightweight aggregate characterized by a porous internal core; it guarantees lightness and has a hard-external skin that gives it mechanical strength.

Many granulometric classes are carried out to guarantee a wide range of lightweight concretes with different requirements. The small spheroids (< 20 mm) have high mechanical strength [4].

Clays are typically crushed and dried to prepare raw material. The preferred agglomeration process for this context is extrusion, but other methods can also be used.

The critical process for producing expanded clay is that of heat treatment. This treatment is used to expand the clay particles physically.

For expanded clay, sintering plays a fundamental part; it causes gas release due to various changes that occur within the material. Among many, we note the decomposition and reduction of ferric oxides [4].

The release of these gases causes a physical expansion, causing them to obtain a lower density at the expense of higher porosity and a large surface.

To obtain the best results, various production factors must be optimized, including:

- Processing temperature: expansion occurs at temperatures just below the melting point of the clay.
- The grain size of the clay.
- Pellet size: a decrease in the pellet size corresponds to a smaller expansion.
- Retention time: varies according to the type of clay used.

5.1 Why clay as a light aggregate

Being a light aggregate (LWA), using expanded clay means taking advantage of many economic and environmental advantages.

- Economic advantages: using LWA, we have a reduction in transport cost, a reduction in structural costs for construction applications, and less dependence on imports [4].
- Environmental advantages: the expanded clay, according to the EXCA, is considered a sustainable material, if used instead of fossil fuels, it involves a reduction of CO2, allowing a better efficiency of buildings, it is recyclable, it brings advantages in the filtration of water and air and is chemically inert [4].

5.2 The production process of expanded clay

The clay is extracted from quarries located near the production plants to reduce transport costs and CO_2 emissions as much as possible. Once the quarries are emptied, they are restored to re-establish biodiversity and to create new natural habitats.

Once it reaches the production plant, the clay is processed in the rotary kiln, and once expanded, it can cool. This process is essential to obtain a high-quality product. The heat released by the hot clay during the cooling process is used as heating for the rotary kiln. The most significant production cost for this process is that of energy [4].

The European plants that perform this operation comply with the European directives on industrial emission.

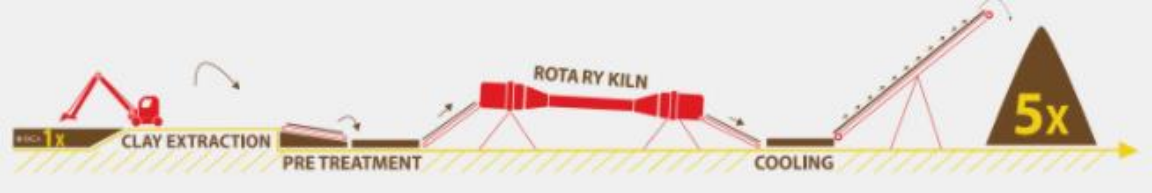

FIGURE 19 - production process of expanded clay [4]

6. Description of the analyzed task

6.1 Explanation

In this section, I describe the work topic on which my thesis is focused.

The work is based on creating a design of the internal structure of a rotary kiln in such a way as to modify the average residence time of the clay particles inside the kiln and obtain more homogeneous mixing of the particle's distribution.

After the analysis and the simulation, there is an explanation of how the mean residence time changes from the designs and the behaviour of the small and big particles inside the kiln.

We focus only on the part of the kiln where the clay particles are already expanded and therefore already exist. For my analysis, I have chosen a numerical simulation of the problem. This section is usually 10 meters long, but to speed up the simulation time and reduce the number of meshes of my component, we carry out the analyses with a length of 3 meters.

To perform the simulations, the material that I choose on Ansys Fluent is anthracite because the material clay is not present in Ansys library. The choice of anthracite is made because I focus more on investigating the effect of the inserts on the behaviour of the barrel.

We don't consider the change in material properties, and we run simulations of 100 seconds in such a way to already have an acceptable result and a simulation time not too long.

6.2 Particle interaction

- Particle-particle interaction

  As the number of particles increases, we also have a collision between them; this collision leads to a loss of kinetic energy [14].

  Two different possible models can be used to describe the collision: the hard-sphere and the soft sphere.

  The hard-sphere model can only be applied to binary collisions and is easy to use.

  The soft sphere model (DEM) is a bit more complex; it is modelled using mechanical elements such as springs; in this type of model, we have higher calculation times than the hard-sphere model, but we have more other fields of applicability [14].

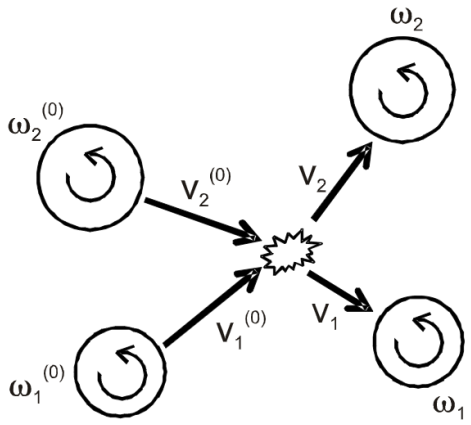

FIGURE 20 - particle - particle collision [14]

- Hard-sphere model

The hard-sphere model is based on the impulsive force, and it is defined by the integral of the force acting on a particle concerning time [14].

$$\mathbf{m_1}\left(\mathbf{v_1} - \mathbf{v_1^0}\right) = \mathbf{J} \qquad \textit{Equation 9}$$

$$\mathbf{m_2}\left(\mathbf{v_2} - \mathbf{v_2^0}\right) = -\mathbf{J} \qquad \textit{Equation 10}$$

$$\mathbf{I_1}\left(\mathbf{w_1} - \mathbf{w_1^0}\right) = \mathbf{r_1 n\ x\ J} \qquad \textit{Equation 11}$$

$$\mathbf{I_2}\left(\mathbf{w_2} - \mathbf{w_2^0}\right) = \mathbf{r_2 n\ x\ J} \qquad \textit{Equation 12}$$

In this application, we have as unknown variables the impulsive force $\boldsymbol{J}$ and the post-collisional velocities $\boldsymbol{v}$. To be able to solve this problem, we apply hypotheses:

We neglect the deformation of the particles, so we have a constant distance between the centres of mass, Coulomb's law controls friction in this system, and there is no more sliding off the particle after it stops sliding.

Regarding the particle-wall interaction, the process is divided into periods of compression and recovery because the coefficient of restitution is defined as the ratio of the impulse forces in the periods of recovery and compression [14].

We have two relative velocities, $\boldsymbol{G^0}$ and $\boldsymbol{G}$, between the centres of the particles:

$$\mathbf{G^0} = \mathbf{v_1^0} - \mathbf{v_2^0} \qquad \textit{Equation 13}$$

$$\mathbf{G} = \mathbf{v_1} - \mathbf{v_2} \qquad \textit{Equation 14}$$

- Soft sphere model

If the bodies exert a force against each other, they undergo a deformation that should show deformation of all the particles if described well. In practical calculation, an approximation is needed for the computational load of many particles [14].

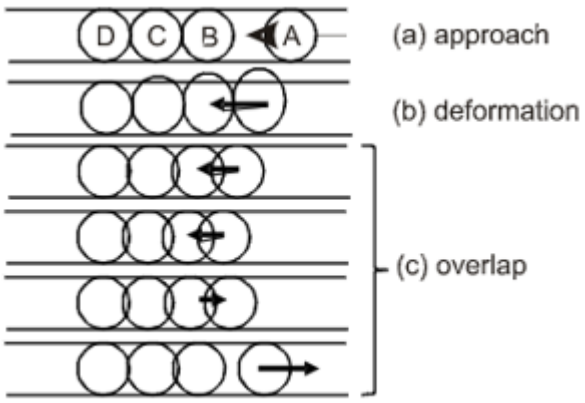

FIGURE 21 - assumption for the sphere model [14]

The movement of the particle has a normal and a tangential part. When two particles meet each other in the soft sphere model, they overlap without changing their shape. This overlap distance has a normal and a tangential component [14].

Based on the expression of Newton's equations of motion, we have a difference between hard-sphere models and soft sphere models.

The integral form describes the hard-sphere model. In this model, the momentum difference between two points in time is equal to the impulsive force [14].

The soft sphere model, on the other hand, is described by differential equations.

Usually, in particle motions, we do not have a linear stress-displacement relationship. For this reason, we obtain the variations of momentum and displacement for arbitrary times as solutions of the differential equations. It is possible to calculate the speeds during the contact process. By doing more calculations, the soft sphere model has higher calculation times [14].

- Hard sphere simulation of a soft sphere model

The soft sphere model has a problem calculating motion during the collision. For this reason, Watson was able to propose an approximation model of the soft sphere to the hard sphere in the case in which the particles are in contemporary contact [14].

This model is based on a rotational and a normal return.

- Cohesive force

The adhesion of the particle to the wall or another particle is due to surface forces and electrostatic characteristics. Various forces interact, and they are:

- Force due to a liquid bridge: due to a very humid environment, condensation is created, and thus a liquid bridge is formed. The pressure inside the bridge is negative, and the surface of the liquid is concave; therefore, a force on the particle acts equal to the sum of these two factors [14].

- Electrostatic force: a force acts on the particles as they are charged. The Coulomb force gives this force.

$$\mathbf{F_C = \frac{1}{4\pi\varepsilon_0}\frac{q_1 q_2}{l^2}} \qquad \textit{Equation 15}$$

Where $\boldsymbol{q_1}$ and $\boldsymbol{q_2}$ express the charge of the particles, $\boldsymbol{\varepsilon_0}$ is dielectric constant, and l express the distance between the particle centres. The cohesive force is given by:

$$\mathbf{F_E = \frac{\pi\sigma_1\sigma_2}{\varepsilon_0}D^2} \qquad \textit{Equation 16}$$

Where $\boldsymbol{\sigma_1}$ and $\boldsymbol{\sigma_2}$ are charge densities ($\frac{C}{m^2}$) of the two particles. This equation is derived assuming that the particles are charged uniformly and that the effective charge is concentrated at the particle centres [14].

- Van Der Waals Forces

We know that the forces between particles due to the above factors cause a particle to join the wall or another particle. The forces of Van Der Waals cause adhere to other particles or a wall.

This force has evidence when there is contact from very smooth surfaces. It is necessary to consider the contribution of the molecules that make up the surfaces.

Hamaker (1973) did calculations for different geometries. The force F between two infinitive plates flat with a separation term z is expressed:

$$\mathbf{F = \frac{A}{6\pi z^3}} \qquad \textit{Equation 17}$$

A is the Hamaker constant, and F is the force per unit area [14].

- Solid particle agglomeration

Due to the Van Der Waals force, liquid bridges and electrostatic effects cause an agglomeration of solid particles.

When two particles collide, they generate energy that is dissipated. To understand if there is energy available for the rebound of the particles, it is necessary to evaluate whether the kinetic energy is greater than that dissipated;

otherwise, there isn't enough energy for the rebound. It is very difficult to determine the fluid dynamic forces due to the different morphologies. The drag coefficient decreases as the fractal dimension decreases [14].

- Fluid forces on approaching particles

Let us take into consideration two particles present inside fluid and approaching each other. The fluid pressure interposed between the two particles increases as the distance between the two particles decreases; this causes the fluid to move outwards. To determine this force, we make an approximation by saying that the spheres have the same size. For this reason, we have a symmetrical flow concerning the central plane of the spheres and asymmetrical along the line that connects the centre of the two spheres [14].

- Particle-wall interaction

It is possible to divide the wall-particle interaction into two different categories: mechanical interaction due to contact with the wall and hydrodynamic interaction caused by proximity to the wall [14].

If a particle is supposed to have an infinitely large diameter, the particle-wall interaction is dominant over that particle-particle [14].

There are two different types of models to manage collisions between particles and particles, and, as described in the previous chapter, they are the hard-sphere model and the soft sphere model [14].
In the hard-sphere model, the instantaneous deformation of the particle does not appear explicitly in the formulation; in the soft sphere model, on the other hand, instantaneous motion is obtained during the entire collision process.

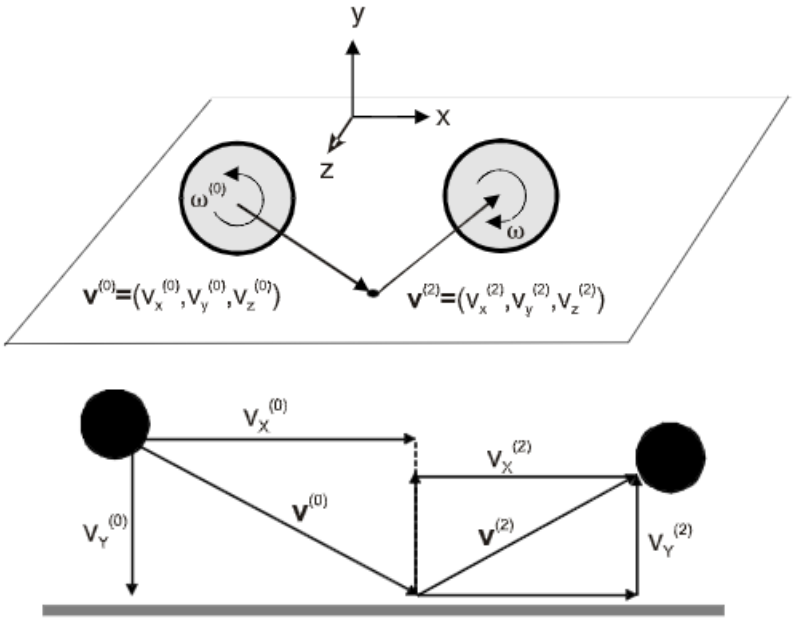

FIGURE 22 - particle colliding with a wall [14]

- Erosion

During the impact between the particle and the wall, erosion occurs.
After a series of experiments, it is possible to state that the maximum erosion for ductile materials occurs close to 15 ° and for brittle materials at 90 ° [14].

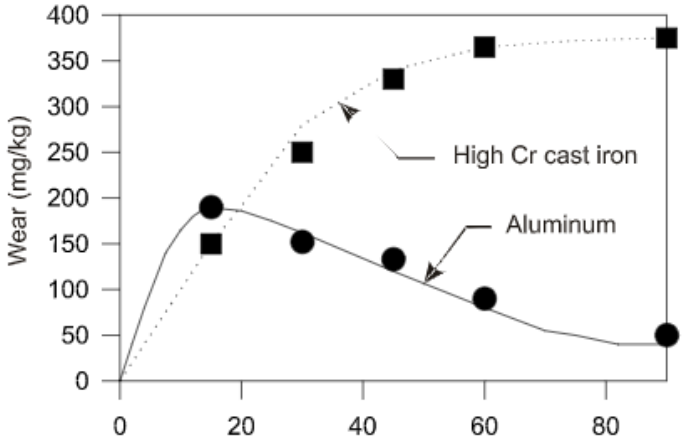

FIGURE 23 - erosion rate of aluminum and high chromium cast iron by alumina particles impinging at 50 m/s [14]

Complete information on erosion due to particle flow can be found in Chapter 12 of the Multiphase Flow Handbook [Crowe (ed.), 2006].

6.3 Mean residence time

Thanks to the experimental rotary kiln, it is possible to show the influences of the structural parameters of mass flow (MFR) and average residence time (MRT). The results show that increasing the slope and rotational speed of the furnace reduces the MRT and instead increases the MFR keeping the same value of the volumetric ratio of particles [7].

The MRT is a very important factor. We can determine the degree of the chemical reaction that occurs between the solid phase and the gas and affects the heat transfer and the mass transfer [7].

Many experiments have been carried out on the rotary kiln with a flow of clay particles inside it; during these experiments, an average residence time of the particles inside a 52-meter-long kiln equal to 42 minutes was obtained.

Taking these data into consideration, through the formula $\boldsymbol{u} = \frac{\boldsymbol{Lenght\ [meters]}}{\boldsymbol{Residence\ time\ [seconds]}}$ we can calculate the average speed of the particles within the kiln, which is equal to $0.021\ \frac{m}{s}$.

Thanks to the value of the average speed of the particles just calculated, it is possible to apply this value on the portion of kiln that has been taken into consideration to calculate the average residence time of the particles; this value is equal to 145 seconds for the length of the model 3 meters.

This average residence time expresses the real condition of the project; during this work, various approximations are taken into consideration to facilitate the calculation and design speed; for this reason, the expected value from the simulations and mathematical formulas must be lower than that extracted from the real situation.

To calculate the MRT, there are several formulas with different approaches from the literature: let us analyse each of them individually.

6.3.1 Boateng mean residence time

The descript formula of Boateng to calculate MRT is the following:

$$\boldsymbol{\tau = \frac{0,23L}{sN^{0,9}D} \pm \frac{BLG}{F}} \qquad \textit{Equation 18}$$

With:

$$\boldsymbol{B = sd_p^{-0,5}} \qquad \textit{Equation 19}$$

τ is the mean residence time expressed in [min]

s is the slope of the kiln expressed in $[\frac{m}{m}]$

N is the revolution per minute of the kiln [rpm]

G is the freeboard gas velocity expressed in $[\frac{kg}{hr.m^2}]$

F is the quantity of the feed that enters in kiln expressed in $[\frac{kg}{hr.m^2}]$

B is the constant that depends on the material dimension

$\boldsymbol{d_p}$ is the particle diameter expressed in [m].

The symbol + in the equation is used if the flow of air and feed is co-current; if these two flows are counter-current, the symbol to use is -.

a. Froude number

   This number is very useful in identifying what kind of movement the particles are making in the transverse plane of the furnace. It can be expressed as:

$$\boldsymbol{Fr = \frac{w^2R}{g}} \qquad \textit{Equation 20}$$

   Where $\boldsymbol{w}$ is the angular velocity expressed in $(\frac{1}{s})$, $\boldsymbol{R}$ is the radius of the furnace expressed in meters [m] and $\boldsymbol{g}$ is the gravitational acceleration $(\frac{m^2}{s})$ [9].

   It is essential to find the best Froude number to be able to have the characteristics of the rotating oven perfectly optimized.

We know that the movement of particles inside the rotary kiln is that of a helical shape; there are six different ranges for the Froude number, which we can summarize in the following table:

TABLE 2 - ranges of Froude number [9]

Mode	Fr
Slipping	$Fr < 1{,}0x10^{-5}$
Slumping	$1{,}0*10^{-5} < Fr < 0{,}3*10^{-3}$
Rolling	$0{,}3*10^{-3} < Fr < 0{,}2*10^{-1}$
Cascading	$0{,}4*10^{-1} < Fr < 0{,}8*10^{-1}$
Cataracting	$0{,}9*10^{-1} < Fr < 1{,}0$
Centrifuging	$Fr > 1{,}0$

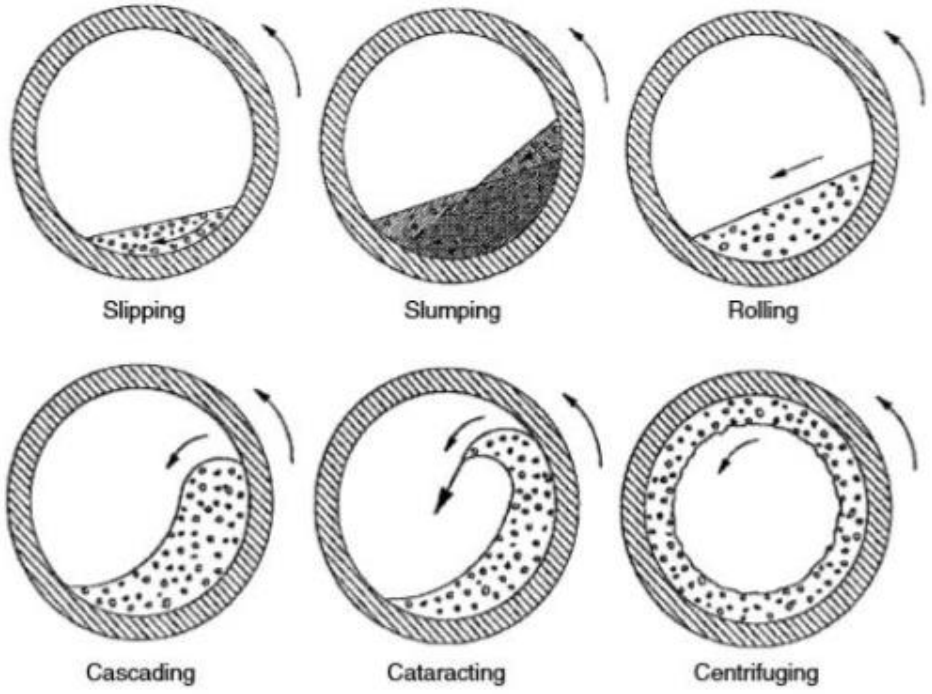

FIGURE 24 - Movement of the particle on Freud number [9]

The cascade concept describes the number of times the particles roll or how many times it is moved from the bottom of the kiln to the top, this concept is derived from the transverse movement of the feed bed.

We can calculate the number of cascades a particle makes for each turn of the kiln [9].

$$z_0 = \frac{L_c(\Phi + \psi \cos\xi)}{\sin\xi} \qquad \textit{Equation 21}$$

Where ψ is the angle of the relative bed is related to the axial plane.

We can also calculate the mean axial velocity:

$$\mathbf{u_{ax} = 2\pi rn\left(\frac{\Phi + \psi cos\xi}{sin\theta}\right)} \qquad \textit{Equation 22}$$

One time we know this velocity, we can calculate the residence time of the permanence of every particle:

$$\mathbf{\tau = \frac{Lsin\xi}{2\pi rn(\Phi + \psi cos\xi)}} \qquad \textit{Equation 23}$$

6.3.2 Sai residence time

The description of the formula from Sai to calculate the mean particle residence time is [10]:

$$\mathbf{\tau = \frac{1315.2\ H^{0,24}}{\theta^{1,02} N^{0,88} F^{0,072}}} \qquad \textit{Equation 24}$$

where: τ is the residence time in [min]

H express the height of the dam in [m]

Θ express the slope of the kiln $[\frac{m}{m}]$

N are the revolutions of the kiln [rpm]

F is the amount of feed $[\frac{kg}{hr}]$

We can calculate *W*, the quantity of the feed content in the kiln:

$$\mathbf{W = \frac{0.66F^{0,86}H^{0,4}}{\theta^{1,11}N^{0,9}}} \qquad \textit{Equation 25}$$

6.3.3 Peary residence time

This formula is an approximation that manages to describe the operation of the kiln under normal working conditions. There must be no internal structures [8].

$$\mathbf{\tau = \frac{CL}{NsD}} \qquad \textit{Equation 26}$$

Where: τ is the residence time in [min]

L express the length of the kiln in [m]

N is the revolution for a minute of the kiln [rpm]

S express the slope of the kiln $[\frac{m}{m}]$

D expresses the diameter of the kiln [m]

There is a variable that we can calculate with $\mathbf{C = 1,77\sqrt{\xi}}$, where $\boldsymbol{\xi}$ is the dynamic response angle, and in this case, we are not able to calculate it; we can assume it equal to 11.4 [8].

6.3.4 Bernard residence time

It is very similar to Boateng's formula; the only thing that changes is the calculation of B [12]:

$$\boldsymbol{\tau = \frac{0,23L}{sN^{0,9}D} \pm \frac{0,6BLG}{F}} \qquad \textit{Equation 27}$$

$$\boldsymbol{B = 5d_p^{-0.5}} \qquad \textit{Equation 28}$$

Where **s** is the expression of the slope of the kiln $[\frac{m}{m}]$

N is the revolution for a minute of the kiln [rpm]

G is the freeboard gas velocity $[\frac{kg}{hr.m^2}]$

F is the quantity of the feed $[\frac{kg}{hr.m^2}]$

B is the constant that depends on the material dimension [m]

$\boldsymbol{D_p}$ is the diameter of the particles [m]

6.3.5 Lui residence time

This relation is called "passage of the solid particles in the cylindrical rotary kiln", and it is expressed as [11]:

$$\boldsymbol{\tau = 1,77\frac{L\sqrt{\theta}}{DN\beta}} \qquad \textit{Equation 29}$$

Where **β** expresses the inclination of the kiln respect x-axis.

6.3.6 Perry residence time

We also find the space velocity formula, and it is expressed as [13]:

$$\boldsymbol{SV = 148N\varphi D^3 tan\theta} \qquad \textit{Equation 30}$$

The proposal formula for the mean residence time is the following.

$$\boldsymbol{\tau = \frac{L}{60\pi NDtan\theta}} \qquad \textit{Equation 31}$$

where N is in [rpm]

$\boldsymbol{\varphi}$ is the friction of cross-section occupied [$\frac{m_{clay}^2}{m^2}$]

D is the diameter in [m]

L is the length in [m]

τ is mean residence time in [h]

SV is the space velocity in [$\frac{ton}{day.m^3}$]

We can resume and make a comparison in the following table of the mean residence time analysed:

TABLE 3 - summary mean residence time

EQUATION	FORMULA	AUTHOR
27 28	$\tau = \frac{0{,}23L}{sN^{0,9}D} \pm \frac{0{,}6BLG}{F}$ $B = 5d_p^{-0.5}$	Bernard [12]
18 19	$\tau = \frac{0{,}23L}{sN^{0,9}D} \pm \frac{BLG}{F}$ $B = sd_p^{-0.5}$	Boateng 1 [9]
29	$\tau = 1{,}77\frac{L\sqrt{\theta}}{DN\beta}$	Lui 1 [11]
26	$\tau = \frac{CL}{NsD}$	Peary 1 [8]
31	$\tau = \frac{L}{60\pi NDtan\theta}$	Perry [13]
24	$\tau = \frac{1315.2\ H^{0,24}}{\theta^{1,02}N^{0,88}F^{0,072}}$	Sai [10]

From these formulas, I use just Bernard, Boateng 1, Peary 1 and Perry. This choice comes because the other formulas need some materials parameters that I do not have and are not useful for reaching the thesis's aim.

I can also calculate the Sai residence time related to the geometry of the cylinder with the dam and compare the result with the results from the simulation of the kiln with the dam.

6.4 How to analyse mean residence time

The dimension of the particle, influences many properties of particulate materials; it is a valuable indicator of quality and performance. Using a sedimentometer, we can measure

the rate of fall of the particle through a viscous medium, with the other particles and/or the walls of the container that tend to slow down their movement [19].

A spherical particle can be described using the diameter as an indicator because each dimension is identical. For this reason, many techniques and theories make assumptions that usually use an equivalent diameter as diameter [19].

Two techniques analyse the particle size without approximating the diameter; they are microscopy and automatic image analysis. Thanks to this last technique, using different variables, we can describe the particle as non-spherical. Usually, for the particle distribution analysis, a graph is used on the x-axis, the equivalent spherical diameter is indicated, and on the y axis, the percentage [19].

- Mean:

  We can calculate the mean of a given set of numbers using the concept of average. We can use the mean of volume to determine which is the centre point of a sample of data, but usually, the mean is used to do this type of analysis [19].

- Median:

  The median is used to define a value for which we have half of the population below this value, and the other half is above. We can indicate this value with the symbol $\boldsymbol{D_{50}}$, it also represents the second quartile. The median is one of the most easily understood values. For particles size populations, we use $\boldsymbol{DV_{50}}$ [19].

- Mode:

  Mode indicates which is the highest point of our population, the highest peak. Our application indicates the size of the particles most present in our population [19].

Thanks to the method described before, we can obtain a report from the measure of the particle size distribution. Base on which type of particle sizing technique we use, we produce different results; that is why there are a lot of things that we must consider: the algorithm used, which physical properties are used, the dynamic range of the instrument, and the number/volume of the particles.

- Number distribution

  The number distribution is difficult to understand, but we can simplify it by considering a measuring particle from a microscope. The person that does the observation gives a size value for every particle inspected. Thanks to this approach, every particle has equal weighting, and it is possible to calculate the final distribution [19].

- Number distribution and Volume distribution

  As we said, the number distribution is based on a microscope or image analyse. On the other hand, the volume distribution is a result of the laser diffraction construct.

  Software can transform the results from Number distribution to volume distribution and vice versa [19].

To make these tests, we have a lot of type of different apparatus; we analyse 4 of them:

1. LA-960

   The LA-960 is an apparatus used to measure wet and dry samples measuring from 10 nanometres to 5 millimetres. The main idea of laser diffraction is that the particle can scatter light with a reflection angle affected by the particle's size.

   We have a dispersion difference based on the particle size; the larger ones have wide dispersion angles while the smaller ones have narrower dispersion angles. There are four different ways in which light interacts with particles: diffraction, reflection, absorption, and refraction [19].

   Simplification hypotheses are made for the calculation; it is assumed that the particles are spherical, opaque, diffuse in an equivalent way and the light interacts differently in relation to the medium.

   This instrument, LA-960, is composed of two high-intensity light sources and an optical bench in cast aluminium. LA-960 uses the laser diffraction method to measure dimensional distributions; it uses the widest range of sizes currently available [19].

   Due to its characteristics, laser diffraction is the most popular method in modern industry.

2. LA-350

   This tool is perfect for applications such as sludge, minerals, and paper chemistry. It is based on the optical design expressed above and manages to be balanced and with good ease of use [19].

3. SZ-100

   This tool measures the particle size, zeta potential, and molecular weight from 0.3 nm to 0.8 µm.

   The zeta potential is a measurement of how much is the charge on the surface of a particle placed in a specific liquid medium. Thanks to this value, we can understand and predict the interactions between particles and suspension. Thanks to manipulating the zeta potential, we can improve the stability of the suspension to accelerate the flocculation of the particles, such as in water treatment [19].

   Through the electrophoretic light diffusion technique, in which the movement of particles in an applied electric field is detected, the SZ-100 apparatus can measure the zeta potential [19].

4. Camsizer x2 & P4|PSA300

   The microscope is the gold standard in particle characterization as it is accepted as the most direct measure of particle size and morphology. Automation has been introduced to replace a boring and somewhat subjective measurement with a

sophisticated technique to quantify the size and shape of the particles more precisely based on the algorithm of image analysis [19].

6.5 Calculation of theoretical mean residence time

In this chapter, we do the analytical calculations of the mean residence time using the formulas that I expressed above in chapter 6.2.

Firstly, we need to define the properties of the kiln, particles, and air that form the system under our analysis.

We are focusing on the last part of the kiln where the expanded clay particles are already formed; this part is usually 10 meters long, but to simplify the calculations during the simulation, we assume this length is equal to 3 meters.

The internal diameter of the kiln is 3 meters with an inclination of 5°; thanks to this data of the inclination, we can determine the slope of the kiln that is equal to 0.087 $\frac{m}{m}$.

The rotational speed of the kiln is set equal to 5 revolutions per minute, and the flow of the particles of clay (density equal to 1760 $\frac{kg}{m^3}$) is 5.56 $\frac{kg}{s}$. The air enters counter-current with respect to the flow of the particles, and it enters with a velocity equal to 3.7 $\frac{m}{s}$ and a density equal to 1.225 $\frac{kg}{m^3}$.

All these data and calculated supported data like for example, the area of the kiln is summarized in the following table:

TABLE 4 - data of the analyzed case

Di:	3	m
Li:	3	m
ϕ:	0,087	radiant
w:	5	rpm
M_{flow}:	5,56	$\frac{kg}{s}$
ρ:	1760	$\frac{kg}{m^3}$
V_{gas} = G:	3,7	$\frac{m}{s}$
Slope:	0,087	$\frac{m}{m}$
L*cosϕ:	2,989	m
L*senϕ:	0,261	m
ρ_{air}:	1,225	$\frac{kg}{m^3}$
Pi:	3,142	/
A:	7,069	m^2
μ_{air}:	1,803E-05	Pas
Tan(ϕ):	2,43E-05	/
SV_{clay}:	0,5	$\frac{tons}{m^3 day}$
Fraction of cross-section:	0,447	$\frac{m_{clay}^2}{m^2}$
A_{clay}:	0.316	m^2
U_{clay} :	0.100	$\frac{m}{s}$

After the calculations of the formulas, I obtained the following results:

TABLE 5 - results of analytical calculations

Formula	Results
Bernard	17.71 sec
Boateng 1	25.46 sec
Peary 1	26.06 sec
Perry	43.66 sec

Analysing this table, it is possible to notice that the mean residence time from Bernard, Boateng and Peary are close to each other while Perry means residence time value is distant from others; this difference comes from the approximation taken from the given data expressed in table 4.

The results given from Table 5 given the first confirmation that perform simulations of 100 seconds can be fit for the data that analysed. I can affirm this because in Perry means residence time, that is the higher one. I perform a simulation 2,3 times bigger than the particles residence time obtained.

6.6 Reynold number and configuration of the software ANSYS Fluent

Before starting the configuration of Ansys Fluent 2020 R1, I did some calculations regarding the Reynold number to determine if my flow is turbulent or laminar.

The Reynold number is defined as the ratio between the inertial forces and the viscous forces of a fluid undergoing an internal movement caused by the different velocities of the fluid. The region where these forces change behaviour is called the boundary layer. A comparable effect can be generated by introducing a high-velocity flow into a low-velocity fluid. This generates fluid friction, which develops turbulent flow. The factor that tends to counter this effect is the fluid's viscosity, which tries to inhibit turbulence. The Reynolds number is a guide to determining whether the turbulent flow occurs in a situation.

We have two different flow regimes: laminar flow and turbulent flow, laminar flow occurs for Re lower than 2300, and in this type of flow, the viscous forces are the dominant ones, the movement of the fluid is regular and constant in a close channel.

For Reynolds numbers greater than 2300, in a close channel, we enter a turbulent regime; this regime is dominated by inertial forces that produce vortices and other flow instabilities

The formula to calculate the number of Reynolds is the following:

$$\mathbf{Re} = \frac{\boldsymbol{\rho_{gas} u_{gas} D_{kiln}}}{\boldsymbol{\mu_{gas}}} \qquad \textit{Equation 32}$$

Where ρ is the density of the fluid expressed as ($\frac{kg}{m^3}$) equal to 1,225 ($\frac{kg}{m^3}$), u is the flow speed ($\frac{m}{s}$) equal to 3,7 ($\frac{m}{s}$), D is a characteristic linear dimension (m) equal to 3 (m), and μ is the dynamic viscosity of the fluid (Pas) equal to 0,00001803 (Pas).

For my specific case, the value of Reynold that I obtained from the data that I expressed above is: Re = 754159,7.

Thanks to Reynolds's result, I know that the case under investigation is in a turbulent region. I use the standard k- ε model. The realizable k-e turbulence model gives close agreement with the experimental data. The standard $\boldsymbol{k–\varepsilon}$ model was seen to predict the

gas phase turbulence for the freeboard region of cement kilns quite satisfactorily and therefore was used in this work [2].

This turbulence model is the most used mathematical model in computational fluid dynamics to simulate the mean flow characteristics in turbulent conditions. It is part of the two-equation models and gives a general description of turbulence using two partial differential equations for the transport of $\mathbf{k}$ (turbulent kinetic energy) and $\boldsymbol{\varepsilon}$ (the dissipation rate of turbulent kinetic energy). The initial impetus for the development of the model came from the improvement of models based on mixing length and as an alternative to models that require the specification of turbulent length scales through algebraic equations.

Compared to past turbulence models, the model focuses on the mechanisms that influence turbulent kinetic energy. This makes the model more general than the mixed length-based models. The model's basic assumption is that turbulent kinetic energy is isotropic, or in other words, that the relationship between the Reynolds stress tensor and the mean strain tensor is the same in all directions [16].

The model contains terms that cannot be evaluated analytically and which therefore require numerical modelling. The standard model proposed by Launder and Spalding is the most used in the industrial field, given the important validation effort behind the model. The model equations are presented, starting with that of turbulent kinetic energy:

$$\frac{\delta(\rho k)}{\delta t} + \frac{\delta(\rho k u_i)}{\delta x_i} = \frac{\delta}{\delta x_j}\left[\frac{\mu_t \delta k}{\sigma_k \delta x_j}\right] + 2\mu_t E_{ij} E_{ij} - \rho\varepsilon \qquad \textit{Equation 33}$$

Where this equation express: variation of k or ε + Transport k or ε by convection equal to transport k or ε by diffusion +production k or ε – reduction k or ε

Where:

$\boldsymbol{u_i}$ represent the component of velocity along with i

$\boldsymbol{E_{ij}}$ is the tensor of deformation

$$\mu_t = \rho C_\mu \frac{k^2}{\varepsilon} \qquad \textit{Equation 34}$$

The value of the constants $\boldsymbol{\sigma_k}$ and $\boldsymbol{C_\mu}$ derived from some experiment result and the standard values for them are: $\boldsymbol{\sigma_k} = 1{,}00$ and $\boldsymbol{C_\mu} = 0{,}09$ [16].

6.6.1 Constitutive equations

I found all the following equations from the ANSYS GUIDE Theory Guide [15].

6.6.1.1 Volume fraction

The concept of phasic volume fractions is created to calculate the volume fraction; it represents the effective space that each phase occupies in each volume and that the laws of momentum and mass conservation are satisfied by each phase individually.

The assumption that is made is that the functions are continuous in the space of time and that the sum of the two fractions is equal to one [15].

The volume of phase for fluent is defined as:

$$\mathbf{V_q} = \int \boldsymbol{\alpha_q} \mathbf{dV} \qquad \textit{Equation 34}$$

Where:

$\boldsymbol{V_q}$ is the Volume of phase q expressed in [m^3]

$\boldsymbol{V}$ is the volume expressed in [m^3]

$\boldsymbol{\alpha_q}$ is the phasic volume fraction [vol.%]

$\sum_{q=1}^{n} \boldsymbol{\alpha_q} = \mathbf{1}$

With: q is the effective density of phase and $\boldsymbol{\rho_q} = \boldsymbol{\alpha_q \rho_q}$ is the physical density of phase q.

6.6.1.2 Conservation equations

The conservation of mass that I found in the ANSYS FLUENT guidebook is the following:

$$\frac{\boldsymbol{\delta}}{\boldsymbol{\delta t}}(\boldsymbol{\alpha_q \rho_q}) + \boldsymbol{\nabla}(\boldsymbol{\alpha_q \rho_q v_q}) = \sum_{\mathbf{p=1}}^{\mathbf{n}} (\dot{\mathbf{m}}_{\mathbf{pq}} - \dot{\mathbf{m}}_{\mathbf{qp}}) + \mathbf{S_q} \qquad \textit{Equation 35}$$

Where:

$\boldsymbol{v_q}$ is the phase velocity expressed in [$\frac{m}{s}$]

$\dot{\boldsymbol{m}}_{\boldsymbol{pq}}$ and $\dot{\mathbf{m}}_{\boldsymbol{qp}}$ characterize the mass transfer in between the phase expressed in [$\frac{m}{s}$]

$\boldsymbol{S_q}$ is the source term, on ANSYS is by default equal to zero.

6.7 Methods for the simulations

DEM: method of discrete elements; this method is recommended for doing simulations of large particles, this is the most realistic approximation that can be done with ANSYS.

This model uses Spring / Dashpot interactions to calculate the element interactions; for these interactions, all the parameters for each material are required. The disadvantage of this model is that being so realistic, it requires considerable IT power, and for this reason, it is used only by large research companies [15].

DDPM: Dense Discrete Phase Model, this model is a simplified version of the DEM model, here the interactions between particles are simplified only to normal and tangential factors; these factors identify how much heat energy is absorbed and how much is used for the rebound [15].

This model allows the simulation of particles with different shapes, aggregation, lifting, and displacement. To get the tracking time, we need to use the tracking particles.

DPM: Discrete Phase Model, this model keeps the particles as individuals; with the use of this model, we can consider the lifting resistance and the normal and tangential factors. This model, although simple, is capable of processing approximately correct simulations [15].

Granular Flow: the simplest model that allows us to analyse discrete particles, the flow is simulated as a continuous flow and not as single particles. It is not possible to obtain the average value of the residence time of the particles.

To do this work, I use the second and the third model described above.

7. Simulations of basic geometries

Now let's start talking about my specific case; I deal with a rotary kiln with dimensions of 57 meters in length, 3 meters in diameter, and a slope of 5°. The particles that we are going to analyse have a diameter from 1 mm to 16 mm.

We focus only on the part where the clay particles are already expanded; this part is about 10 meters long in reality but, in our simulations, we approximate it with a length of 3 meters to speed up the simulations and reduce the number of elements of my system.

To solve this problem, as I told before, we focus more on the investigation of the effect of the inserts on the behaviour of the barrel. One problem that emerged was related to the feed flow rate. Using the feed indicated from the data, I could not perform simulations due to technological limits. A lower flow rate affects the movement of the particle inside the kiln and their interaction. There are fewer contacts particle-particle, and the distribution of the particle is different. After a discussion with my supervisor, it was chosen to decrease the feed flow rate for IT power; the flow rate that is used in this work for the simulations is equal to 0,1 $\frac{kg}{s}$, but the aim is still the comparison of effects on the particles by inserts in the kiln.

For this report, I so CFD analysis using ANSYS 2020 R1 student license software.

Firstly, I perform a simulation of the smooth rotary cylinder to find out the most accurate analytical result that I obtained first and compare the simulation of the discrete phase model and dense discrete phase model.

The initial goal of the thesis is to understand how to carry out a simulation that reflects these parameters, obtain images of the mean particle residence time trend and the data related to the particle residence time after 100 seconds of simulation.

Thanks to these data, I can compare my own designed different four geometries, trying to understand the advantages and disadvantages of each one to find, after an analysis, the better design possible to maximize the mean residence time and the mixing of the particle inside the kiln.

We should go to carry out simulations with a rotating cylinder with an angular speed of 5 rpm; inside it enters the particles that follow the movement of it.

Let start to see which the different alternatives are to perform my simulations

7.1 Configurations of Mesh

The configuration of the mesh is the same for both methods and geometries. I used hexahedral elements. The only thing that is going to change is the values of the qualities of skewness and orthogonal quality for the geometries.

The meshes for this work are made in the same way for all the geometries with an element size equal to 30 mm (by fluent, it is recommended to create elements larger than the maximum size of particles). Thanks to this value, I can respect the limits for orthogonal quality and skewness. The value for the orthogonal quality that I must respect is that the minimum value must be bigger than 0,1. Regarding the skewness, the max must be lower than 0,94.

For my cases, putting element size of meshes equal to 30 mm, I find the following values for smooth cylinder: a maximum skewness is 0,58588 and minimum of orthogonal quality 0,46341.

Regarding the cylinder with the dam, I have the value of minimum for orthogonal quality equal to 0,15219 and the maximum skewness equal to 0,84781.

I can see that for both cases, the values respect the limit values that I expressed above. Now we can see the graphs of the mesh quality for the case of a smooth cylinder.

The number of the elements of meshes that I have after these configurations for the smooth cylinder is 1270500.

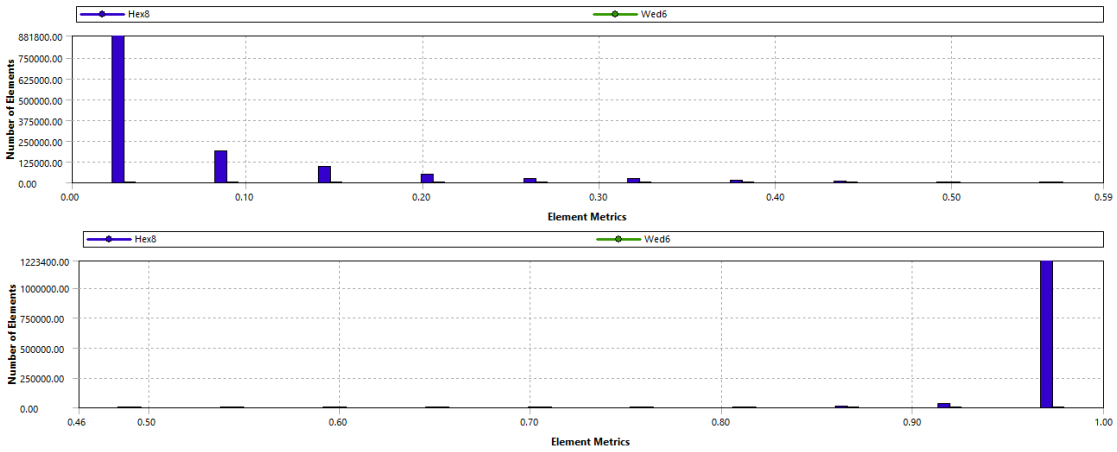

FIGURE 25 - skewness and orthogonal quality smooth cylinder

7.2 Simulations of a smooth cylinder to compare the methods of simulation

In this part, we see how to do the correct configuration of the software ANSYS Fluent for both models.

7.2.1 DDPM

The first thing to do is to lunch the Fluent software; in this method, we have to active the Double Precision to have more accurate results and then press start.

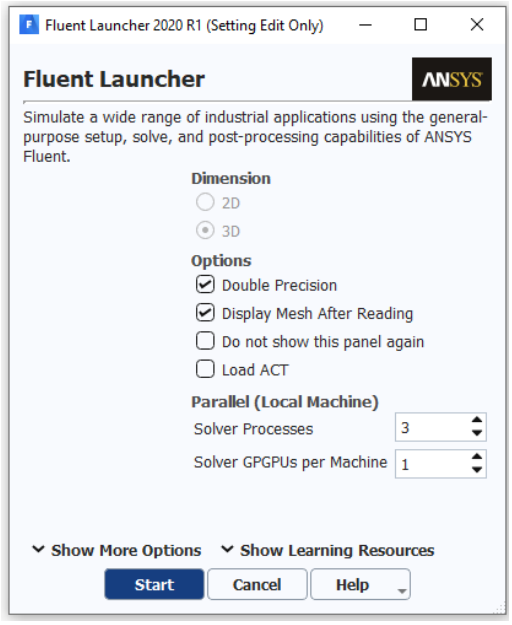

FIGURE 26 - fluent launcher DDPM

When the software is open, we have to do a Check of our Mesh, change the Units for the angular velocity to RPM, switch the time do transient and set the gravitational force according to the slope of my kiln in this way:

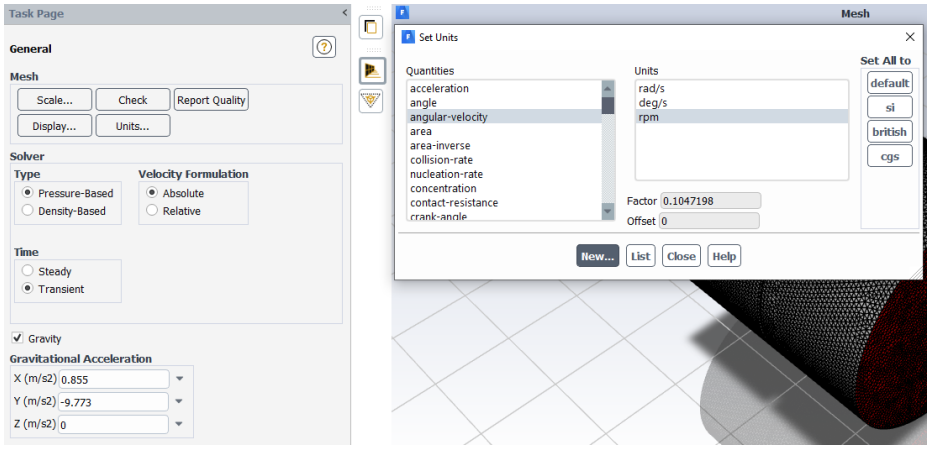

FIGURE 27 - generally set fluent DDPM

We have to put the Multiphase model ON on the Model part and activate the discrete phase. Once the multiphase is turned on, we have to switch to the Eulerian model and activate DDPM.

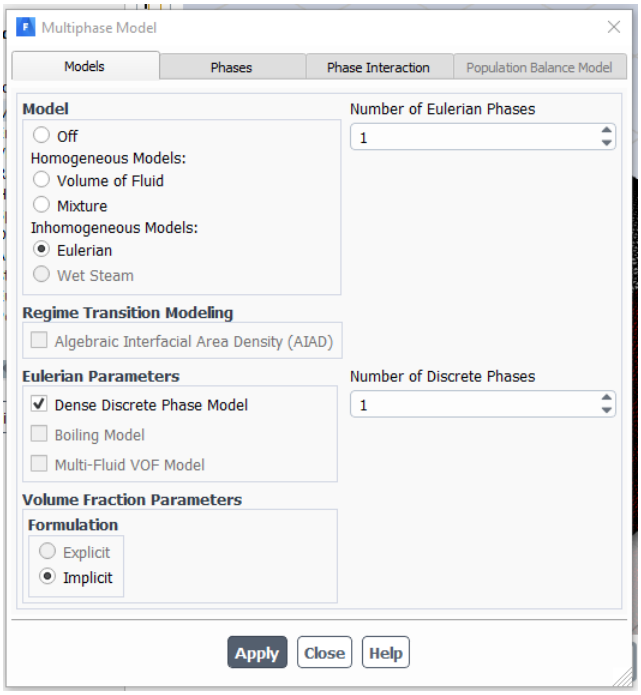

FIGURE 28 - multiphase model DDPM

Then we switch to Set Injection Properties and keep attention to put Discrete phase domain with phase 2, put group inside the Injection type with the number of streams equal to 50. We choose Anthracite in the material section, put Rosin-Rammler distribution, and put the dimension of my particles, the flow rate, and the time.

Anthracite's choice is because the material clay (expanded) is not presented in the library (and we do not have enough data for simulation) of Ansys, and anthracite is the material that better respects the physical and chemical properties of the clay.

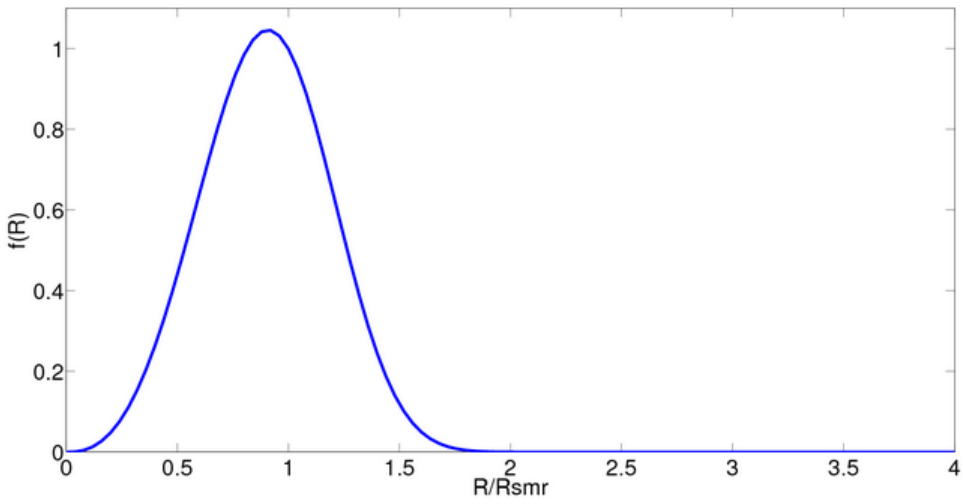

FIGURE 29 - Rosin-Rammler distribution

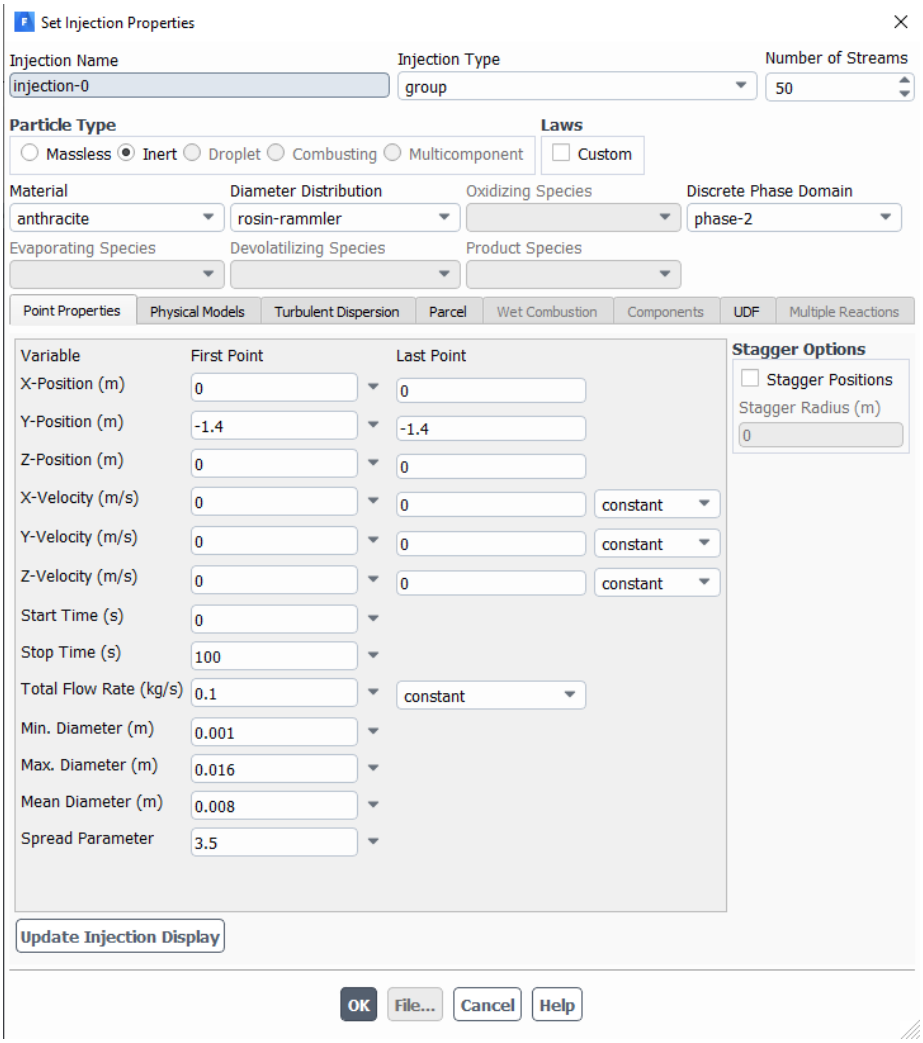

FIGURE 30 - injection properties DDPM

Now we can come back to the multi-phase windows to set the interaction inside my phases correctly.

The first thing to do is to put the phase-2 like granular and change Granular Viscosity to gidaspow (that is good for bed fluidize application) and Granular Bulk Viscosity (indicates the sum of kinetic, collisional, and frictional viscosity components for the solid particles) to lun-et-al (used for granular bulk viscosity). Now I have to put the restitution coefficient of phase 2 – phase 2 equal to 0.5 [17], a normal or tangential coefficient of restitution equal to 1,0 means that the particle retains all of its normal or tangential momentum after the rebound (an elastic collision). If the normal or tangential coefficient of restitution is equal to 0.0 means that the particle retains none of its normal or tangential momentum after the rebound.

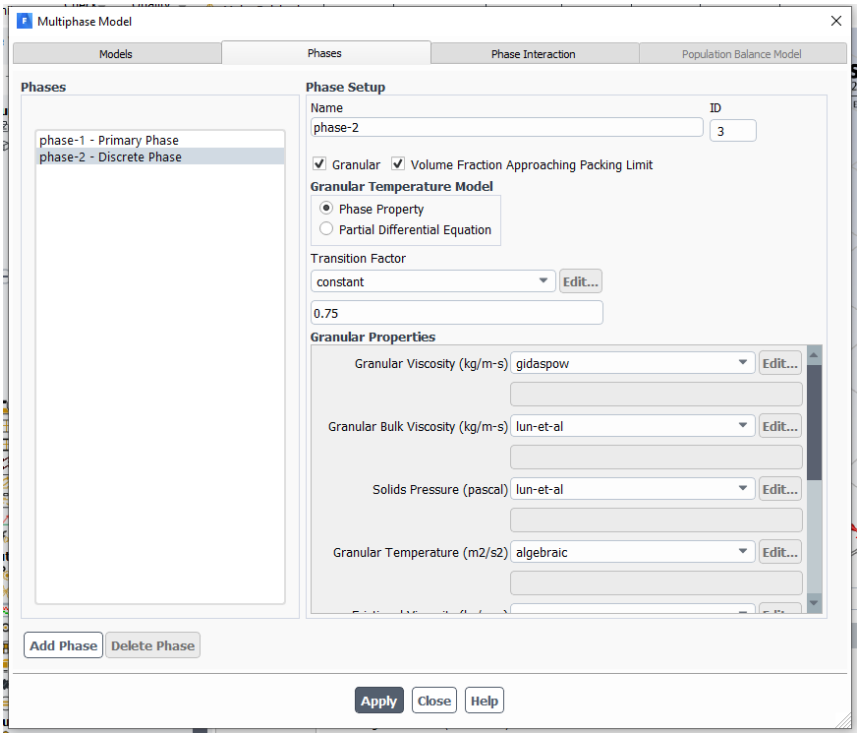

FIGURE 31 - setting discrete phase DDPM

Switching to the material section, we have to change the density of Anthracite to 1760 kg/m3.

Inside the boundary condition, we put the velocity of the input for phase-1 equal to 3.7 m/s, and in the mixture-wall part, we can set the rotation of the wall; we have to select absolute, Rotational and put 1 on the x-axis with a speed of 5 rpm. Now go on the DPM section to digits which are the Discrete Phase Reflection Coefficients [17].

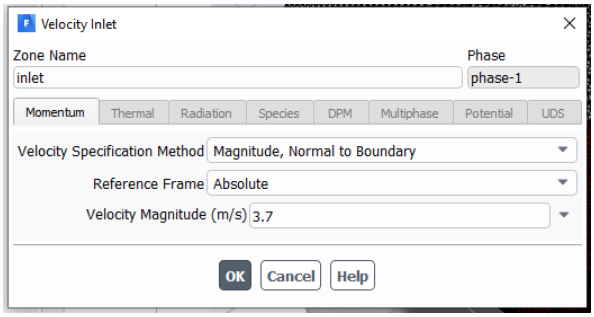

FIGURE 32 - setting inlet velocity DDPM

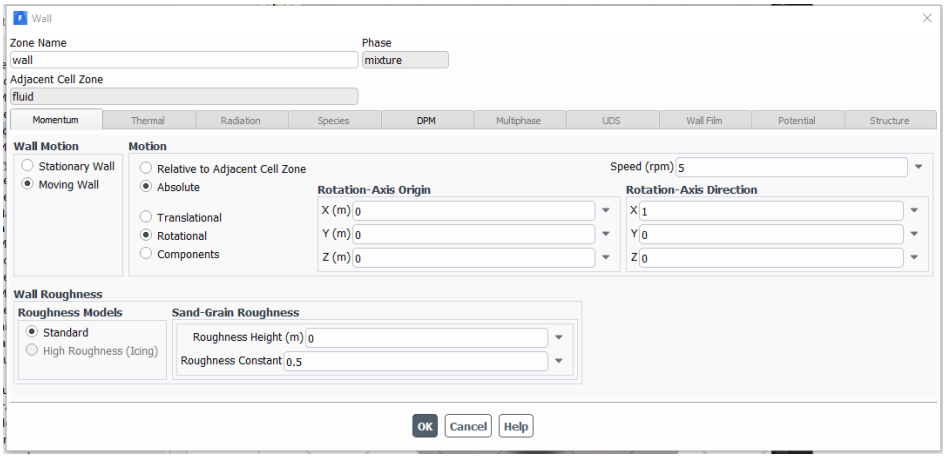

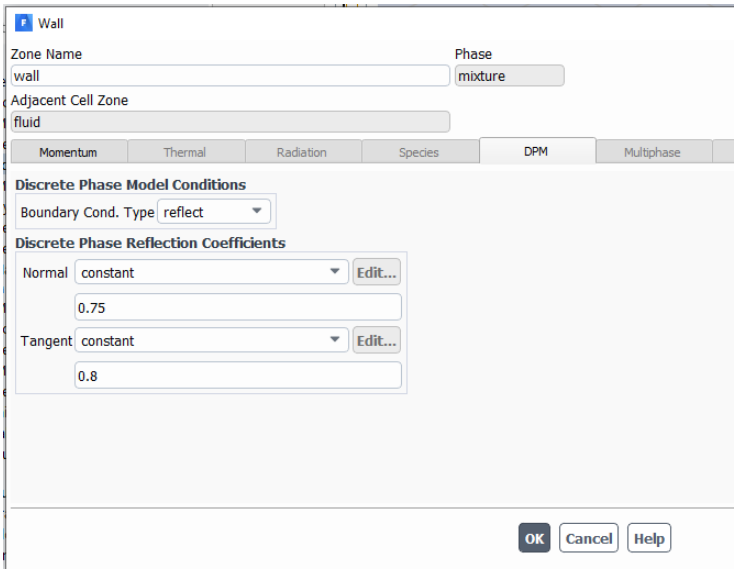

FIGURE 33 - moving wall DDPM

Now we can initialize and do the patch of phase-2 equal to zero, after it, we can save the particle mean residence time and start the calculation with a time step equal to 500, size equal to 0,2, and iteration for every time step equal to 20.
The value of the time step size equal to 0,2; this value was chosen according to pre-analysis and optimization in fluent simulation.

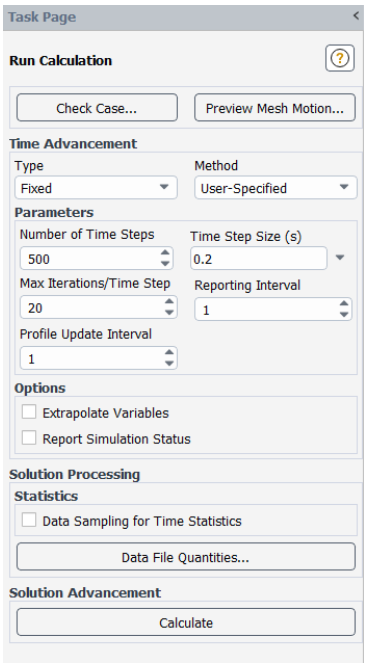

FIGURE 34 - run calculation properties

7.2.2 DPM

To configure this model, it is unnecessary to double precision before starting Ansys fluent because, with DPM, the software works just with one phase.
When the software is open, we have to do a check of our mesh, change the units for the angular velocity to rpm, switch the time do transient, and set the gravitational force according to the slope of my kiln in this way:

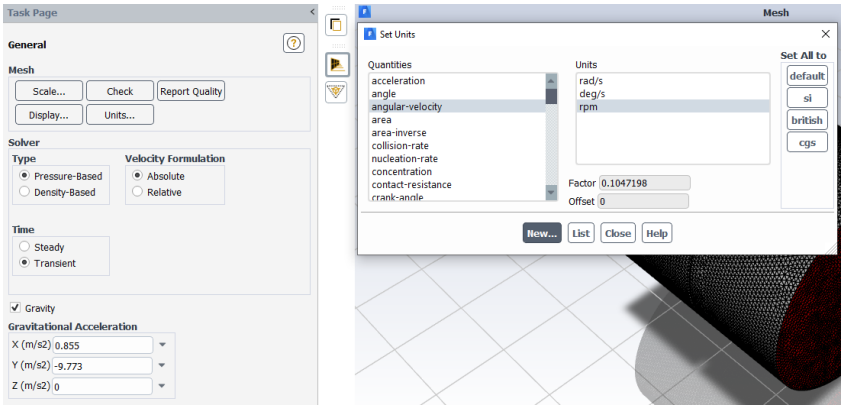

FIGURE 35 - general set fluent DPM

Now we have to activate the discrete phase and add an injection in it; when the window of the injection is open, we have to put injection type equal to a group, number of streams equal to 50, particle type equal to inert, material equal to anthracite and diameter distribution equal to Rosin-Rammler. The other parameters that we must set are showed in the following figure:

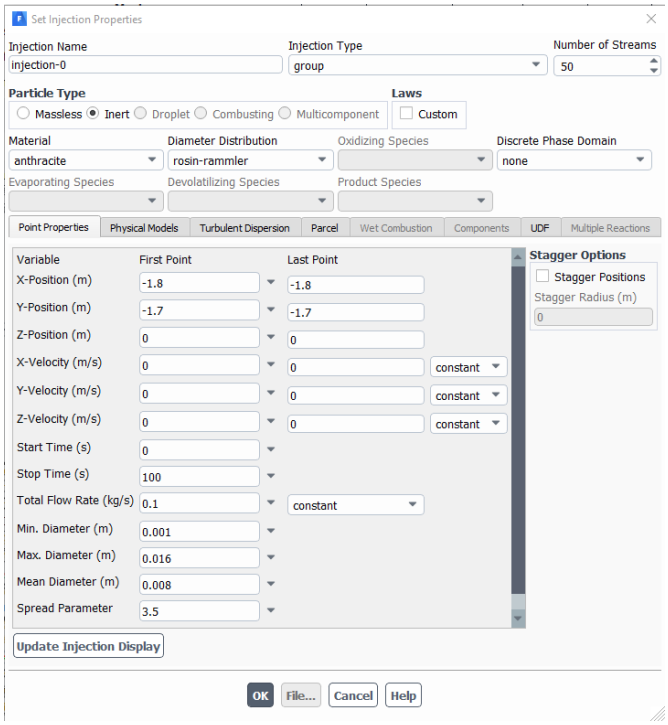

FIGURE 36 - set injection properties DPM

Switching to the material section, we have to change the density of anthracite to 1760 kg/m3.

Now we can set the rotation of the wall. In this model to do this, we have to set the movement of it inside the cell zone conditions, open them, and in fluid, we have to activate mesh motion, then put absolute in the section called relative to a cell zone, put 1 on x in rotation-axis direction and insert the rotational velocity equal to 5 rpm.

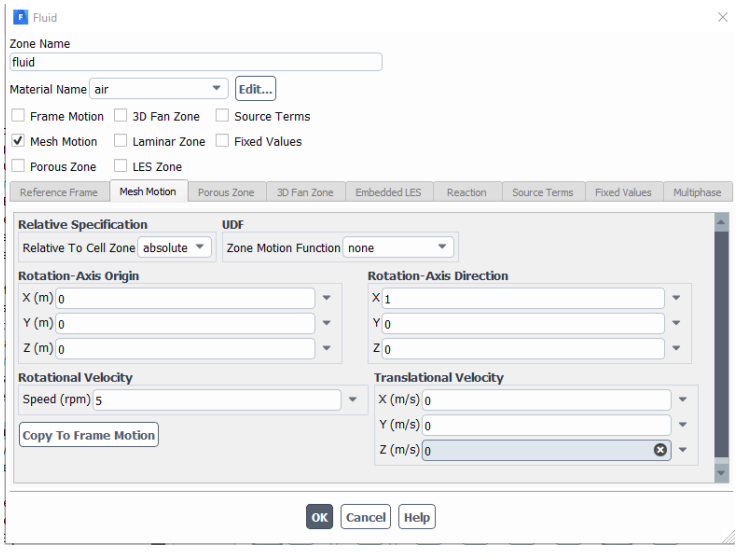

FIGURE 37 - set cell zone conditions DPM

Now we must go to the boundary condition, and inside the wall condition, we have to set the DPM section to digits, which are the discrete phase reflection

coefficients. Then put like in the previous model, the velocity of the inlet equal to 3,7 m/s.

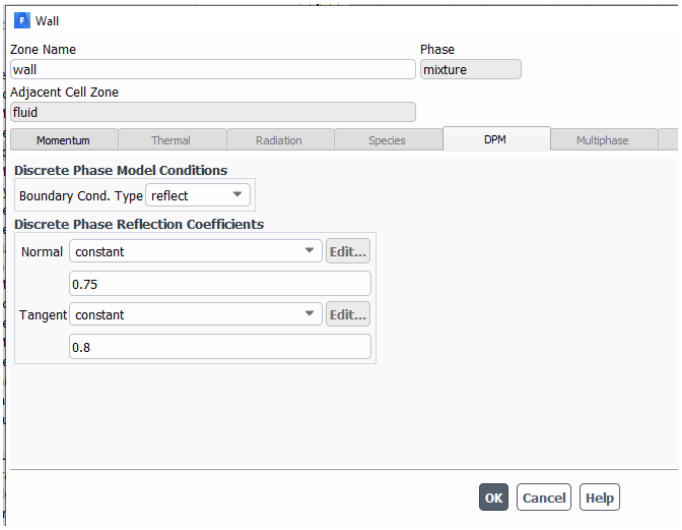

FIGURE 38 - DPM setting for DPM

Now we can initialize. After it, we can save the particle mean residence time and start the calculation with a time step equal to 500, size equal to 0,2, and iteration for every time step equal to 20. To find the value of the time step size, I used the same procedure descript for the DDPM; see equations 36 and 37.

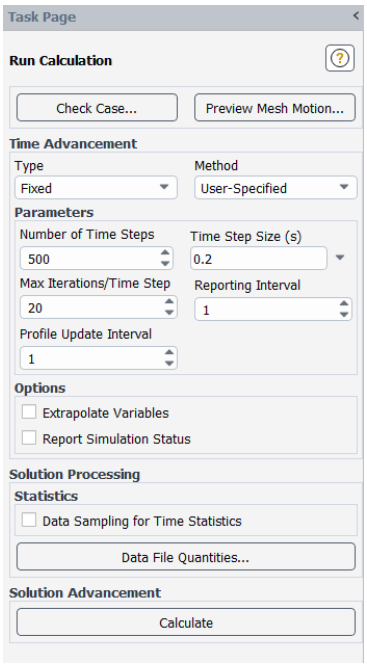

FIGURE 39 - run calculation parameters DPM

7.2.3 Comparison of the models for a smooth cylinder

In this chapter, we find the results of the simulations descript above.

The first simulation that we did is the simulation of the particles inside the smooth rotary cylinder with the model DDPM.

We can notice that the particles follow the rotation of the kiln.

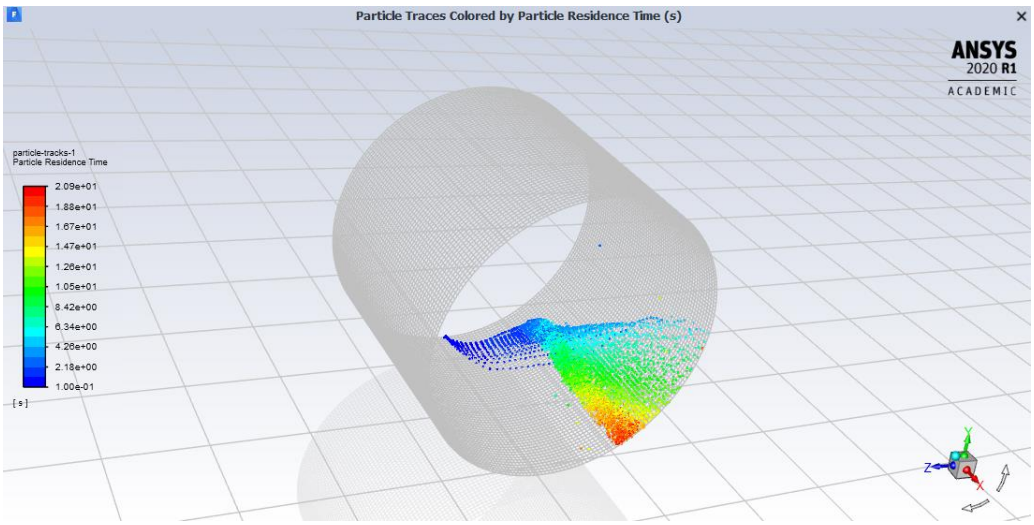

FIGURE 40 - result smooth cylinder DDPM

The second simulation was performed with the DPM model using the same geometry as the first simulation.

We can also notice that the distribution of the particles is following the rotation of the kiln as in the previous case.

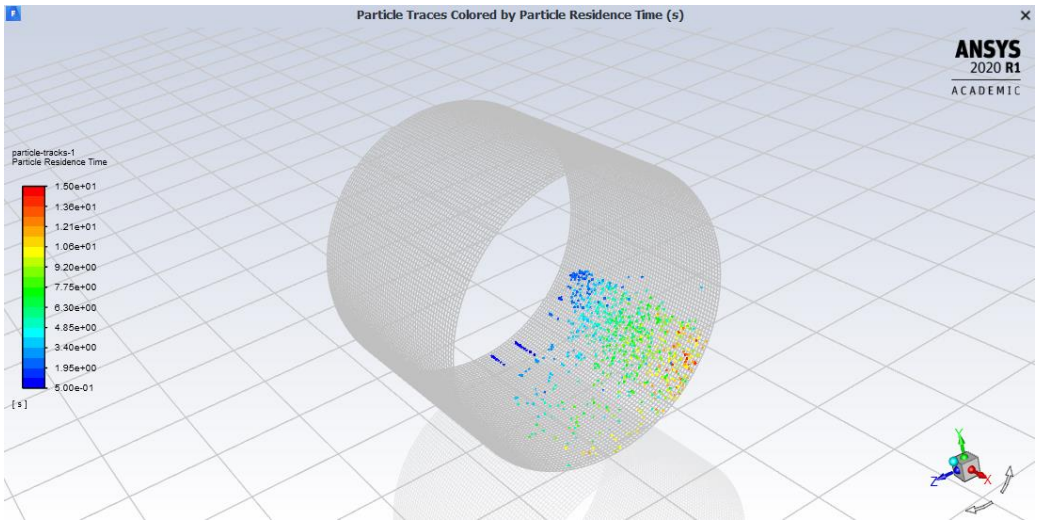

FIGURE 41 - result smooth cylinder DPM

From the analyses carried out, I observed that the most suitable solution model is the DPM, which allows me to have a good quality of the solution without having to carry out simulations that are too sophisticated and costly on a technological level, and we also have enough material parameters for this.

The computational time of the DPM and DDPM present a difference of time equal to 3 hours.

After the simulation and the choice of the model that I am going to use for the other simulations, I can analyse the mean residence time of the simulated case and compare it with the results from the analytical formulas that I already expressed.

We can see this comparison in table 6:

TABLE 6 - comparison between analytical solutions and simulation for mean residence time

Formula	Results
Bernard	17,71 sec
Boateng 1	25,46 sec
Peary 1	26,06 sec
Perry	43,66 sec
Simulation DDPM	35,91 sec
Simulation DPM	21,63 sec

The simulation result with the DPM method performed gives the result equal to 21,63 second instead of the simulation with the DDPM method that gives 35,91 seconds second. The value of the DPM method is closer to the results obtained from Bernard, Boateng and Peary. Instead of this, the Perry formula is the one that presents a larger deviation.

Thanks to this comparison, it is possible to affirm that the DPM method for my specific case is more accurate because it can catch the results of the analytical solution in Bernard, Boateng and Peary. This fully reflects the expectations expressed previously.

Once the comparison between the analytical and simulation results for the particles means residence time is done, it is possible to calculate how many particles enter the kiln with the smooth cylinder design during the 100 seconds of the simulation.

First, it is necessary to calculate how many particles enter the kiln for each second. To calculate the particle flow rate, it is necessary to know the volume of the particles, to take this value, I consider the mean particles diameter of my range, so 8 mm.

I assume that the formula to calculate the volume of the particles is the same used to calculate the volume of the sphere:

$$\mathbf{V_p} = \frac{\mathbf{4}}{\mathbf{3}}\boldsymbol{\pi r_p^3} \qquad \textit{Equation 36}$$

From equation 38, the value of the particle volume for the diameter of 8 mm is equal to 2,145E-06 m^3.

After this calculation, it is possible to proceed with the calculus for the number of particles entering the kiln for each second of simulation.

$$\dot{\boldsymbol{N}}_{\mathbf{p}} = \frac{\dot{\boldsymbol{M}}_{\boldsymbol{flow}}}{\boldsymbol{V_p} * \boldsymbol{\rho_{clay}}} \qquad \textit{Equation 37}$$

The result of equation 39 gives the value of the particles that enter in the kiln for each second; this value is equal to 30082 $\frac{particles}{second}$.

Multiplying the value obtained from equation 39 with the simulation time of 100 seconds, we obtain the total amount of particles entering the kiln during the simulations. This value is equal to 3008200 $\frac{particles}{simulation}$.

To verify if the simulation time equal to 100 seconds is enough to describe the problem, I try to do a simulation of 105 seconds in such a way to make a comparison between the particle's distribution for the 100 seconds simulation and the 105 second's simulation.

It is possible to notice the particles distribution at the output for the simulations time described in table 7:

TABLE 7 - checking of the simulation time

100 seconds	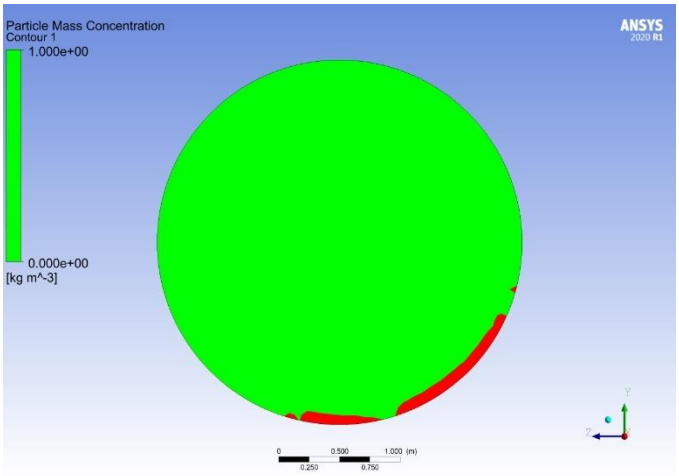
105 seconds	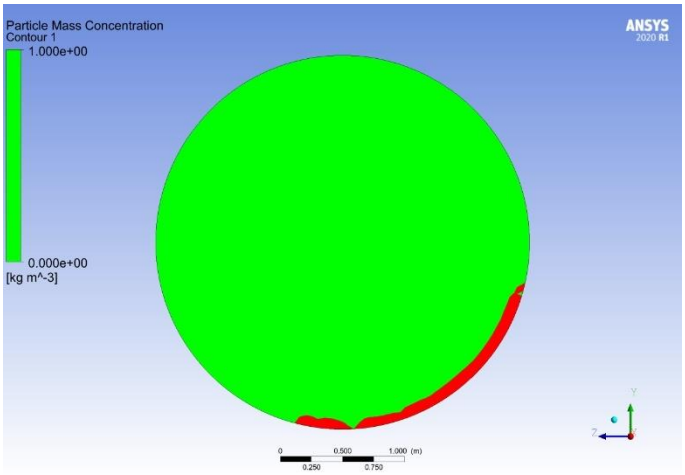

From the analysis of the results obtained from this comparison, it is possible to notice that the distribution of the particles for all three cases is similar.

The particles distribution is mainly concentrated in the bottom right side of the kiln, which means that the particles do the same movement and respect the theoretical things expressed in the chapters above. The particles following the rotation of the kiln.

To find these pictures, I used the post-processing software of Ansys. I created a contour in the kiln outlet section, and the variable chose was the particles mass concentration.

After this, to have better contrast between air and anthracite, I changed a bit the predefined setting, the value list selected equal to the value list to obtain green for the air and red for the particles of anthracite.

For this reason, it is possible to affirm that the chosen simulation time of 100 seconds can give the correct distribution of the particles at the outlet section of the kiln.

For this reason, it would have no sense to perform a simulation with a longer time since the final results are really similar compared with the simulation performed for 100 seconds.

7.3 Simulations of dam, hooks, and mixers

Once we analyse what type of simulation we have to perform to have an accurate result, we decide that the discrete phase model is the correct method; we can start to do the simulations for the geometries with the basic interior designs.

The designs that we are going to analyse are the following:

7.3.1 Cylinder with dam

This section has been analysed the simulation for the cylinder with the dam.

First, it is time to do the mesh. For this geometry, the mesh size is 30 mm; with this mesh size applied to this geometry, it is possible to obtain the correct values for the skewness and the orthogonal quality that respect the standard necessary.

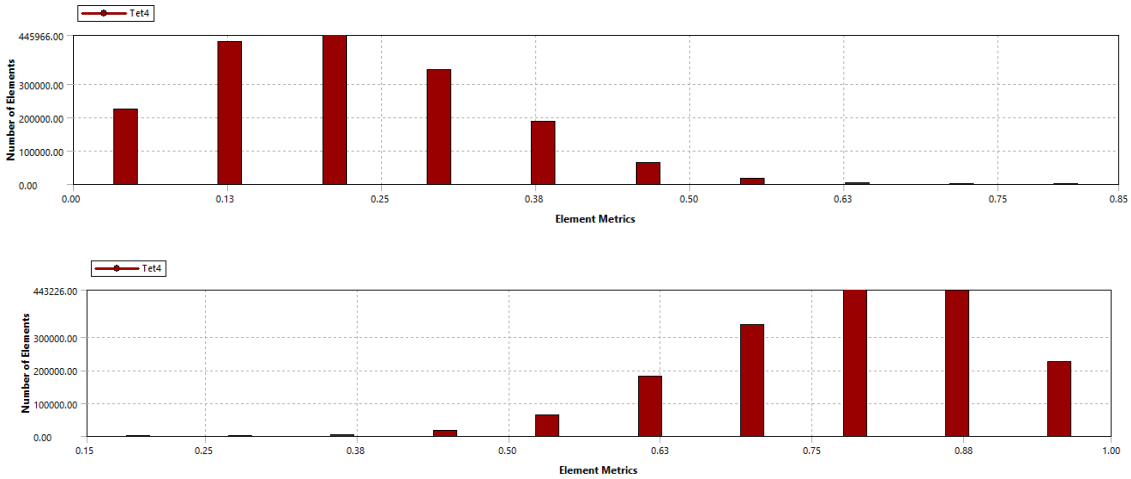

FIGURE 42 - skewness and orthogonal quality cylinder with dam

After the definition of the mesh, it is possible to configure Fluent and perform the simulation.

As has been explained above, the method of simulation used is DPM; thanks to this method and the analysis performed in the previous chapter, it is sure that the result obtained is correct.

The simulation that performed runs for 100 seconds, this amount of time allows performing simulation that gives good result.

The design of the cylinder with the dam is represented in figure 43:

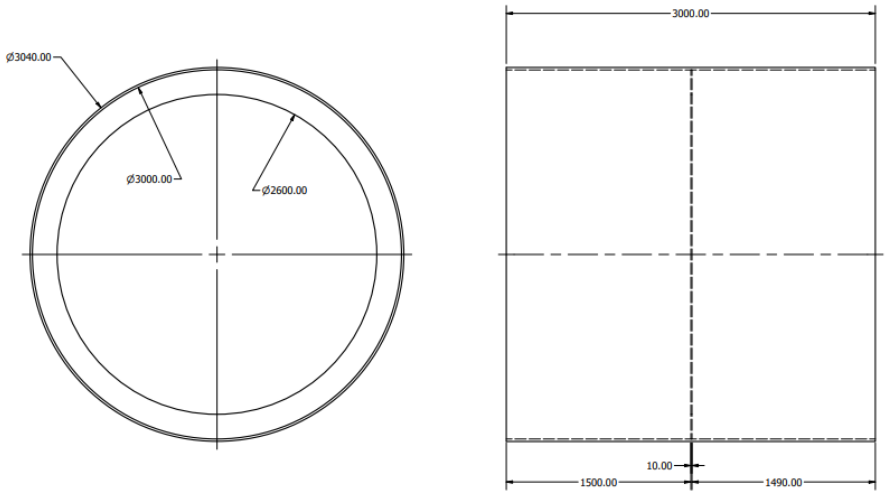

FIGURE 43 - design cylinder with dam

After this amount of time, the following distribution of the particles is obtained; these confirm that the dam increases the mean particle residence time, but it is not able to increase the mixing of the particle in my system.

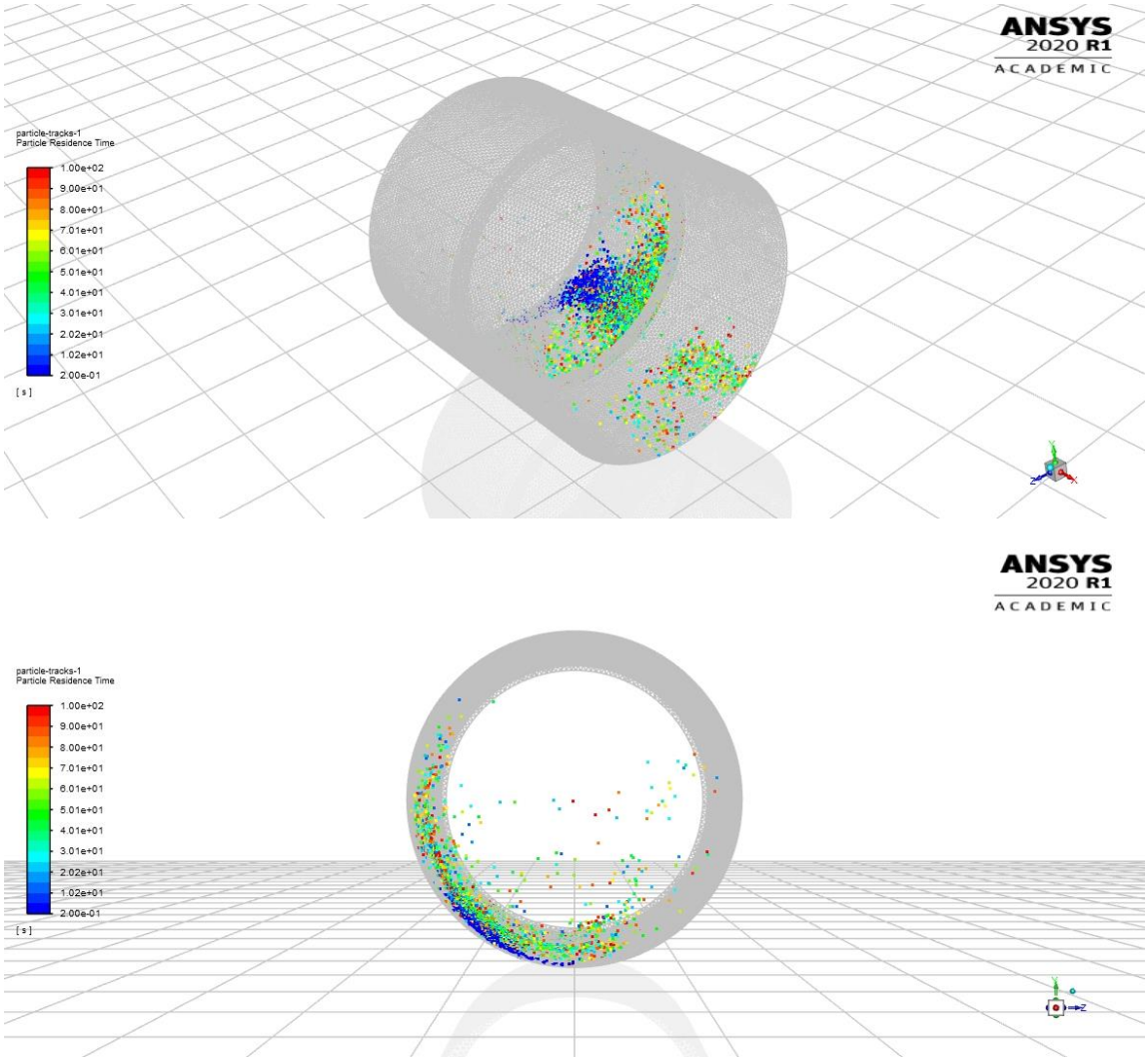

FIGURE 44 - result cylinder with dam

7.3.2 Cylinder with hooks

After the analysis of the cylinder with the dam, now it is time to focus on the next geometry that is the cylinder with hooks.

Theoretically, the hooks can increase the mixing of the particle inside my system without affecting much of the mean residence time.

For these reasons also without any simulation, it is possible to affirm that the final design can be composed only with hooks.

The simulation is performed with a length of 100 seconds; the mesh size for this geometry is 30 mm; thanks to this amount of mesh, the value of the skewness and orthogonal quality are respected.

These are the graphs of the mesh quality for skewness and orthogonal quality:

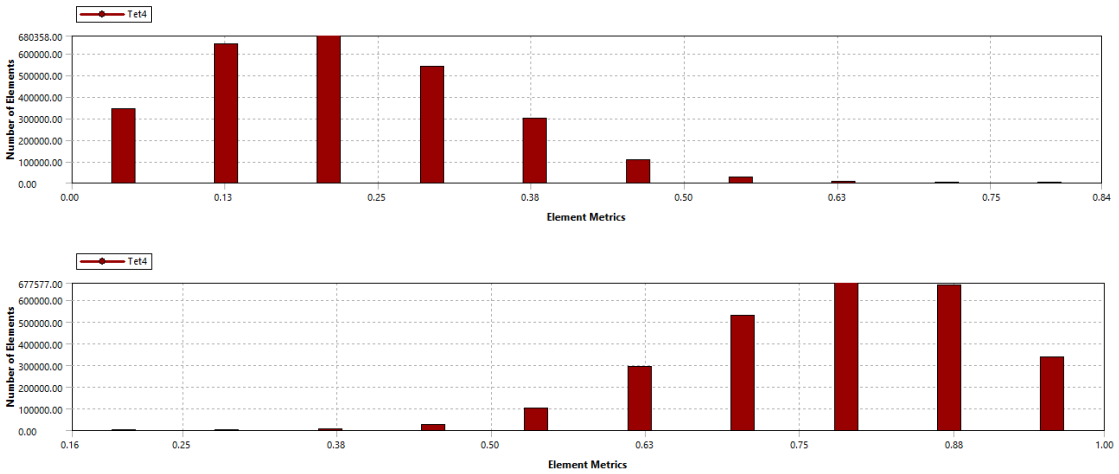

FIGURE 45 - skewness and orthogonal quality cylinder with hooks

Once the mesh is done, it is possible to proceed with the configuration of Fluent for the discrete phase model.

The design of the cylinder with hooks is the figure 46:

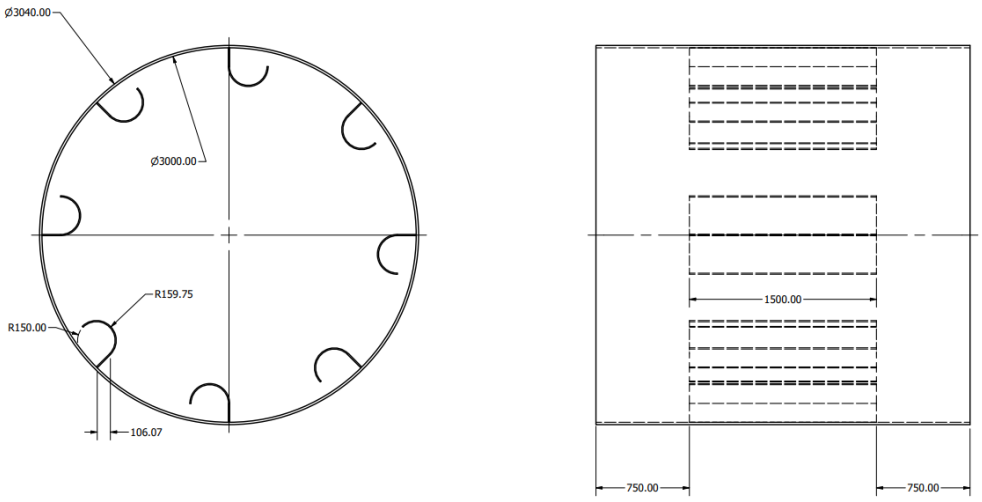

FIGURE 46 - design cylinder with hooks

After the simulation, the following distribution of the particles is obtained and, as the theoretical background told, the hooks can take the particle from the bottom and lift them up to the cylinder, but they do not increase substantially particle mean residence time.

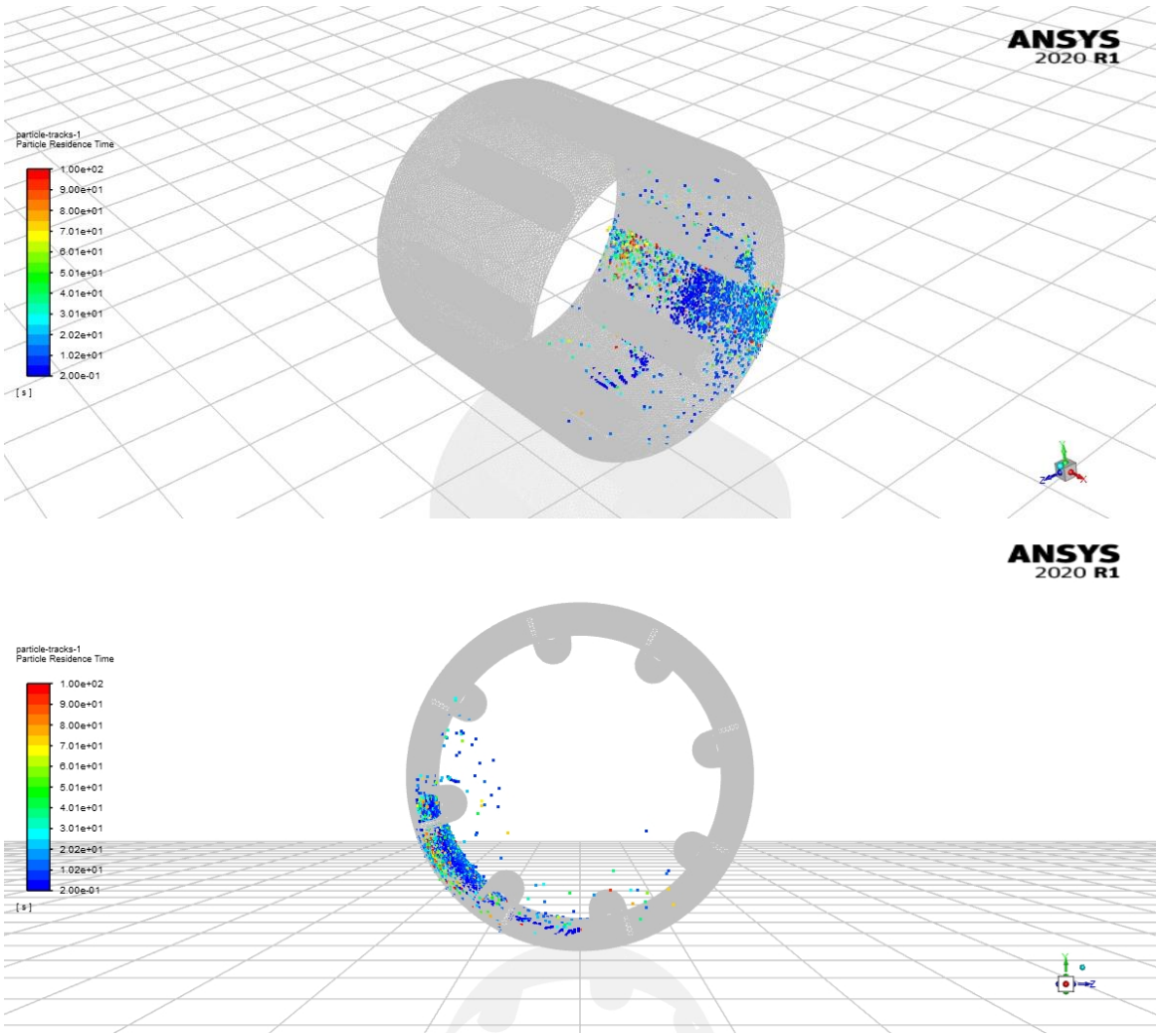

FIGURE 47 - result cylinder with hooks

7.3.3 Cylinder with mixers

The simulation for the cylinder with the mixers should give the homogenization of the flow.

The design of the cylinder with the mixers allows the flow of particles to mix better within the volume of the kiln; thanks to this, there is a more homogeneous exposure of the particles to the flow of hot air.

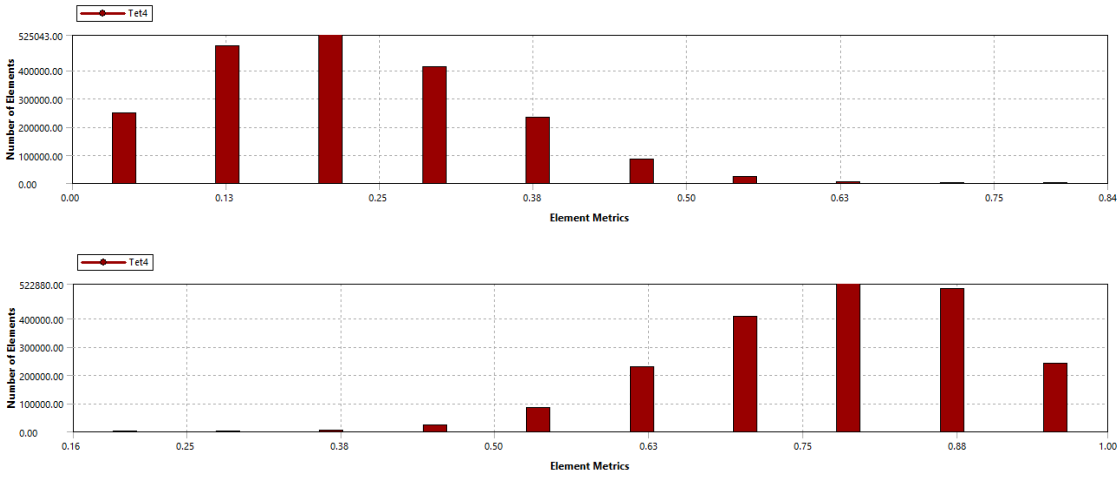

FIGURE 48 - skewness and orthogonal quality cylinder with mixers

Once the mesh is done, the configuration of Fluent was done.

The design of the cylinder with mixers is shown in figure 49:

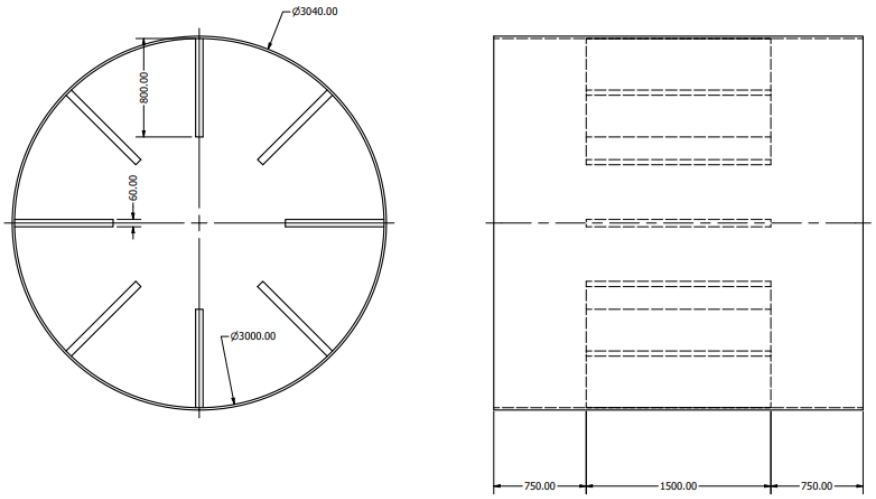

FIGURE 49 - design cylinder with mixers

The simulation takes place for 100 seconds, and the result obtained is shown in figure 50:

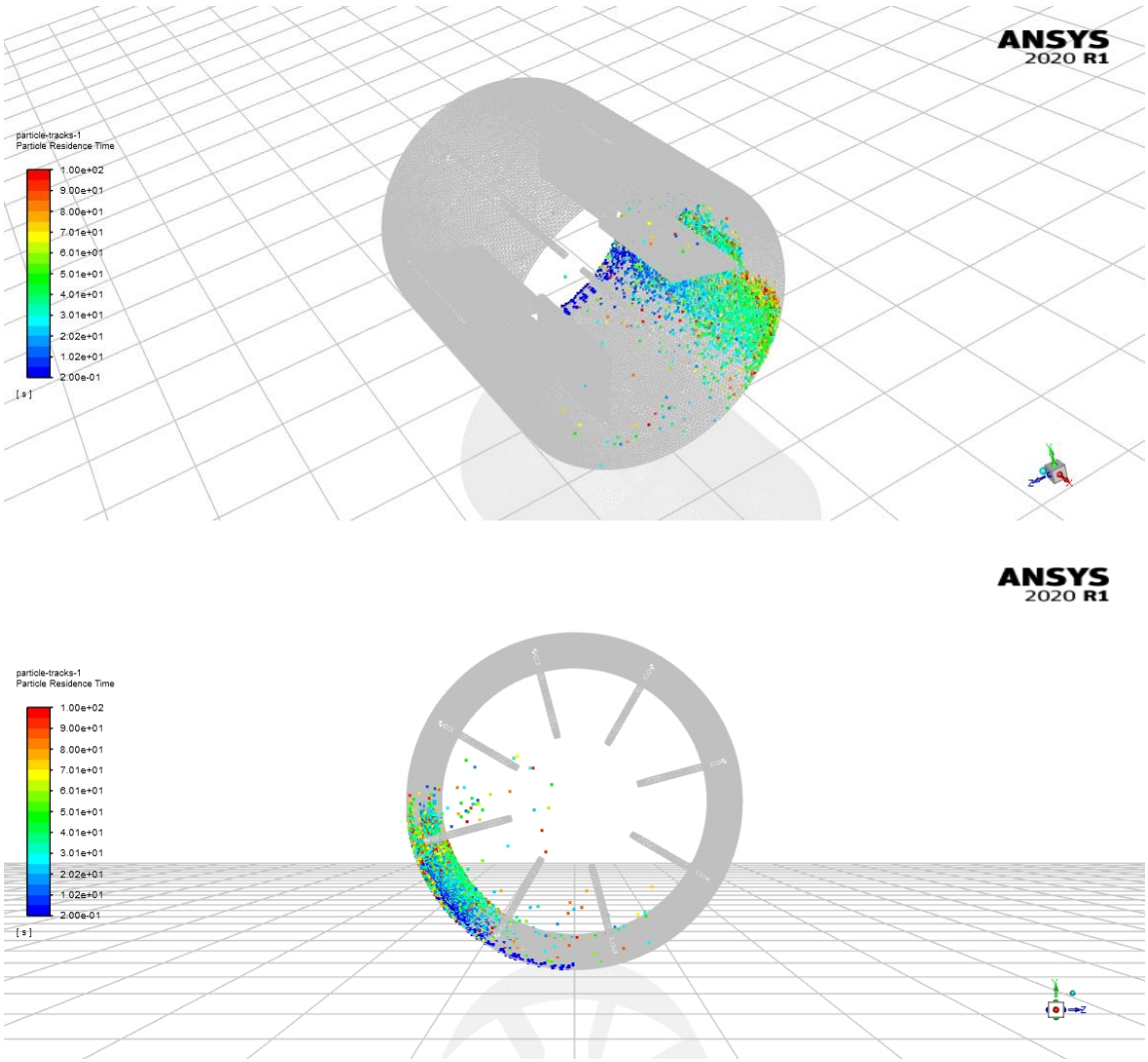

FIGURE 50 - result cylinder with mixers

The mixers do not influence too much on the particle mean residence time, but, as expressed in the previous chapter, the mixers can create a better mixing for the flow of the particles in the kiln.

Thanks to this characteristic, the heat transfer between the particles and the air increase and is obtained a more homogenization of the heat.

7.4 The first study of design

After the simulations, it is possible to start to study the differences between these designs.

The first thing that was done was to calculate the mean residence time of the particles for each geometry in such a way as to compare them and discover which geometry can help the increasing of particles mean residence time.

TABLE 8 - comparison of results for mean residence time for basic geometries

	Smooth	Dam	Hooks	Mixer
MODE [sec]	18,50	27,50	28,80	31,00
MEAN [sec]	21,63	30.04	28,82	34,36
MEDIAN [sec]	16,50	24,50	23,2	27,50

From table 8, it is possible to notice that the geometry with the dam, as expected from the theory part, helps the increasing of the particles mean residence time; also the design with mixers gives a good value of mean residence time, but the highest value has a mixer. The geometry with the hooks gives lower advantages compared with others given geometries.

After calculating these variables and their analysis, it is possible to generate the graph of the normal distribution of mean residence time of particles after 100 seconds for each geometry.

To construct these graphs, it was necessary to normalize the data of the particles mean residence, and I did it using Microsoft excel, and the function used is ***NORM.DIST(X, MEAN, STANDARD-DEVIATION, CUMULATIVE-FLAG).*** Where:

x corresponds to the cell of particles mean residence time [sec].

mean corresponds to the cell of the average value of the particles mean residence time [sec].

standard-deviation corresponds to the cell of the standard deviation of the particles mean residence times [sec].

cumulative flag is a logical value, it can be True or False; if True, the function gives the cumulative distribution function; if False, the probability of masses function is returned.

After having normalized each value of the particles mean residence times, I created a graph by placing the newly created normalized distribution on the y-axis, and the non-normalized particles mean residence time on the x-axis.

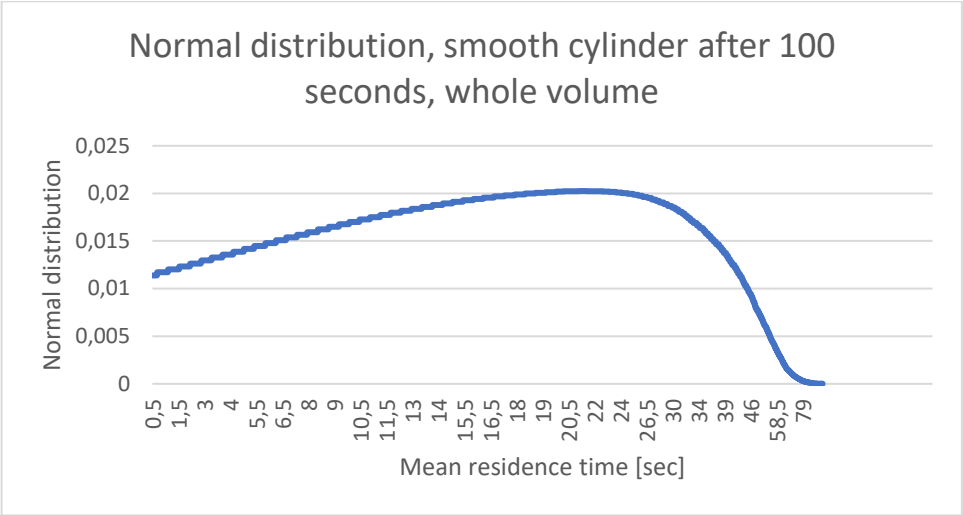

FIGURE 51 - normal distribution smooth cylinder

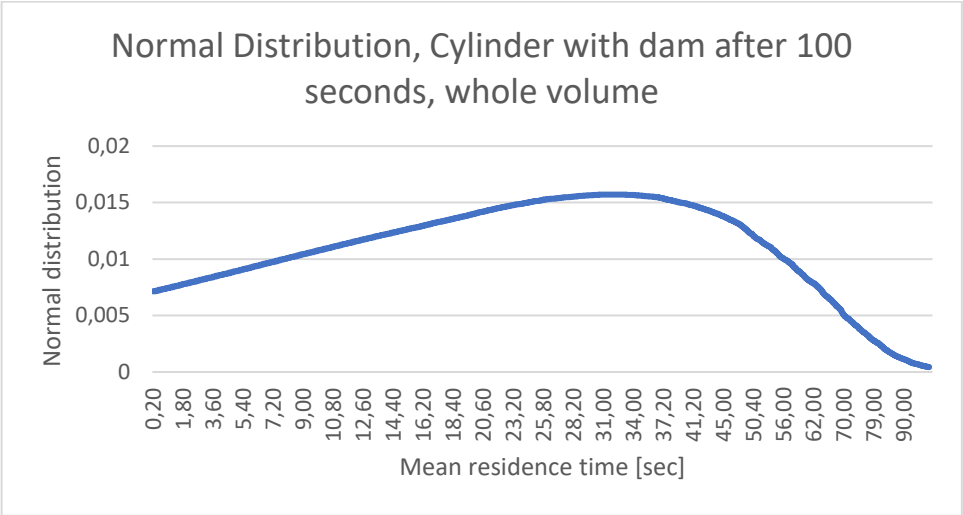

FIGURE 52 - normal distribution cylinder with dam

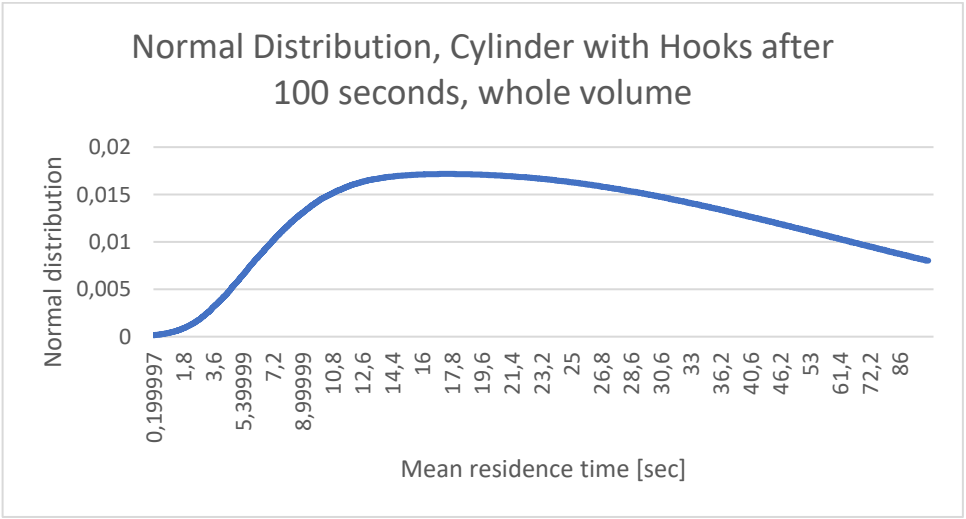

FIGURE 53 - normal distribution cylinder with hooks

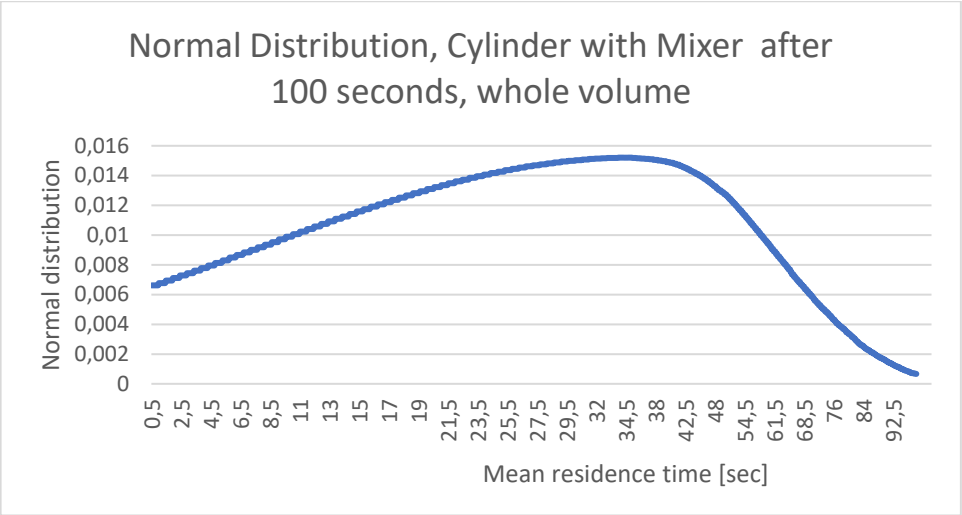

FIGURE 54 - normal distribution cylinder with mixers

The normal distribution, or Gauss distribution, is a distribution of continuous probability that is used to describe the value that tends to concentrate around a single medium value. The normal distribution depends on two mean variables and variance. Increasing the value of the variance, the curve becomes wider; decreasing the value of the variance, the curve narrows and rises.

Analysing the final pictures of the simulations is possible to notice that the dam creates an effect of accumulation of the particle on it; they continue the accumulation while following the rotation of the kiln and can overtake the dam just when they reach height bigger than the height of the dam or when they drop down thanks to the gravitational force.

For this reason, it is possible to affirm that the dam gives big support for the increasing of the particles' mean residence time, but it is not able to increase the mixing of the particles too much.

The second set of pictures that are shown above are for the hooks, it is possible to see that the hooks have a great ability to transport the particle from the bottom part of the kiln until the upper part for dropping them down; in this way, they can increase the mixing of the particles in the kiln, so the heat transfer between particles and air is enhanced.

Speaking of the pictures for the mixers, it is easily visible that they have a big ability to mix the flow of the particles inside the kiln; they affect the particle mean residence time more than the hooks.

Focusing on the mixing of the particles inside the kiln is possible to analyse the data in such a way as to obtain a graph that can help to understand also numerically if the particles are mixed or not.

This graph is possible to find on the y-axis the mean residence time of the particles and on the x-axis the diameter of them. Figure 55 is the graph obtained for: smooth cylinder:

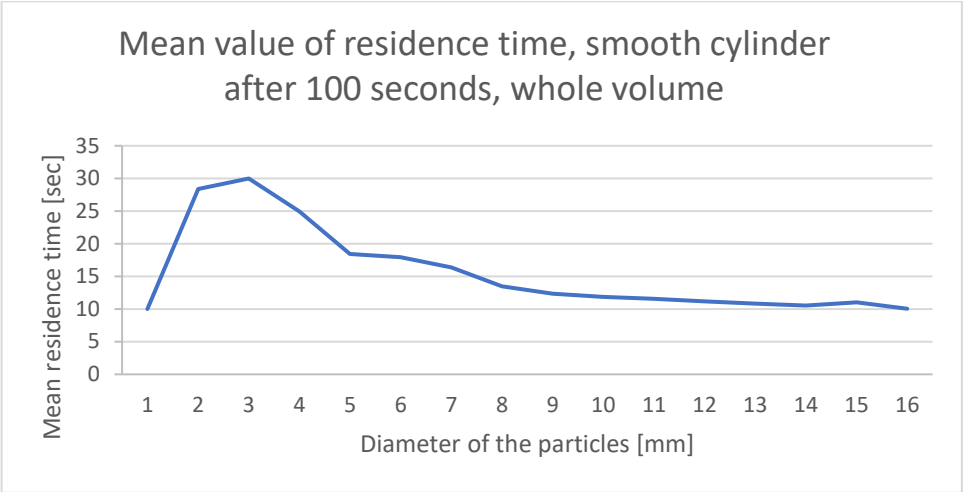

FIGURE 55 - comparison diameter and particle mean residence time for smooth cylinder

For the cylinder with a dam, the following graph is obtained:

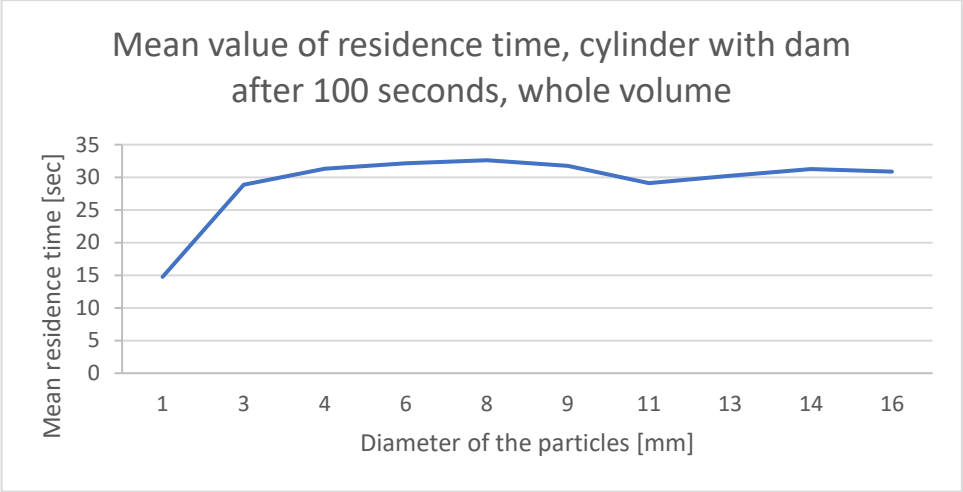

FIGURE 56 - comparison diameter and particle mean residence time for a cylinder with dam

For the cylinder with hooks, the following graph is obtained:

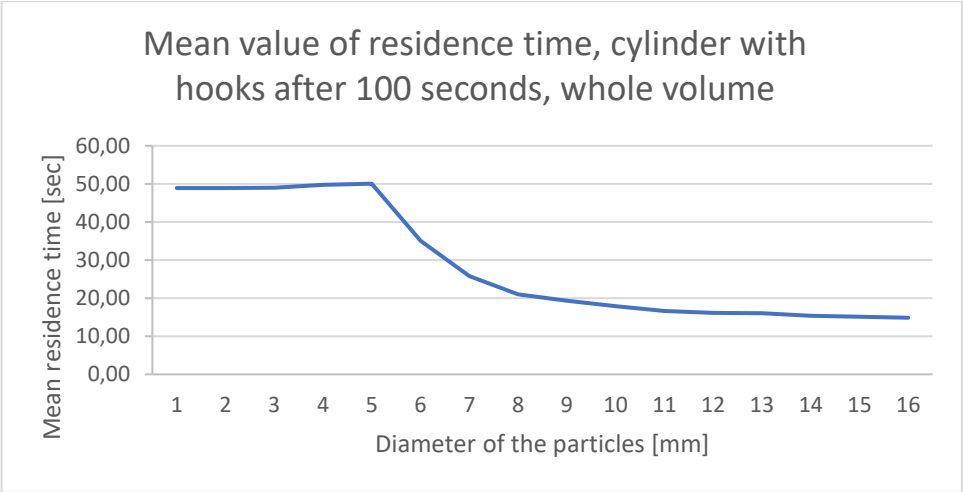

FIGURE 57 -comparison diameter and particle mean residence time for a cylinder with hooks

The graph obtained for the cylinder with mixers is the following:

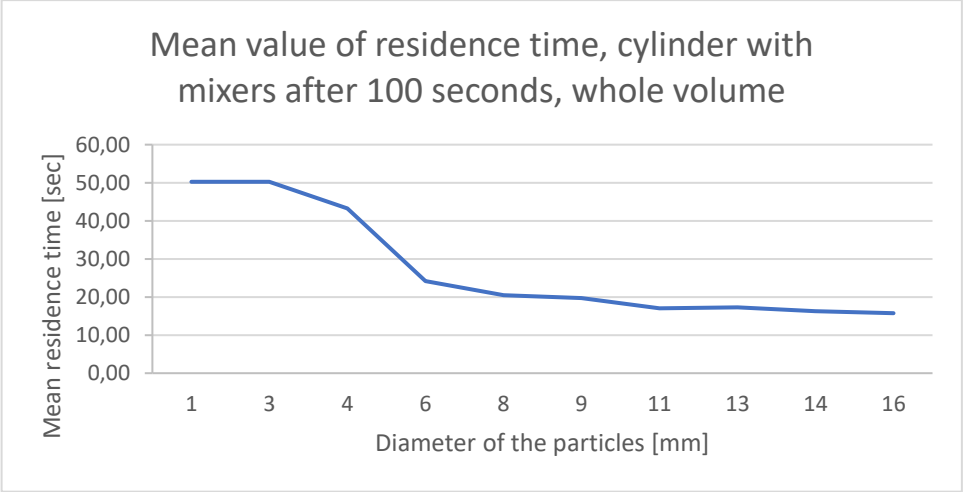

FIGURE 58 - comparison diameter and particle mean residence time for a cylinder with mixers

From the study of the graphs expressed above, it is possible to notice that the dam is the worst configuration if the aim is to increase only the homogenization of the particles in the kiln.

Looking at the graphs for hooks and mixers, the curve of the data obtained is almost the same for both configurations; that is why both configurations have the characteristic to increase the mixing of the particles in the system and homogenize the flow.

These results perfectly express the concept expressed in the article written by Wen Zhong, Chun Hua Wang, Tie Liu, Chun You Zuo, Yuan Hang Tian, Tian Tian Gao (2009), “Residence time and mass flow rate of particles in carbon rotary kilns”, College of Materials and Metallurgy, Northeastern University, Shenyang 110004, China.

In this article, it is possible to find Sai residence time, equation 24. Calculating this equation using the data (table 4), I find the value of the particles mean residence time for the geometry cylinder with the dam.

TABLE 9 - comparison mean residence time cylinder with dam between Sai residence time and simulation

	Mean residence time
Cylinder with dam simulation	30,04 sec
Sai residence time	28,104 sec

The result obtained is equal to 28.104; thanks to this comparison is possible to affirm that we can catch the analytical solution results in Sai residence time.

8. Proposed Designs

This chapter aims to discuss the proposed designs that are thought of after studying the simulations for the basic geometries.

The first part focus on the analysis of the new geometries in such a way to make clear the choice, after this part, it is presented the simulation's chapter in which the method of the simulations are explained, and the results of the proposed geometries are analysed to select the more accurate.

The third part of the chapter is focused on the study of the design of the selected geometries to understand if, with some small modification of them, it is possible to obtain a better result in the form of mean residence time and mixing of the particles in the kiln.

The fourth part is a presentation of the final geometries proposed.

8.1 Proposed geometries

After analysing the statistical data for the mean residence time in the previous chapter and the analysis from the point of view of the mixing of the particles in the kiln, it is possible to start thinking about some final design.

The proposed designs are three; these three designs come after a study of different geometries and consequential simulations that were done to understand well how the particles work inside the kiln and how they react with different structures in the kiln.

8.1.1 Hooked blade design

The first geometry thought is a combination of mixers and hooks.

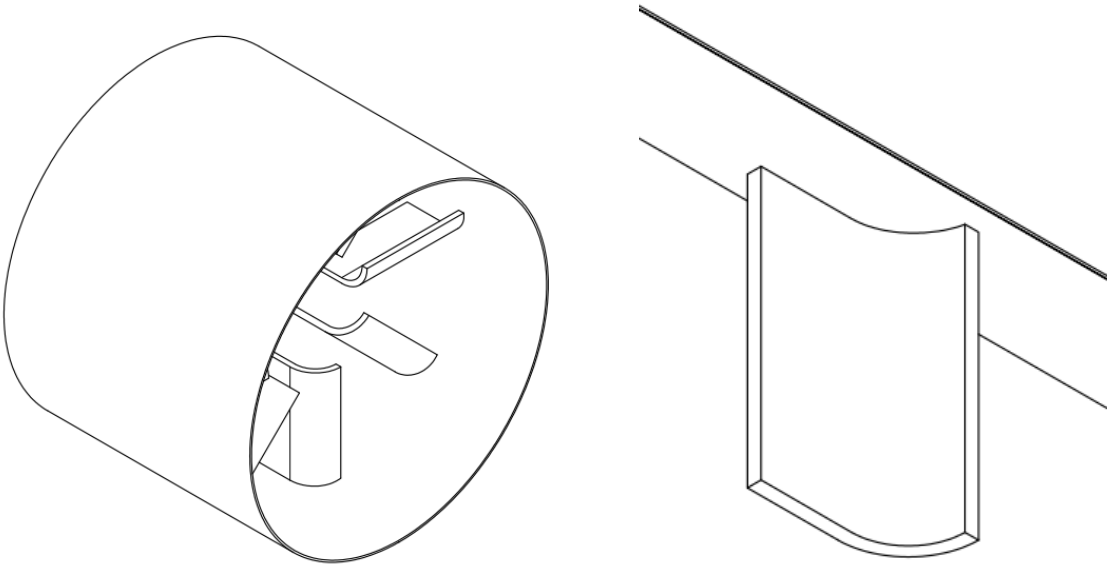

FIGURE 59 – hooked blade design

This geometry was thought just to see how is possible to reach the best mixing in the kiln, it is already clear from the previous study that this design cannot give a high value

of particles mean residence time because both hooks and mixers are not perfect for this goal.

The internal geometry is composed of eight components equal to them; they present the following geometry:

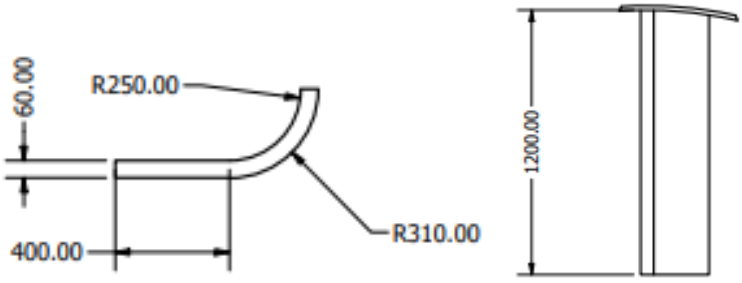

FIGURE 60 - details of the hooked blade design

8.1.2 Inclined mixers with dam design

The second design proposed is the following ones:

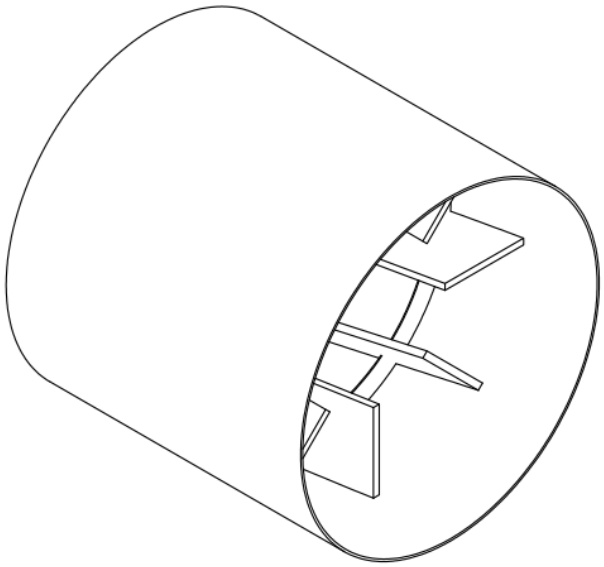

FIGURE 61 – inclined mixers with dam design

It is a combination of dam and mixers; the peculiarity of this design is that the mixers are inclined by 10 ° concerning the horizontal.

This geometry should give a high particle mean residence time because of the studies done in the previous chapter we know that the dam increases too much this parameter, and the mixers can increase it a bit.

Thanks to the combination of the properties of the dam and mixers also a good mixing and homogenization of the particle flow should be reached; this allows the particle to have a good heat transfer with the air.

Specifically for this geometry, the mixers begin to create a rotational movement of the particles, which then, having reached the middle of them, are blocked by the dam, increasing the average residence time. Once over the dam, they continue the rotation movement thanks to the second part of the mixers. This geometer also gets a good mixing of the system.

The internal geometry is composed of one dam and eight mixers:

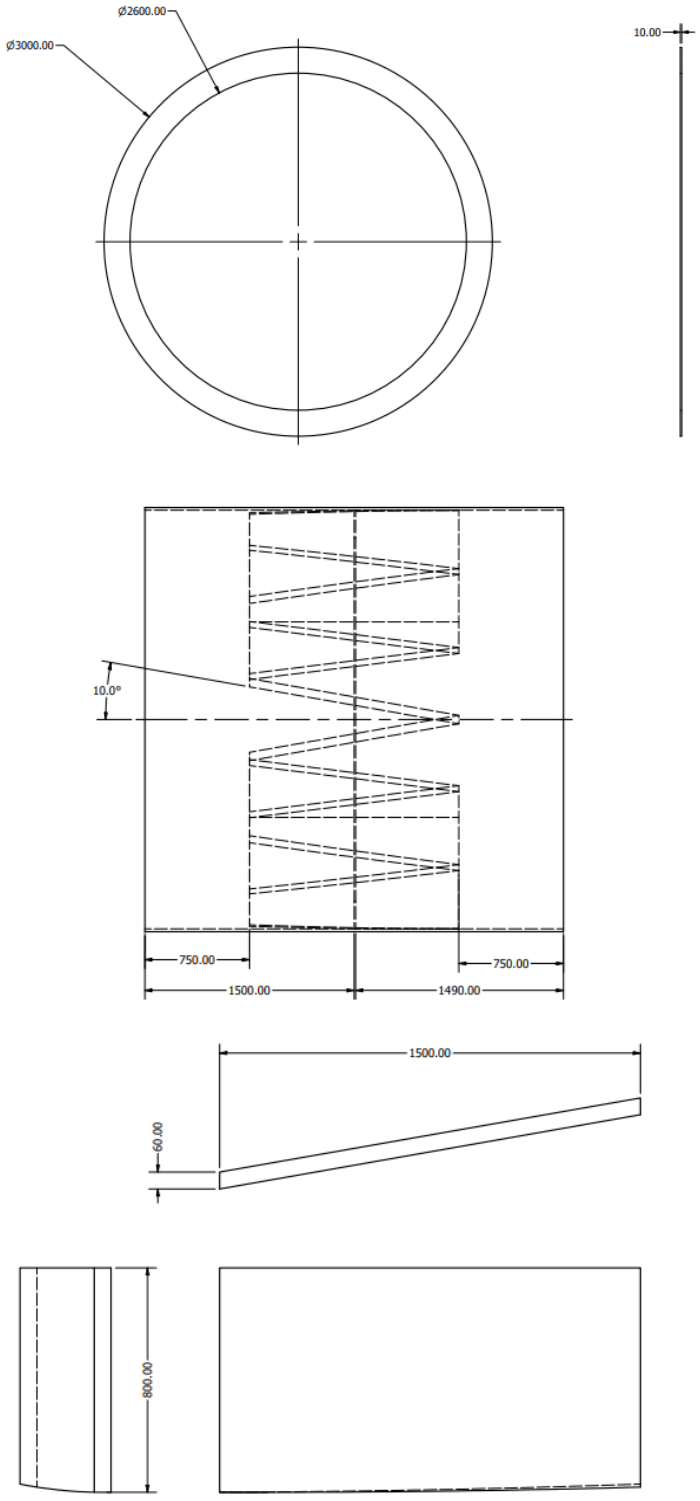

FIGURE 62 - details of the inclined mixers with dam design

8.1.3 Shovels with dam design

The third design is the following:

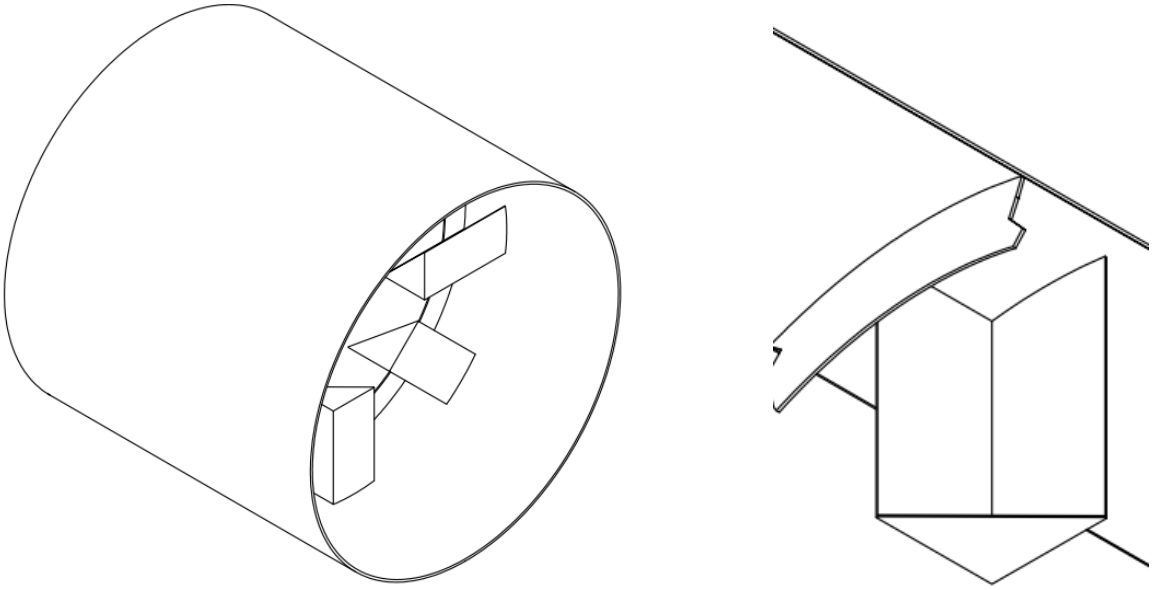

FIGURE 63 – shovels with dam design

This design is a combination of a dam and a structure thought to trap the particles inside it to be able to transport them along with the rotation of the kiln and let them fall from when the highest point of the kiln has been reached.

Through this structure, the idea is to be able to create a homogeneous mixing of the particles inside the kiln in such a way as to increase the heat exchange between them and the air.

With the combination of this geometry to that of the dam, we tried to create a design that could combine the properties of increasing the particle's mean residence time with that of mixing the mixers with a structure that can be conducted to that of the hooks.

The internal geometry is composed of the following compounds:

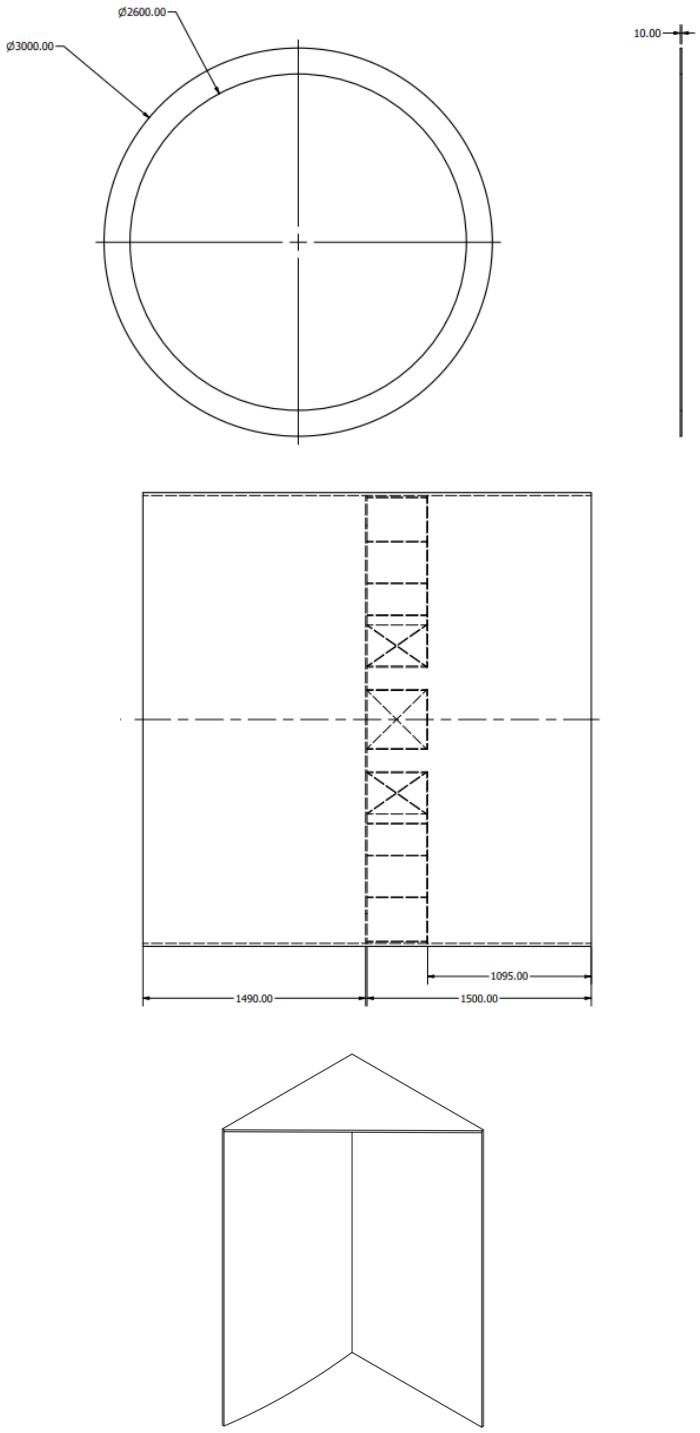

FIGURE 64 - details of the shovels with dam design

The blueprint of all the geometries is presented in the last part of the work.

8.2 Configurations of mesh

This chapter aims to describe how the meshes for the geometries described above were performed to be able to respect the limit values for skewness and orthogonal quality.

For the hooked blade design, the size of the mesh is equal to 30 mm, this size generates 2589552 elements and 477917 nodes.

Thanks to this mesh size I can respect the limit values for skewness and orthogonal quality.

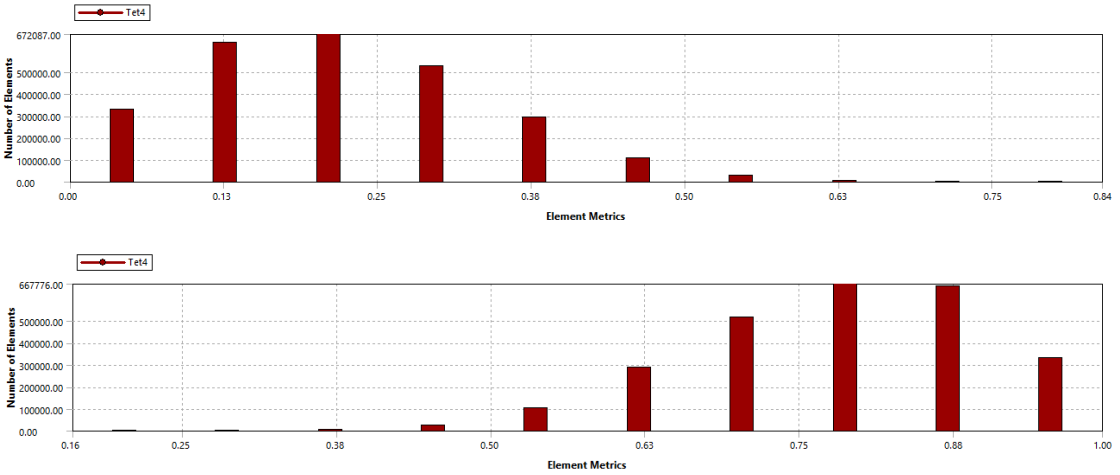

FIGURE 65 - skewness and orthogonal quality for hooked blade design

Speaking of the inclined mixers with dam design, to be able to respect the limit values for orthogonal quality and skewness, the size that is used is equal to 30 mm; this divides the geometry into 2071518 number elements and 386928 number nodes. The following graphs for skewness and orthogonal quality are generated:

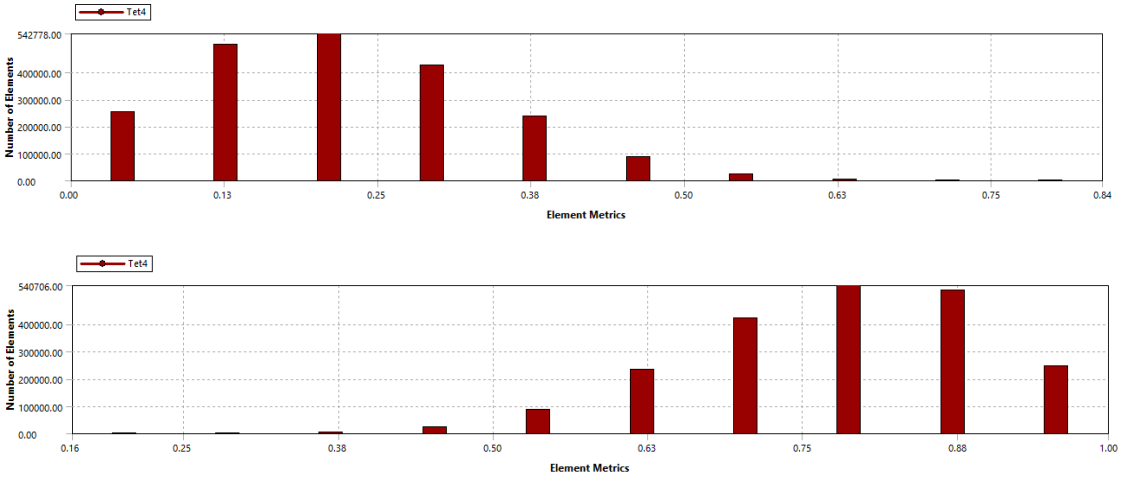

FIGURE 66 - skewness and orthogonal quality for inclined mixers with dam design

The shovels with dam design is the most complex from the point of view of design and number of plane present in it so for this geometry neither the size of 50 mm and the size of 40 mm are enough to satisfy the quality of orthogonal quality and skewness, for this reason, the size of the mesh that it is used for this design is equal 30 mm.

This mesh's size divides the geometry into 1924754 number of elements and 358027 number of nodes.

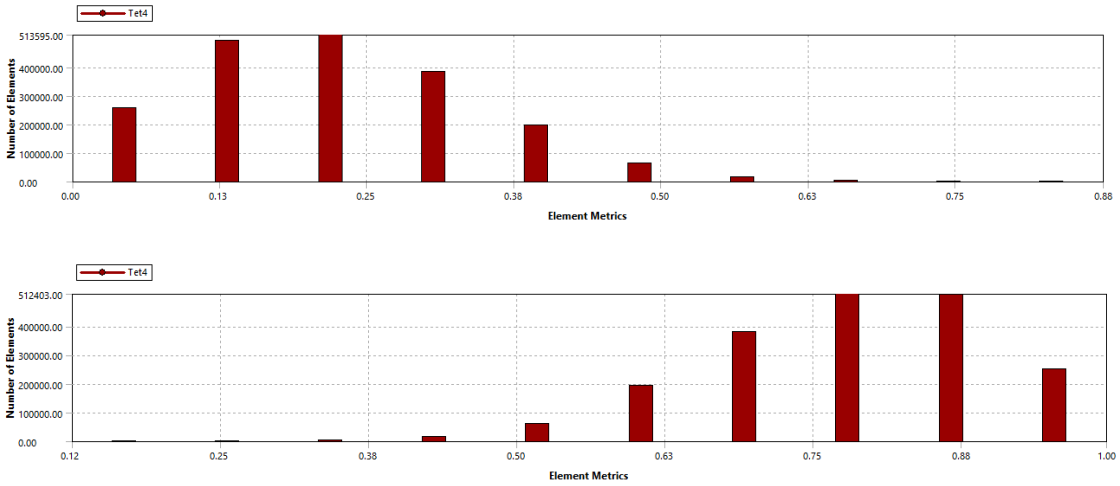

FIGURE 67 - skewness and orthogonal quality for shovel with dam design

8.3 Simulations

This section aims to describe how the simulations of the designs are configurated in the software Fluent with student license and what are the results of the simulations from the point of view of the mean residence time, analysed in a statistical way as for the basic geometries, and of the mixing of the particles inside the kiln.

As explained in chapter "7.2.3.", the simulations are performed using the discrete phase method; this method allows to obtain a reliable result and to perform simulations that do not need too much time to complete.

Once did the meshes for the design, it is possible to start with the configuration of the software Ansys Fluent 2020 R1 with a student license to perform the simulation.

Opened the software, the first thing to do is modify the unit measure of the angular velocity; this is necessary because the kiln that we are analysing rotates with an angular velocity of 5 rpm.

The kiln is inclined concerning the horizontal with an angle of 5°, so the gravitational force that acts on it is directed on the x-axis and the y-axis. The values of the gravitational force, in this case, are 0,855 $\frac{m}{s^2}$ for the x-axis and -9,773 $\frac{m}{s^2}$ for the y-axis.

It is important to utilize the transient regime in such a way as to obtain a more accurate result.

The model used for these simulations is the k-ε, all the explanation about this model is expressed in the chapter "6.6" because the flow regime is turbulent (Reynolds number bigger than 2400).

To set up the particles of clay that enter the kiln, you have to activate the discrete phases and insert an injection. This injection is composed of anthracite as a material; the group of particles that enters the kiln is equal to 5, and the distribution is that of Rosin-Rammler as descript in chapter 8.1.

The diameter of the particles entering the oven, for our case study, is between 1 mm and 16 mm; for this reason, in the Rosin-Rammler distribution, it is set as a minimum diameter value of 1 mm, a maximum diameter value of 16 mm and an average value of the particle diameter 8 mm.

With the hypothesis used for this work, the particles enter the kiln with a flow rate equal to 0,1 kg / s as I explained in chapter 8.

Since the model chosen is the phase model, to set the rotation of the kiln, you have to go to the cell zones conditions; in this section, it is necessary to activate the "mesh motion" button and set the x-axis as the rotation axis with a speed of 5 rpm.

Moving on to boundary conditions, we need to set an air input speed of 3,7 $\frac{m}{s}$ with a flow-directed against the current to the x-axis as my oven works in a counter-current mode.

To set the correlation between particles and wall, on the other hand, it is necessary to go to the boundary conditions of the wall and entering the window called DPM; one must set the discrete phase reflection coefficient constant for both the normal and the tangent and enter the values 0,75 and 0,8 respectively [17].

8.4 Results and comparison

Once the method for configuring the meshes and simulations had been defined, it was possible to carry out the simulations.

The unwinding time of them was 100 seconds; this value allows us to obtain quite reliable results both in terms of the number of particles that enter the kiln and in terms of the number of rotations that the kiln performs on itself (approximately 8 rotations over 100 seconds).

8.4.1 Results hooked blade design

The result of the first proposed design shows us that, as previously explained, the union of the hooks and the mixers does not increase the average residence time of the particles inside the kiln as much.

TABLE 10 - statistical results for mean residence time of hooked blade design

	Hooked blade
MODE [sec]	49,40
MEAN [sec]	32,96
MEDIAN [sec]	26,40

This geometry, however, allows the particles to create a homogenized mix and distribute themselves well in the kiln; thanks to this property, there is a good heat exchange.

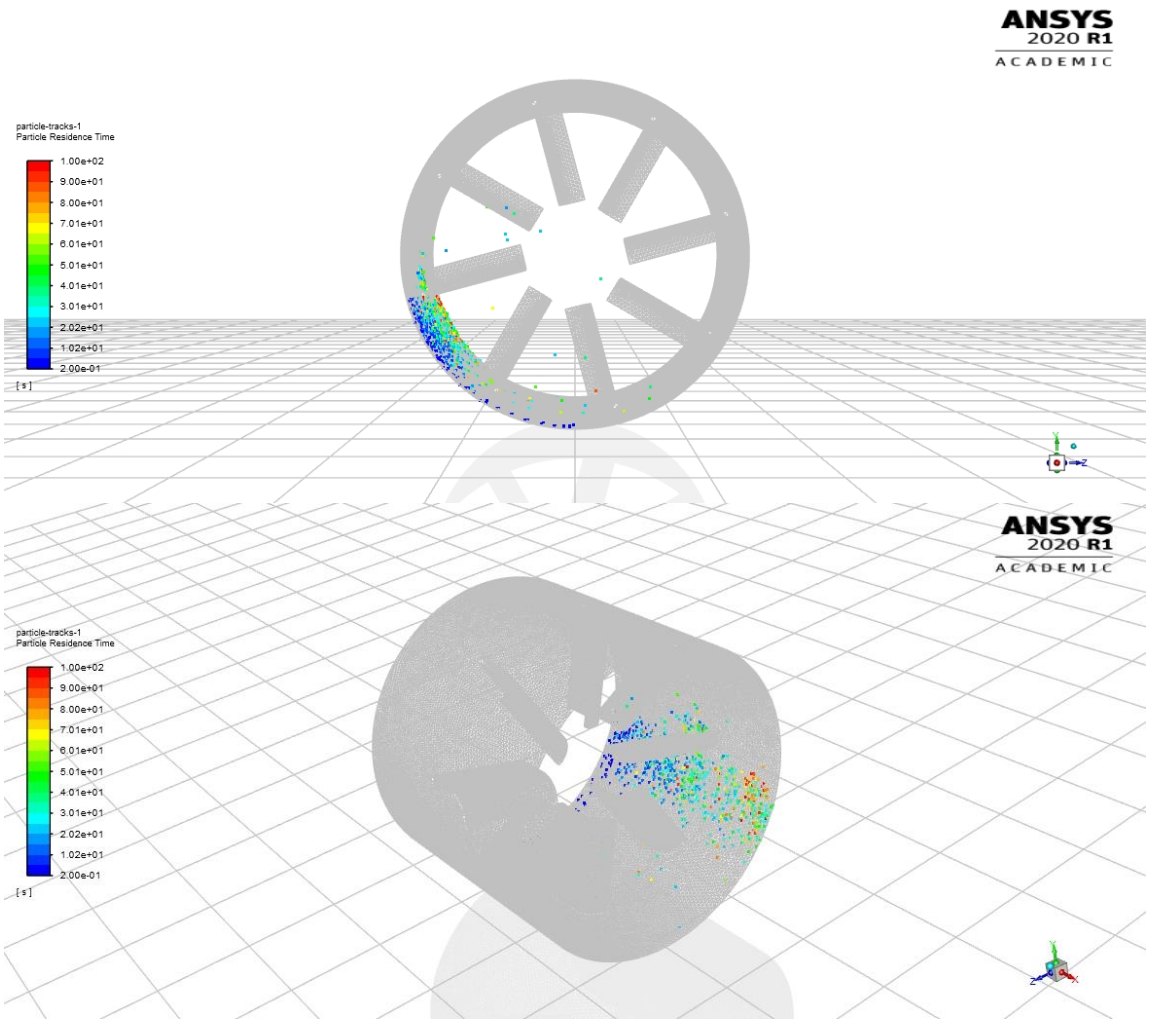

FIGURE 68 - result of hooked blade design

After the analysis of the pictures obtained from the simulation performed, it is possible to analyse the data in such a way to obtain statistic that can measure the mixing of the particles inside the kiln; the object that it was analysed for the mixing of the particles is a graph on which there is the diameter of the particles on the x-axis and particles mean residence time on the y-axis.

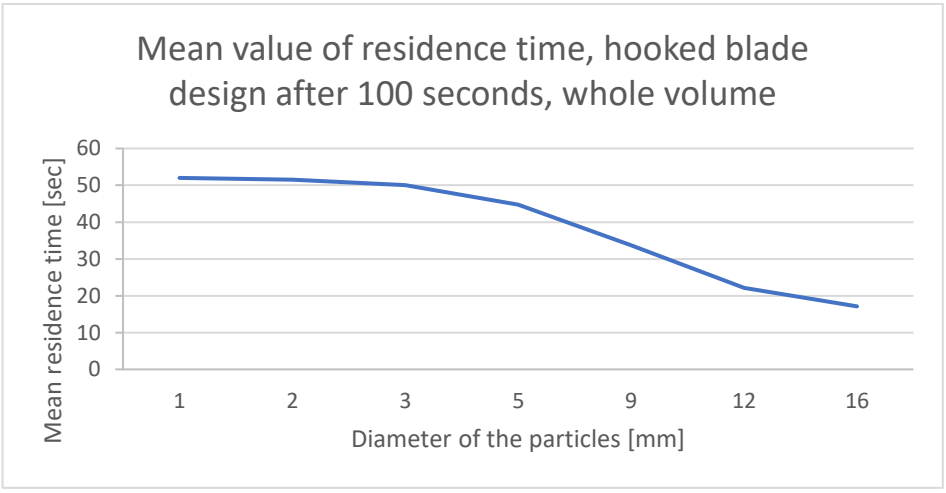

FIGURE 69 - comparison diameter and particle mean residence time for the hooked blade design

8.4.2 Results inclined mixers with dam design

Focusing on the second design, which is composed of the union of a dam and the mixers inclined by 10 degrees with respect to the vertical, we can see that the average residence time of the particles inside the furnace has increased sharply.

TABLE 11 - statistical results for mean residence time of inclined mixers with dam

	Inclined mixers with dam
MODE [sec]	89,20
MEAN [sec]	41,06
MEDIAN [sec]	37,01

Focusing instead on the distribution of the particles, we can see that the inclined mixers do their job well and manage to mix the flow of particles.

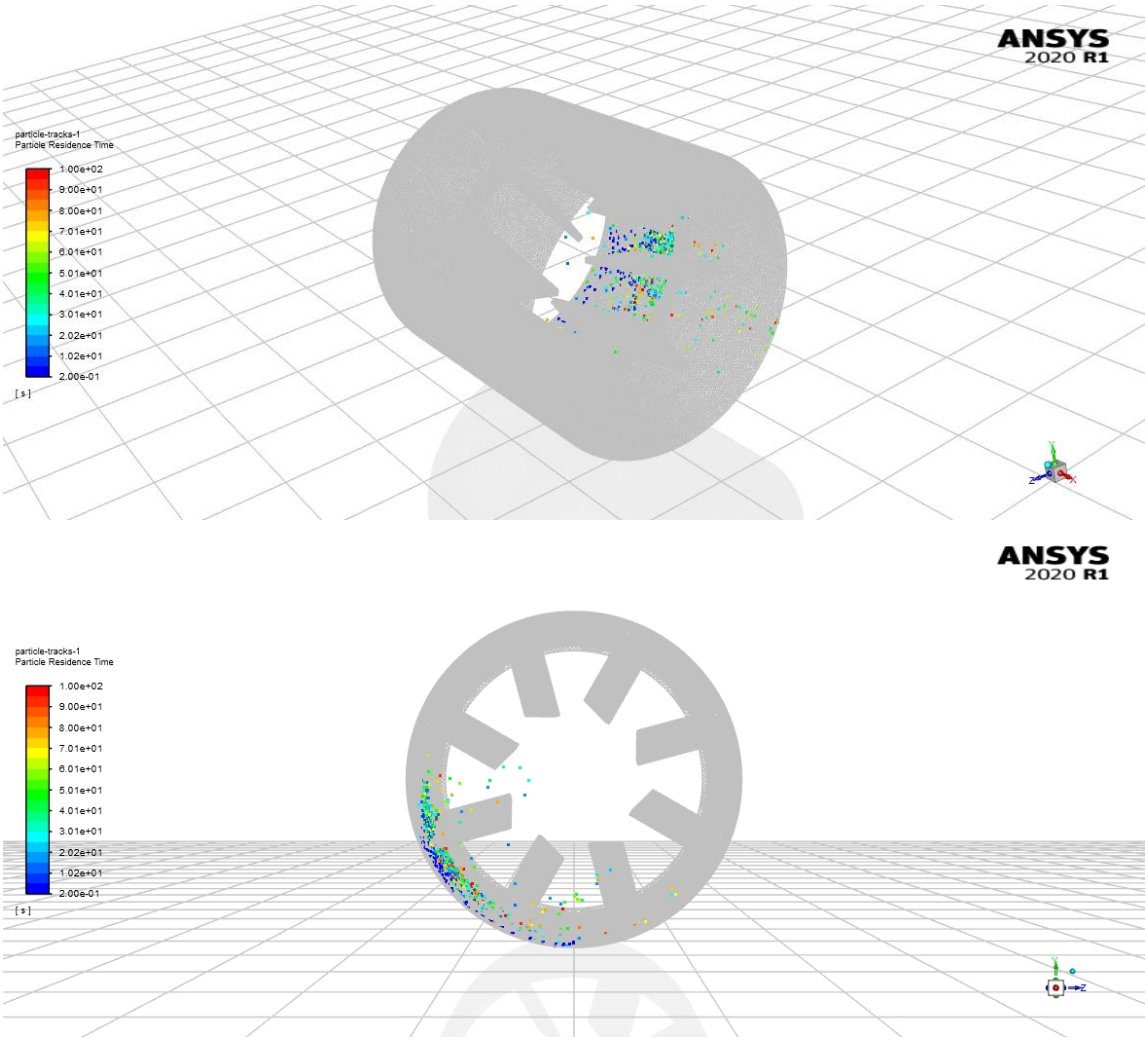

FIGURE 70 - result inclined mixers with dam design

As in the first design, now let keep attention on the graph of the mean value of residence time for the second design:

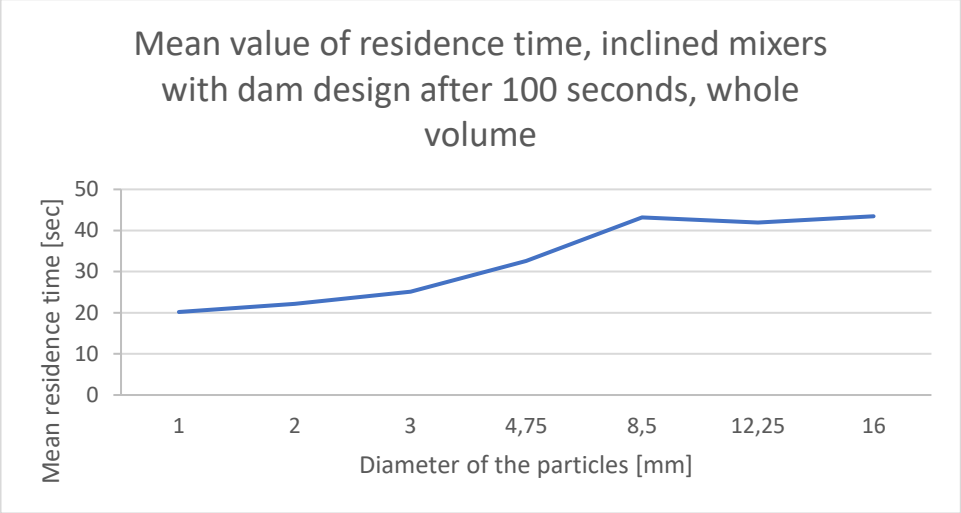

FIGURE 71 - comparison diameter and particle mean residence time for the inclined mixers with dam design

8.4.3 Results shovels with dam design

Speaking of the third design, consisting of a dam and an apparatus that includes a mixer and a hook, it is possible to note that the average time of the particles inside the kiln has significantly increased compared to the basic geometries.

TABLE 12 - statistical results for mean residence time of shovel with dam

	Shovels with dam
MODE [sec]	83,00
MEAN [sec]	44,61
MEDIAN [sec]	41,80

From the analysis of the position of the particles, the flow is well mixed within the kiln, and a lot of particles are in lift.

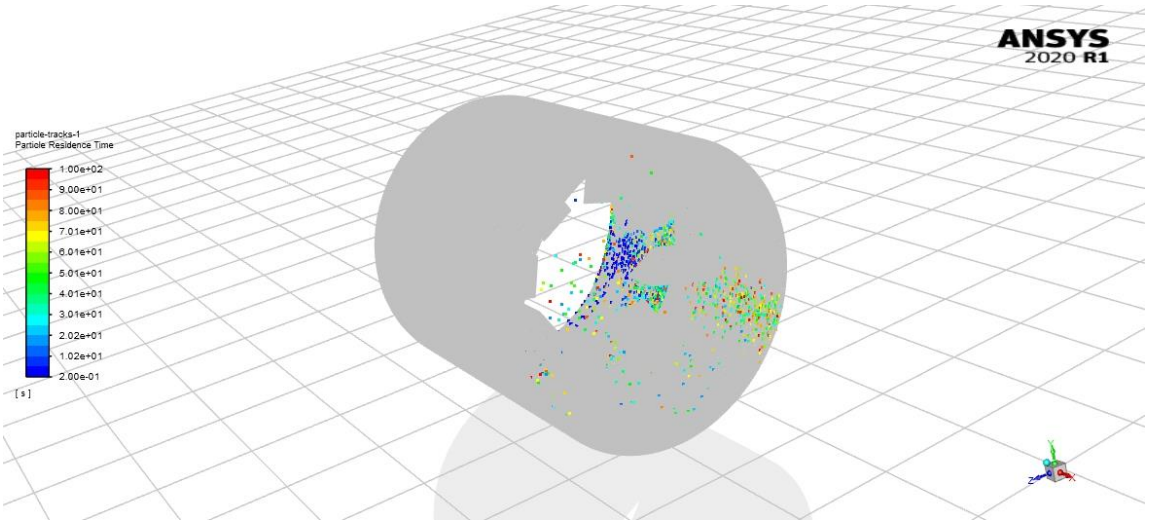

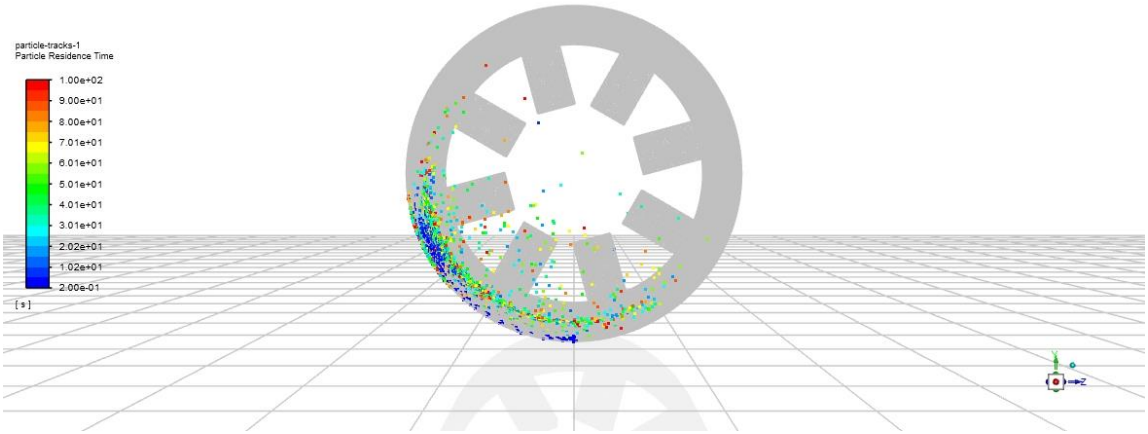

FIGURE 72 - result shovels with dam design

The graph of the mean value of residence time for the third design is:

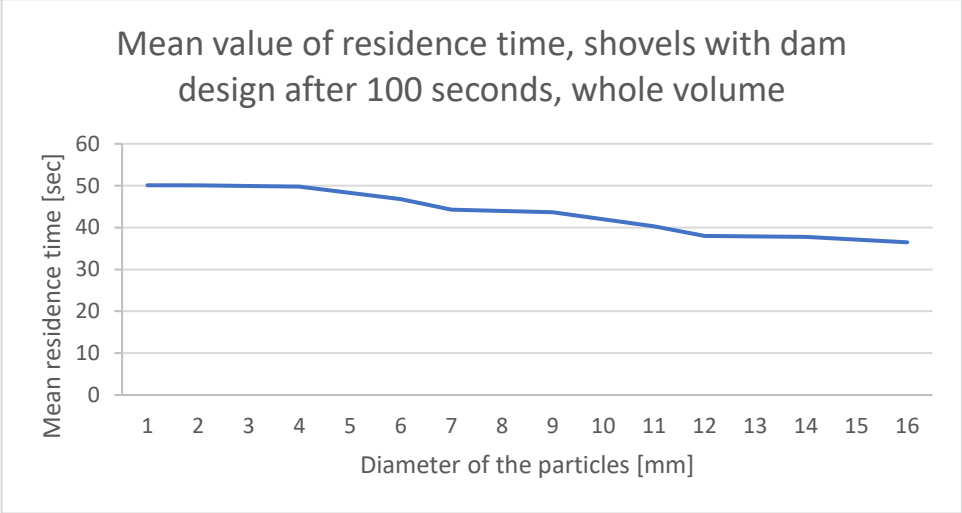

FIGURE 73 - comparison diameter and particle mean residence time for the shovels with dam design

Analysing the results obtained and comparing the average residence times of the particles inside the kiln, it is possible to deduce that design 1 is the one that least manages to optimize this parameter while both designs 2 and 3 manage to have excellent results.

TABLE 13 - comparison analytical solutions for mean residence time of proposed designs

	Smooth cylinder	Hooked blade	Inclined mixers with dam	Shovels design with dam
MODE [sec]	18,50	49,40	89,20	83,00
MEAN [sec]	21,63	32,96	41,06	44,61
MEDIAN [sec]	16,50	26,40	37,01	41,80

The particle distribution analysis points out that hooked blade design and shovels with dam design manage to create a well-distributed mixing. Inclined mixers with dam design, on the other hand, fails to get the particles to mix as efficiently as we can see from figure 70.

The graph represents how the mean residence time is affected by the dimension of the particle diameter. It is possible to see that the distribution of the mean residence time is not constant between the different diameters; particles with lower dimension escape more quickly than particles with a diameter bigger than 8 mm.

Suppose a comparison between figure 70 and figure 71 takes place. In that case, it is possible to notice more clearly that in Figure 71, the mean residence time distribution is almost constant for all the particle diameters considered.

The failure of the hooked blade can be attributed to the fact that the particles are transported along the axis of the furnace by the hooks, this transport causes their speed to increase, and therefore the average residence time decreases.

Since the primary purpose of this work is to increase the mean residence time of the particles, it is decided to continue to analyse inclined mixers with dam design and shovel with dam design.

To perform a better evaluation of the geometry to find the correct setting of the geometry and try different configurations that could increase the efficiency of these geometries, studies of designs occur.

8.5 The second study of design

8.5.1 Inclined mixers with dam

In this section, we make a design study for the second geometry proposed to try to understand if it is possible to improve the results obtained from the first simulation.

This geometry features a dam with eight mixers arranged at a 45 ° angle to the circumference of the furnace.

These mixers in the initial geometry are mounted with a 10 ° angle of inclination with respect to the vertical, as shown in the following figure.

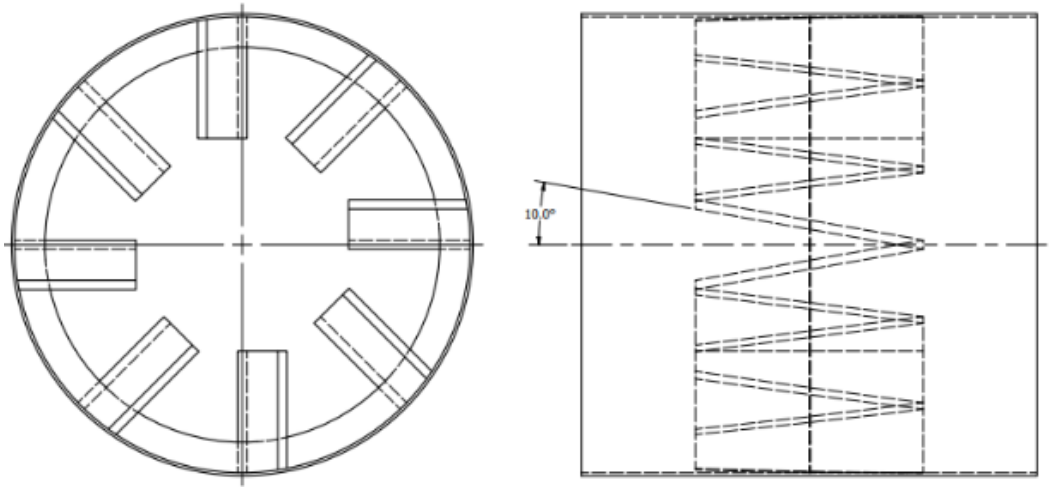

FIGURE 74 – inclined mixers with dam design, first configuration

The idea of modifying this geometry is to vary the angle of inclination of the mixers with respect to the vertical axis.

The first test that was made was to increase the angle from 10 ° to 20 ° slightly.

In both cases, the mixers are placed in such a way that, following the rotation of the kiln, the inclination of the mixers generates in the first part a backflow of the particles generated by gravitational force.

The following figure shows how the geometry test looks.

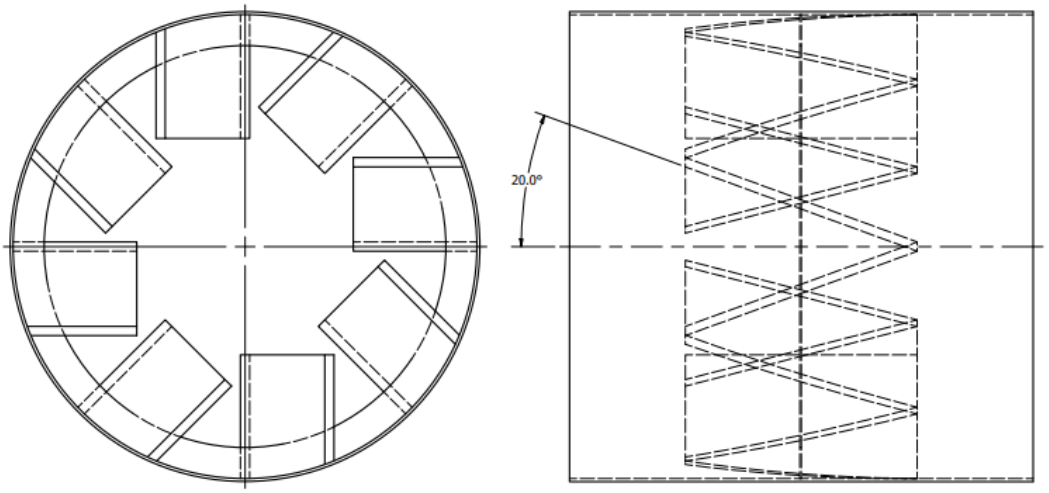

FIGURE 75 – inclined mixers with dam design, second configuration

Once these two tests had been carried out, it was decided to accentuate this angle of inclination of the mixers even more in such a way as to try an extreme case to see if through the extreme modification gains were obtained or not.

The third test has the angle respect the vertical equal to 35°.

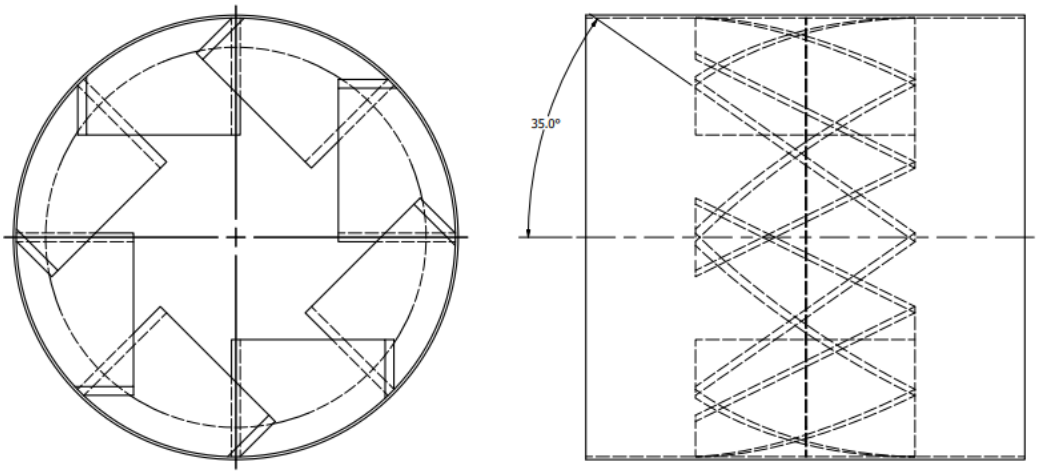

FIGURE 76 – inclined mixers with dam design, third configuration

The simulations were all carried out with a time of 100 seconds in order to obtain reliable results.

The settings of the Ansys Fluent program have been set as described in the previous paragraph.

At the end of the simulation, the analysis of the data expressing the average residence time of the particles within the kiln was carried out.

The following table summarizes this aspect:

TABLE 14 - comparison analytical results for mean residence time of inclined mixers with dam design

	10°	20°	35°
MODE [sec]	89,20	98,20	50,20
MEAN [sec]	41,06	43,77	37,98
MEDIAN [sec]	37,01	40,00	32,40

By analysing the data expressed in the table above, we can see that the bigger value of the mean residence time is achieved in the second configuration with an inclination of 20°.

As previously described, this configuration has the mixers inclined by 20 degrees with respect to the vertical.

8.5.2 Shovels with dam

The next geometry analysed for improving the particles' mean residence time is the third design proposed above.

The parameter taken into consideration for the design study in question is the angle of inclination of the mixer after the dam.

The simulation of this design which was carried out in the previous chapter, presents the angle of inclination of the mixer with respect to the dam equal to 90 ° as shown in the figure below.

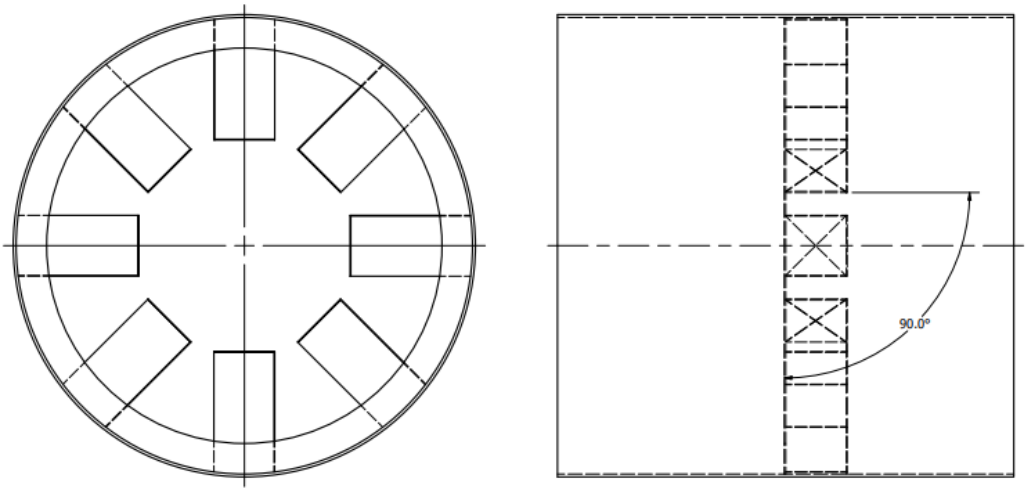

FIGURE 77 – shovels with dam design, first configuration

The idea in changing the angle of inclination of the mixer with respect to the dam is to be able to create an angle that creates a kind of basin that manages to trap the particles inside it.

The blocking of these particles within the geometry should allow the particles to be transported up to the top of the oven and then drop under the force of gravity and thus create a good mixing inside the kiln.

The decision to insert a dam, on the other hand, stems from the study carried out on the basic geometries, in which it was understood that the dam has an important influence on increasing the average residence time of the particles in the kiln.

As shown in the figure below, the variation present in the second design test presents a variation with respect to the original as the mixer, in this case, is inclined by 80 ° against the 90 ° of the first prototype.

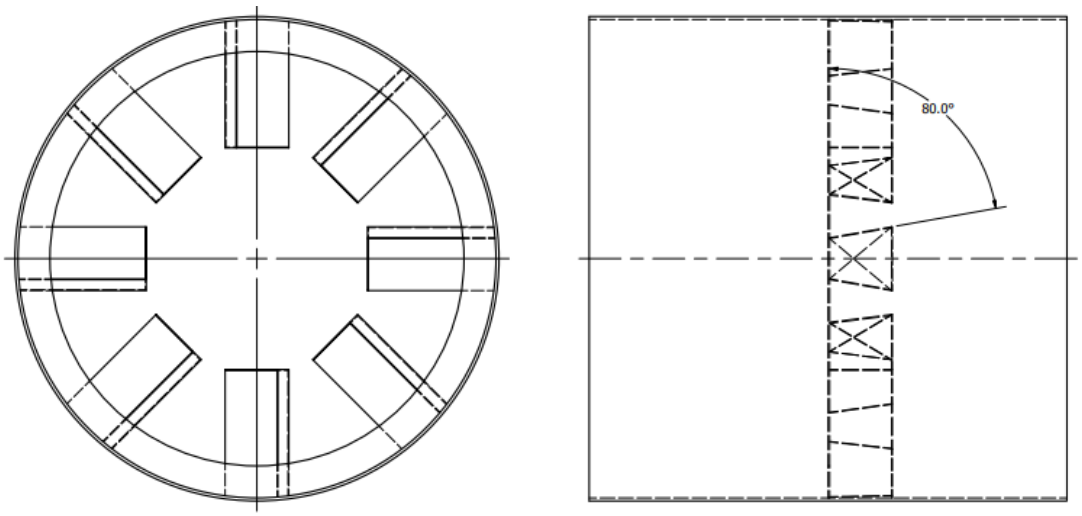

FIGURE 78 – shovels with dam design, second configuration

The third test that has been carried out increases the angle of inclination of the mixer even more; in this case, it is 70 °.

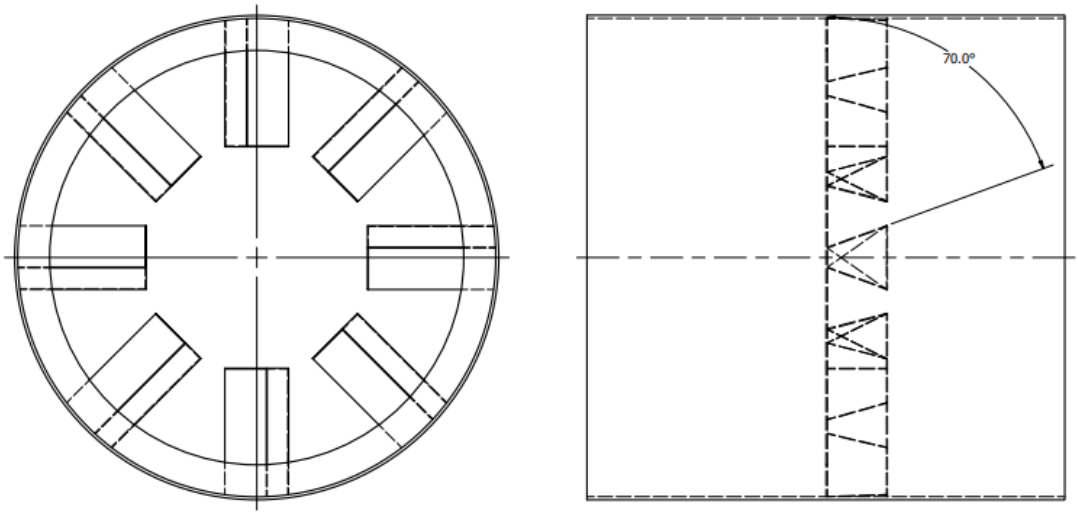

FIGURE 79 – shovels with dam design, third configuration

The Ansys Fluent 2020 R1 software setting with student license has been set as described in the previous chapter.

The simulation lasted for 100 seconds in order to obtain efficient results.

The following table summarizes the data relating to the average time of appearance of the particles in the kiln that have been extrapolated from the simulations of this design.

TABLE 15 - comparison analytical results of mean residence time of shovels with dam design

	90°	80°	70°
MODE [sec]	83,00	39,20	75,24
MEAN [sec]	44,61	31,93	40,44
MEDIAN [sec]	41,80	26,00	31,40

Analysing the data summarized in the table above, we can see that the biggest average residence time of the particles is obtained in the first configuration of this design, that is, the one with an angle between the shovels and the dam equal to 90 °.

There is a significant difference between the mean residence time of the configuration with an inclination equal to 90° and the one with an inclination equal to 80°. The cause of this big difference is that by changing the angle of the inclination, the particles can escape from the shovels and escape from the kiln. This thing doesn't happen for the configuration with 90°, so probably close to 80° of inclination, the maximum escaping point for the particles exists.

Studying the other data of the table makes it possible to see that the first configuration is also a good parameter for the other aspects.

9. Discussion of the final results

Once the simulations with the basic geometries have been carried out, new possible design choices to be proposed, and the design study carried out to identify the best configuration; it is possible to start discussing the results obtained and comparing them with each other.

The first thing to be compared and analyzed in the table below, which summarizes the statistical variables of the two previously selected geometries.

TABLE 16 - comparison analytical results for mean residence time of geometries after the second study of design

	Inclined mixers with dam 20°	Shovels with dam 90°
MODE [sec]	98,20	83,00
MEAN [sec]	43,77	44,61
MEDIAN [sec]	40,00	41,80

Thanks to these results, it is possible to know the increase of the residence time compared with the result of the smooth cylinder expressed in percentage.

The idea of expressing the results as a percentage comes from the fact that many simplifications have been taken to carry out this work.

In this way, it is possible to guess which increase in the average residence time of the particles within the kiln is obtained with the selected geometries.

The table below shows the percentage increases of the average residence time of the two selected designs.

TABLE 17 - results of mean residence time expressed in percentage for selected designs

	Inclined mixers with dam 20°	Shovels with dam 90°	Smooth cylinder	% Inclined mixers with dam 20°	% Shovels with dam 90°
MEAN	43,77 sec	44,61 sec	21,63 sec	50,58 %	51,51 %

The first difference that can be noticed is that the average residence time of the particles inside the kiln is very similar even if, in the simulation of shovels with dam, it is slightly higher.

Focusing on the mixing of the particles inside the kiln for the configurations selected, it is possible to analyse the graphs obtained from the study of the data.

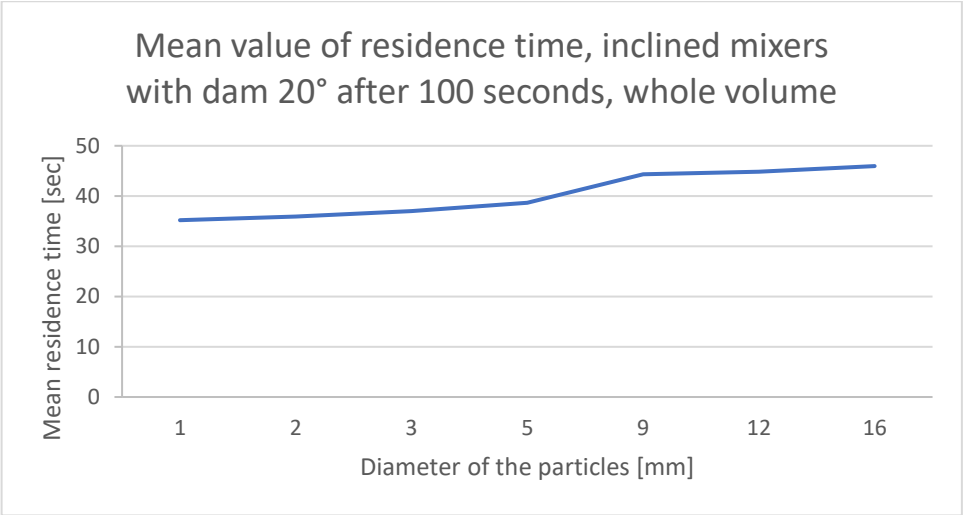

FIGURE 80 - comparison diameter and particle mean residence time for inclined mixers with dam design with 20° of inclination

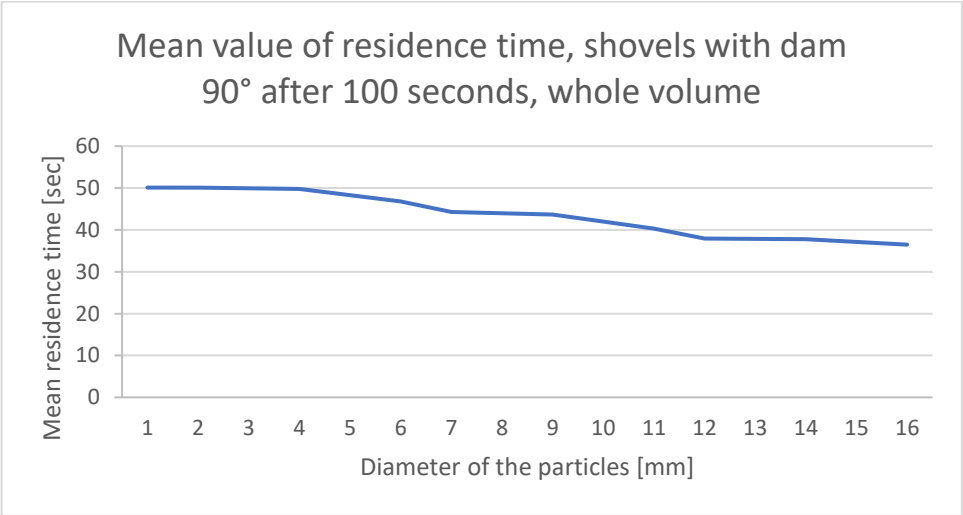

FIGURE 81 - comparison diameter and particle mean residence time for shovels with dam design with 90° of inclination

Turning to the observation of the figures deriving from the simulations carried out, we can determine which of the two configurations is able to create a less homogeneous mixing of the particles within the kiln.

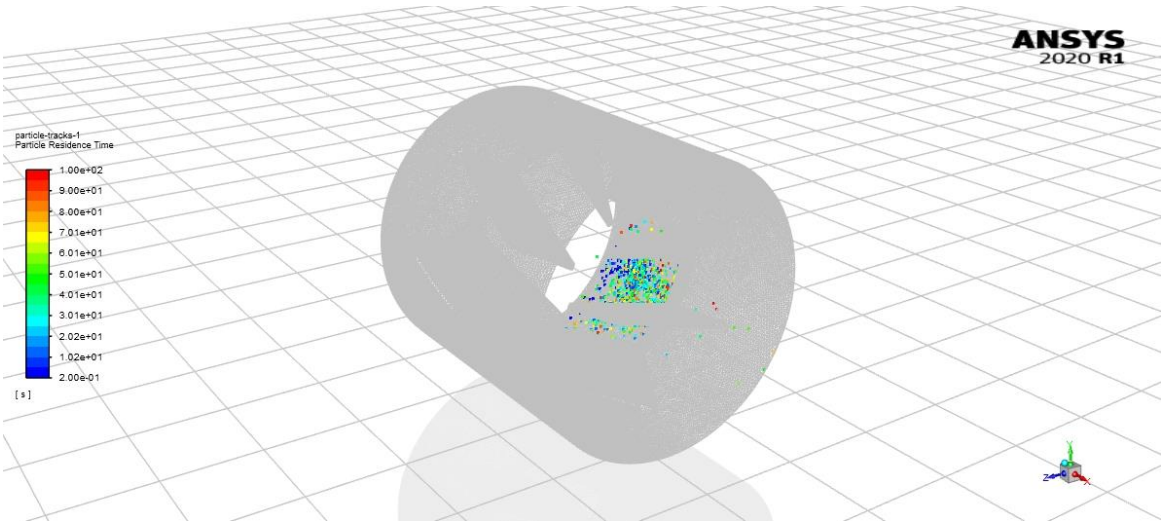

FIGURE 82 - final result inclined mixers with dam design 20°

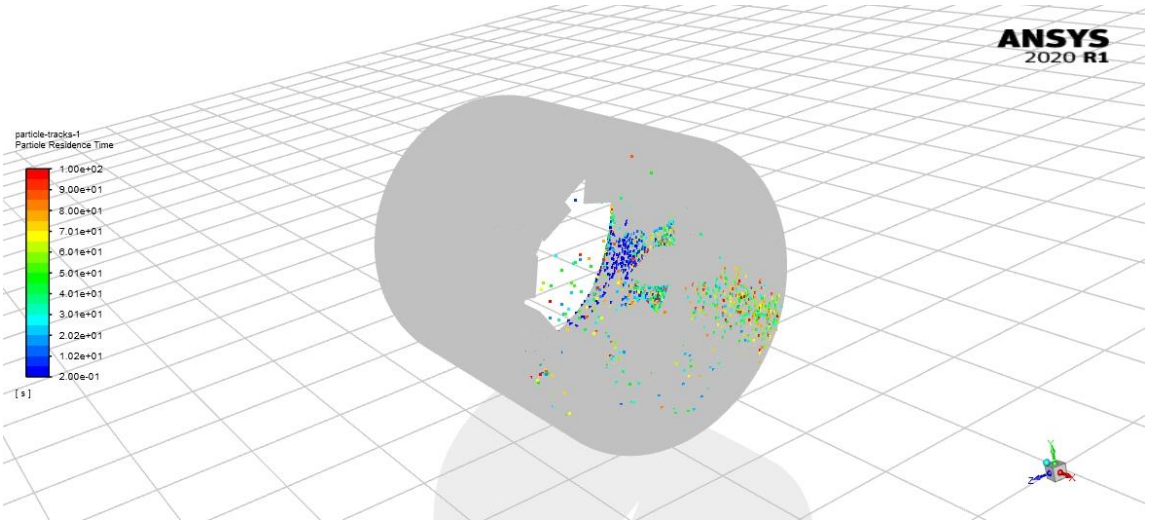

FIGURE 83 - final result shovels with dam design 90°

It is possible to notice that this configuration of shovels with dam gives a good mixing of the particles inside it; on the other hand, inclined mixers with the dam is not able to create a good mixing of the particle.

For these reasons, from the point of view of the analysis of the graphs and the pictures for the mixing of the particle is preferable to shovels with a dam with the configuration at 90°.

10. Conclusion

Given the considerations scattered throughout the thesis in question, several conclusions can be deduced:

The student licensed Ansys 2020 R1 software is able to simulate the rotating kiln with a flow of clay particles inside. A problem that emerged during the simulations is that the software is heavy. Therefore, it is necessary to use a new generation computer with powerful processors to perform reliable measurements. The average required time to complete the simulation is around 10 hours.

If it had been decided to run longer simulations and/or with a higher number of particles, the simulation time would have been drastically higher and would not have allowed the correct execution of the work due to lack of time.

For this reason, some assumptions have been made, such as the number of meshes that have never been excessively high, the number of particles present in the incoming stream, the simulation time, the kiln length, the simulation time, and the flow rate of the particles.

Only two simulation methodologies were analysed as the others would have greatly extended the simulation time or would have been too heavy to support the computer used for the work under examination.

The two simulation methods analysed are the discrete phase model (DPM) and dense discrete phase model (DDPM), both of which could return acceptable and concrete results for the case study.

After several feasibility and reliability studies, it was decided that the discrete phase model was the one that best meets the needs described; for this reason, the model used for all simulations is the DPM.

The simulation performed using the smooth cylinder geometry was very useful to compare the different simulation methodologies and compare the analytical results with the simulation result.

Thanks to the simulations carried out on the basic geometries (the dam, the hooks, and the mixers), it was possible to obtain tangible results on which tasks to perform at their best. Three geometries were proposed, hooked blade design, inclined mixers with dam and shovels with the dam. Only inclined mixers with dam and shovels with dam are chosen.

A design study was carried out to understand if the geometries conceived in the first place could be improved to obtain better results. This study deduced that in the inclined mixers with dam design, the best configuration is the one with the mixers inclined by 20 degrees. Thanks to this modification, it is possible to gain about 6.6% on average compared to the initial geometry.

Both final designs give a huge increase in the particle mean residence time compared with the geometry of the smooth cylinder. For the first final design, inclined mixers with a dam

inclination of 20°, gives an increase of 50,58% and, the second final geometry increases 51,51%.

Regarding the mixing of the system, it is possible to notice that for inclined mixers design with 20° the small particles present lower mean residence time compared with particles with bigger diameter. For the shovels with dam 90°, there is a lower difference between small and big particles, and the value of the mean residence time is almost the same with a small difference in favour of small particles.

How mean residence time is changed with the changing of the inserts? The answer to this question can be summarized in the following table:

TABLE 18 - discussion of all results

	Smooth	Dam	Hooks	Mixer	Hooked blade	Inclined mixers with dam 20°	Shovels with dam 90°
MEAN [sec]	21,63	30,04	28,82	34,36	32,96	43,77	44,61
%	0,00%	27,99%	24,94%	37,04%	34,37%	50,58%	51,51%

From this table, it is possible to see that thanks to the proposed designs, I could increase the particles' residence time of the smooth cylinder for more than 50%.

How big and small particles behaves? To answer this question, we can observe the following graph that summarizes all the data find from the simulations:

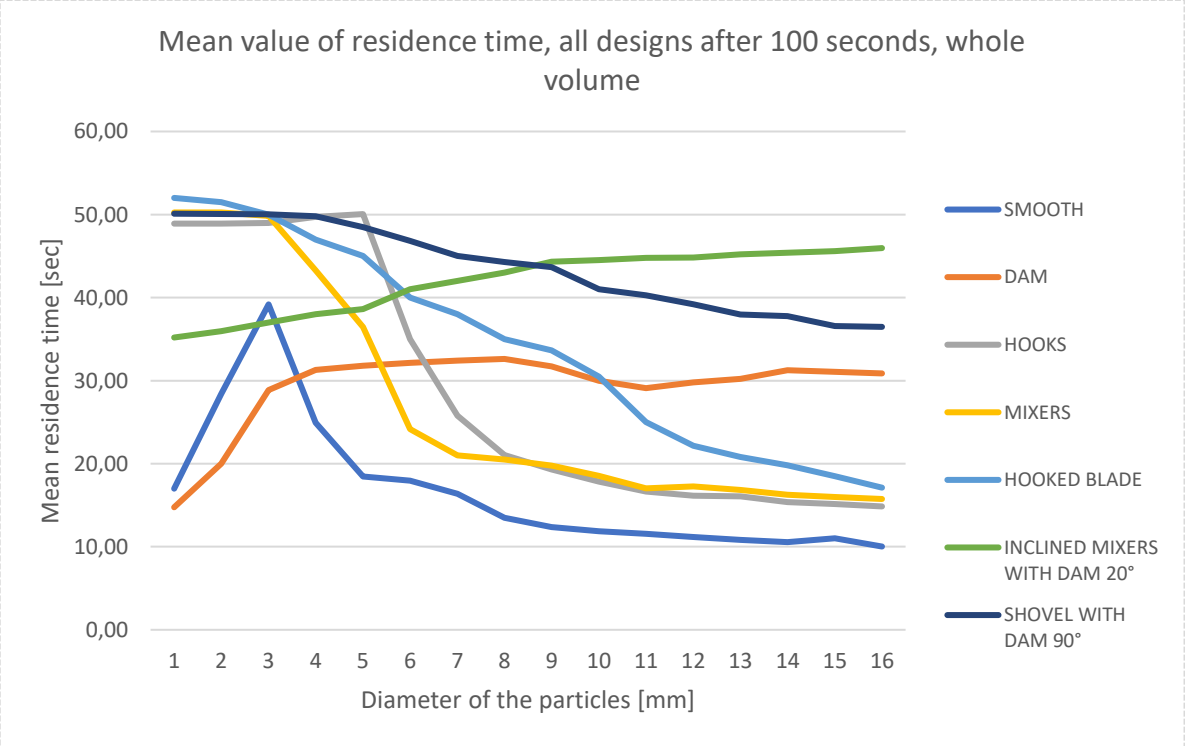

FIGURE 84 – discussion of diameter and particle mean residence time for all designs

From this graph, it is possible to analyse the average value of all design simulated with the same mesh size, simulation time, type, and dimension of particles.

We can see that particle from 1 to 5 mm has bigger mean residence time equal to 42,71 seconds, this means that the smallest particles are on average trapped more inside the inserts placed in the rotary kiln.

The big particles, from 9 to 16 mm, instead present a more constant distribution compared with the small particles; the average value of the mean residence time for these diameters is 25,24 seconds. The constant distribution means that these particles have the same behaviour inside the kiln.

List of symbols

SYMBOL	NAME	MEASURE UNIT
τ	Mean residence time	[s]
L	Length	[m]
s	Slope of the kiln	$[\frac{m}{m}]$
N	Rotational velocity	[rpm]
G	Freeboard gas velocity	$[\frac{kg}{hr.m^2}]$
B	Constant on material dimension	[-]
F	Quantity of the feed that enters the kiln	$[\frac{kg}{hr}]$
d_p	Particle diameter	[m]
Fr	Freud number [-]	[-]
w	Angular velocity	$[\frac{1}{s}]$
R	Radius	[m]
z_0	Number of cascades	[-]
ψ	Angle of the relative bed related to the axial plane	[°]
u_{ax}	Axial velocity	$[\frac{m}{s}]$
H	Length of the dam	[m]
Φ	Slope of the kiln	$[\frac{m}{m}]$
W	Quantity of the feed	$[\frac{kg}{hr}]$
β	Inclination of the kiln concerning x-axis	[°]
SV	Space velocity	$[\frac{m}{s}]$

q_i	Charge of the particles	[C]
ε	Dielectric constant	$[\frac{F}{m}]$
σ_i	Charge of densities	$[\frac{C}{m^2}]$
A	Hamaker constant	[-]
Re	Reynolds number	[-]
ρ	Density	$[\frac{kg}{m^3}]$
u	Velocity	$[\frac{m}{s}]$
μ	Dynamic viscosity	[Pas]
V_q	Volume of phase q	$[m^3]$
α	Phasic volume fraction	[-]
ρ_q	Physical density of phase	$[\frac{kg}{m^3}]$
u_q	Phase velocity	$[\frac{m}{s}]$
$\dot{m}_{ij}$	Mass transfer between the phases	$[\frac{kg}{hr}]$
S_q	Source term	[-]
φ	Fraction of cross-section occupied	$[\frac{m^2_{clay}}{m^2}]$

References

[1] Mr. Rozon (2018), "Investigation of the particle movement in the rotary kiln", Master's thesis, CVUT Prague.

[2] Kaustubh S. Mujumdar and Vivek V. Ranade, Asia-Pac. J. (2008), "CFD modelling of rotary cement kilns", Chem. Eng. 3: 106–118.

[3] S.-Q. Li, L.-B. Ma, W. Wan and Q. Yao (2005), "A mathematical model of heat transfer in a rotary kiln thermo-reactor", Chem. Eng. Technol. 2005, 28, No. 12.

[4] Fabian Herz, Iliyan Mitov, Eckehars Specht, Rayko Stanev (2012), "Influence of operational parameters and material properties on the contact heat transfer in rotary kilns", International Journal of Heat and Mass Transfer 55, 7941-7948.

[5] Deliang Shi, Watson L. Vargas, J.J. McCarthy (2008), "Heat transfer in rotary kilns with interstitial gases", Department of Chemical and Petroleum Engineering, University of Pittsburgh, Pittsburgh, PA 15261, USA.

[6] Bormans, P. (2003), "Ceramics are more than clay alone: raw materials, products, applications.", Retrieved from http://ebookcentral.proquest.com

[7] Wen Zhong, Chun Hua Wang, Tie Liu, Chun You Zuo, Yuan Hang Tian, Tian Tian Gao (2009), "Residence time and mass flow rate of particles in carbon rotary kilns", College of Materials and Metallurgy, Northeastern University, Shenyang 110004, China

[8] Peray, K. E., Edward Arnold. (n.d.), "The Rotary Cement Kiln (2nd ed.)".

[9] A.A. Boateng (2008), "Rotary kilns", ELSEVIER,

[10] Sai, P., Surender, G., Damodaran, a., Suresh, V., Philip, Z., & Sankaran, k. (1990, December), "Residence Time Distribution and Material Flow Studies in a Rotary Kiln", metallurgical transaction, 1005-1011

[11] Xiao Yan Lui and Eckehard Specht (2006, April 6), "Mean residence time and hold up of solid in rotary kiln", Chemical Engineering Science, 61

[12] Pavel Bernard (2015), "Ph.D. Thesis Rotary Kiln model", CVUT Prague

[13] Robert H. Perry and Don W. Green (1999), "Perry's Chemical Engineering Handbook", Mc Graw Hill

[14] "Multiphase flow with droplets and particles", CRC Press, second edition, 119 - 157–

[15] C. T. Crowe, J. D. Schwarzkopf, M. Sommerfeld, and Y. Tduji (2012), "Fluent Theory Guide 16.2. Retrieved August 13", ANSYS, from http://www.afs.enea.it/project/neptunius/docs/fluent/html/th/node1.htm

[16] https://it.wikipedia.org/wiki/Modello_k-epsilon

[17] Mr. Mehdi Abedi (2009), "Effect of Restitution coefficient on Inertial Particle Separator's Efficiency", Master's thesis, North-eastern University Boston, Massachusetts

[18] J. K. Brimacombe and A. P. Watkinson. "Heat transfer in a direct fired rotary kiln: Part I. Pilot plant and experimentation," Met Trans. B, 9B, 201–208, 1979.

[19] "A guidebook to particle size analysis", Horiba Instruments Inc.

[20] "A review on kiln system modelling", R. Saidur, M.S. Hossain, M.R. Islam, H. Fayaz, H.A. Mohammed, Department of Mechanical Engineering, University of Malaya, Faculty of Engineering, 50603 Kuala Lampur, Malaysa (2011)

Appendices

Design 2 - 20°
SCALE 1:20

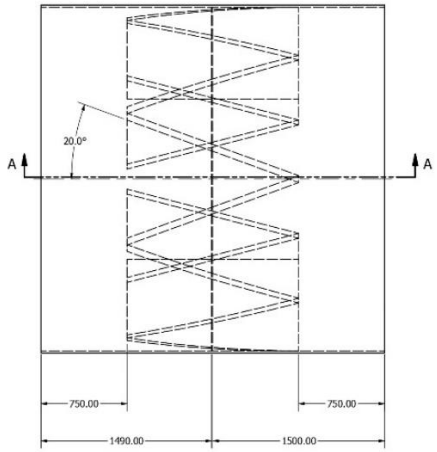

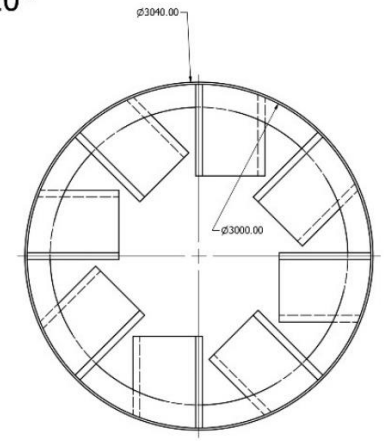

Detail mixer Design 2 - 20°
SCALE 1:10

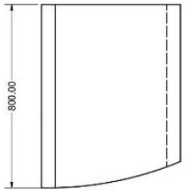

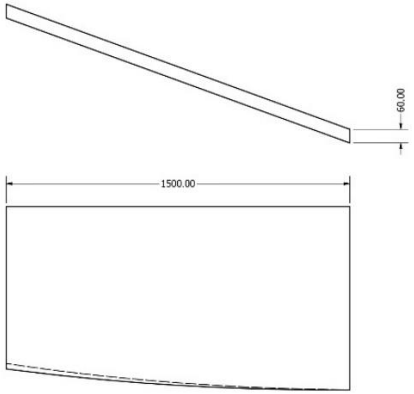

Detail dam Design 2 - 20°
SCALE 1:20

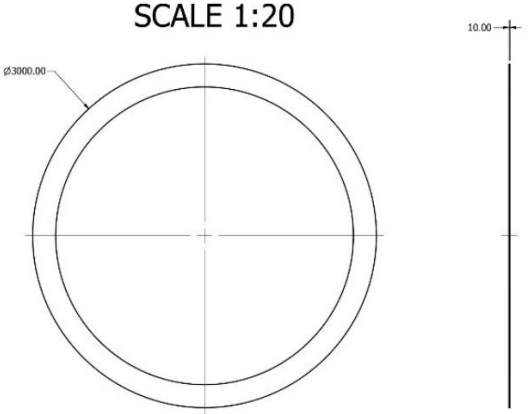

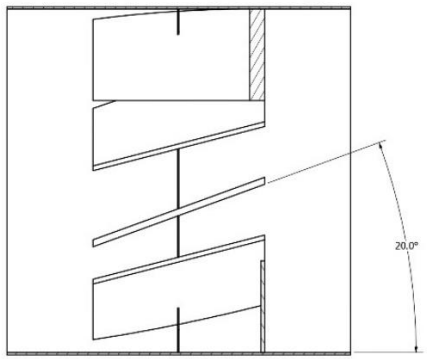

SECTION A-A
SCALE 1:20

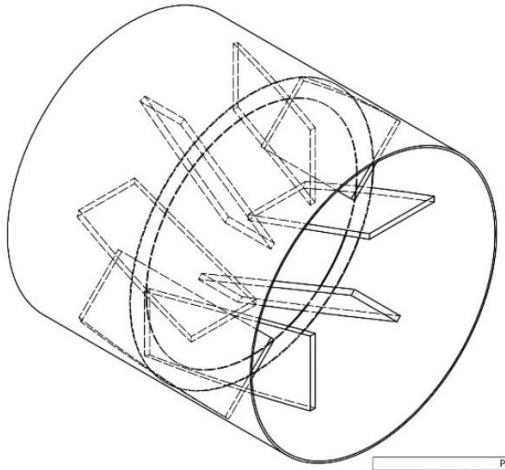

PARTS LIST		
ITEM	QTY	PART NUMBER
1	1	Cylinder
2	1	Dam
3	8	Mixer design 2 - 20°

TITLE: Design 2 - 20° FME - CVUT	DRAWN BY: Alessandro Sechi	PROJECTION:
REVIEWED BY: Ing. Jan Skocilas Ph.D.	SHEET FORMAT A4	PROCESS ENGINEERING
	DRAWING 1/2	DIMENSION IN mm

Design 3 - 90°
SCALE 1:20

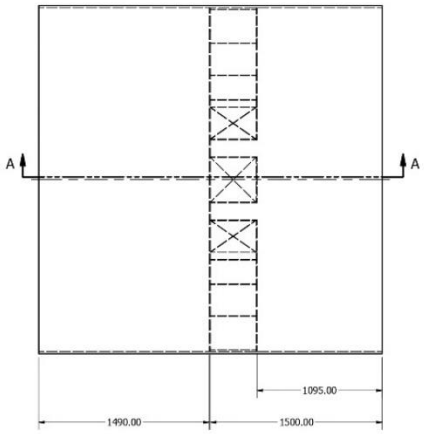

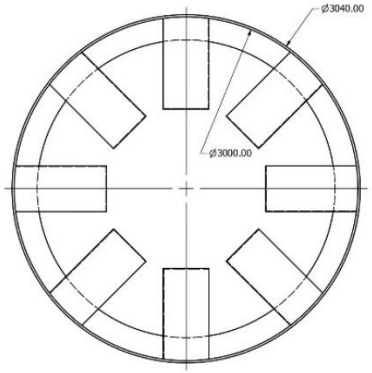

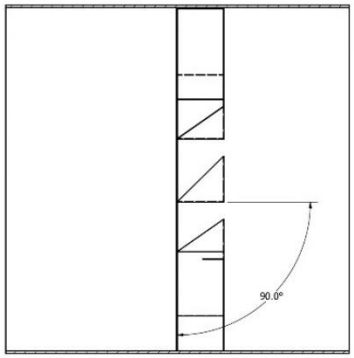

SECTION A-A
SCALE 1:20

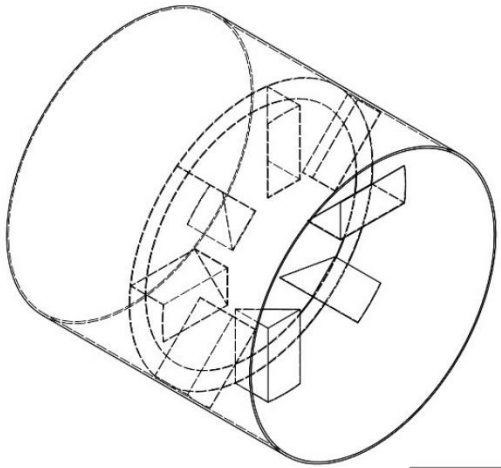

Detail component design 3 - 90°
SCALE 1:10

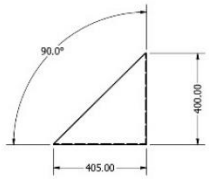

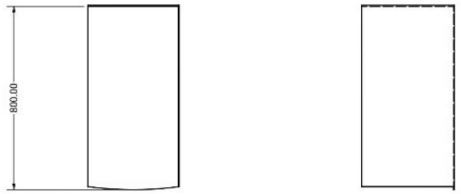

Detail dam design 3 - 90°
SCALE 1:20

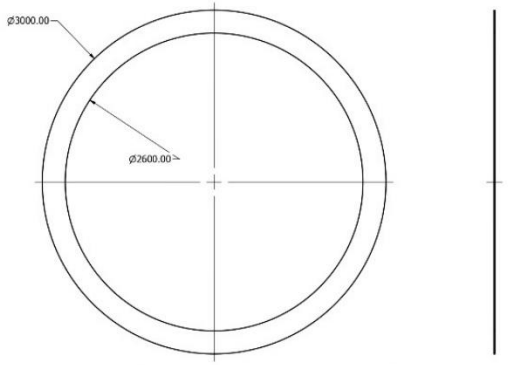

PARTS LIST		
ITEM	QTY	PART NUMBER
1	1	Cylinder
2	1	Dam
3	8	Component design 3 - 90°

TITLE: Design 2 - 20° FME - CVUT	DRAWN BY: Alessandro Sechi	PROJECTION:
REVIEWED BY: Ing. Jan Skocilas Ph.D.	SHEET FORMAT A4	PROCESS ENGINEERING
	DRAWING 2/2	DIMENSION IN mm